

Characterization of a putative separase Esp1p and a novel interacting protein in
regulating mitosis in the fungal pathogen *Candida albicans*.

Samantha Sparapani

A Thesis
in
The Department
of
Biology

Presented in Partial Fulfillment of the Requirements
for the Degree of Master of Science (Biology) at
Concordia University
Montreal, Quebec, Canada

September 2015

©Samantha Sparapani, 2015

ABSTRACT

Characterization of a putative separase Esp1p and a novel interacting protein in regulating mitosis in the fungal pathogen *Candida albicans*.

Samantha Sparapani

C. albicans is an important fungal pathogen of humans, and an understanding of the regulation of its cell cycle may reveal new targets for anti-fungal therapies. We previously characterized the *C. albicans* Anaphase Promoting Complex/Cyclosome regulatory co-factors Cdc20p and Cdh1p, and showed that they are important for the metaphase-to-anaphase transition and mitotic exit. In order to determine the mechanisms of action of Cdc20p, we searched the genome for factors that bind it in other systems, and found that *C. albicans* lacks the conserved Cdc20p target, securin. Securins bind and prevent separase from cleaving cohesin, and must be targeted for degradation by Cdc20p for separase-dependent sister chromatid separation. We hypothesized that *C. albicans* contains a divergent securin, which may be uncovered by identifying proteins that bind separase. We demonstrated that the *C. albicans* separase homologue, *ESP1*, is required for chromosome segregation. We then identified Esp1p-interacting factors using affinity purification and mass spectrometry, and uncovered Orf19.955p, a protein of unknown function with homologues only in *Candida* species. Orf19.955p contains Destruction and a KEN box, like other securins. While not essential, depletion impairs cell growth and phenotype. Chromosomes could segregate; unlike in Esp1p-depleted cells, but chromosome organization and microtubules were adversely affected. In contrast, depletion of securin Pds1p in *S. cerevisiae* prevented chromosome separation and phenocopied absence of Esp1p. Future experiments will clarify if Orf19.955p is a securin. Collectively our results provide new insights on factors involved in the metaphase-to-anaphase transition, and thus cell proliferation in *C. albicans*, including a novel fungal-specific protein.

Acknowledgements

I would like to thank my supervisor Dr. Catherine Bachewich for providing me with the opportunity to conduct my research on an area that is extremely important and very interesting. Thank you very much for your knowledge and patient guidance throughout my degree. You have truly helped me and inspired me in a multitude of ways academically.

I would also like to thank my committee members, Dr. Whiteway and Dr. Piekny for your guidance and for kindly being my committee for my thesis.

I would also like to thank my former colleague Amandeep Glory, for your patience and guidance throughout each and every day in the lab. I would also like to thank my previous colleague Vinitha Chidipi.

Also, I would like to thank Dr. Bonneil from the Proteomic Centre of University of Montreal, who helped with mass spectrometry.

Table of Contents

List of Figures	x
List of Tables.....	ix
List of Acronyms.....	xi
1. Introduction.....	1
1.1 Cell cycle regulation.....	1
1.1.1 General overview	1
1.2 Mitosis	1
1.2.1 Overview of Stages.....	1
1.2.2 Regulation of the G2/M transition: Mitosis Promoting Factor (MPF)	1
1.2.3 Regulation of the metaphase-to-anaphase transition	2
1.2.3 (a) Separase.....	3
1.2.3 (b) Securin.....	4
1.2.3 (c) Anaphase Promoting Complex/Cyclosome.....	6
1.2.3 (d) Mitotic Exit Network (MEN) and Cdc14 Early Anaphase Release (FEAR).....	7
1.3 <i>Candida albicans</i>	9
1.3.1 General Overview	9
1.4 Virulence-determining traits: Morphogenesis.....	10
1.4.1 Cell Types	10
1.4.2 Environmental Regulation of Morphogenesis	12
1.4.3 Virulence-determining trait: Cell proliferation	13
1.4.3.1 General.....	13
1.4.3.2 Regulation of mitosis in <i>C. albicans</i>	13
1.4.3.2 (a) MPF, FEAR and MEN homologues.....	13

1.4.3.2 (b) APC/C cofactors Cdc20p and Cdh1p.....	14
1.5 Objectives	15
2. Materials and Methods	17
2.1 Strains, oligonucleotides and plasmids.....	17
2.2 Medium and growth conditions.....	21
2.3 Construction of strains.....	21
2.3.1 <i>ESP1-TAP</i>	21
2.3.2 <i>ESP1-TAP</i> in Cdc20p conditional background.....	23
2.3.3 <i>ESP1-HA</i>	23
2.3.4 <i>ESP1-MET3</i>	23
2.3.5 <i>ORF19.955-MYC</i>	25
2.3.6 <i>ORF19.955-MYC/ESP1-HA</i>	26
2.3.7 <i>ORF19.955-MET3</i>	26
2.3.8 <i>TUB2-GFP/ORF19.955</i>	27
2.3.9 <i>TUB2-GFP/ESP1</i>	28
2.4 Transformation of <i>C. albicans</i>	28
2.5 Genomic DNA (gDNA) extraction.....	29
2.6 PCR screening	29
2.7 Protein Extraction.....	30
2.7.1 Protein extraction by bead-beating.	31
2.7.2 Protein extraction by lyophilization.....	31
2.8 Western Blotting.....	32
2.9 Co-Immuoprecipitation	32
3.0 Affinity Purification	33
4.0 Cell imaging	34

3. Results.....	36
3.1 Characterization of the <i>C. albicans</i> Separase homologue Esp1p.....	36
3.2 <i>C. albicans</i> Esp1p is required for separation of chromosomes.....	44
3.3 Identification of Esp1p-interacting proteins reveals strong enrichment of a novel, previously uncharacterized protein, Orf19.955p.....	51
3.4 Orf19.955 is a <i>Candida</i> -specific protein with KEN and putative Destruction boxes	62
3.5 Co-immunoprecipitation confirms a physical interaction between Orf19.955p and Esp1p.....	65
3.6 Depletion of Orf19.955p results in a pleiotropic phenotype including cells that are large-budded, multi-budded, pseudohyphal or chains of yeast cells	70
3.7 Absence of <i>Orf19.955</i> results in abnormalities in chromosome organization and segregation	75
3.8 Orf19.955p levels increase in response to MMS-mediated DNA damage	76
4. Discussion	79
4.1 <i>C. albicans</i> Esp1p may be a functional separase.....	80
4.2 Putative <i>C. albicans</i> Esp1p-interacting proteins include previously unidentified factors, suggesting additional functions	81
4.3 Orf19.955p binds Esp1p and influences chromosome organization.....	82
4.4 Summary.....	84
References:	85
Supplemental Data:	92
Table S.1.....	92
Table S.2.....	93

Figure S.1.....	94
Figure S.2.....	95
Figure S.3.....	96
Figure S.4.....	97
Figure S.5.....	98

List of Figures

Figure 1: Cohesin complex and its role in sister chromatid separation.....	4
Figure 2: The Anaphase Promoting Complex/Cyclosome (APC/C), its targets and effect on mitotic progression.....	7
Figure 3: Mitotic regulatory pathways	9
Figure 4: Cell types in <i>Candida albicans</i> produced from mitotic arrest.....	11
Figure 5: Strategy for replacing a single copy of a Gene of Interest (GOI) with a marker.....	38
Figure 6 : One-step PCR strategy for tagging a gene with TAP, HA, MYC or GFP epitope.....	39
Figure 7 : Strategy for creating a strain containing a single copy of a Gene of Interest (GOI) under control of the <i>MET3</i> promoter.	40
Figure 8: Confirmation of a <i>esp1::URA3/MET3::ESP1-HIS1</i> strain.....	41
Figure 9: Yeast cells depleted of Esp1p form large buds followed by filamentous and multi-budded growth.....	42
Figure 10: <i>ESP1</i> is essential while <i>ORF19.955</i> is not.....	48
Figure 11: Cells depleted of Esp1p impairs chromatin separation.....	49
Figure 12: Cells depleted of Esp1p impairs progression to telophase and microtubule organization in a proportion of cells	50
Figure 13: Confirmation of strain <i>esp1::HIS1/ESP1-TAP-URA3</i>	53
Figure 14: Confirmation of strain <i>ESP1/ESP1-TAP-ARG4</i> in Cdc20p-conditional background.....	54
Figure 15: Esp1p-TAP expression is not significantly modulated in the presence vs. absence of Cdc20p	55
Figure 16: Amino acid sequence of Orf19.955p.....	63

Figure 17: Confirmation of strain *orf19.955::URA3/ORF19.955-MYC-HIS1*66

Figure 18: Confirmation of strain *ESP1/ESP1-HA-URA3* 67

Figure 19: Confirmation of strain *ESP1/ESP1-HA-URA3*,
ORF19.955/ORF19.955-MYC-HIS1 68

Figure 20: Co-immunoprecipitation demonstrates an interaction between Esp1p and
Orf19.955p 69

Figure 21: Confirmation of a *MET3::ORF19.955-HIS1/orf19.955::URA3* strain.....72

Figure 22: Yeast cells depleted of Orf19.955p demonstrate a pleiotropic phenotype
including cell enlargement, multi-budding and pseudohyphal growth 73

Figure 23: Cells depleted of Orf19.955p demonstrate abnormal chromosomal
segregation including fragmentation..... 77

Figure 24: Cells depleted of Orf19.955p demonstrate abnormalities in spindle and
cytoplasmic microtubule organization and position in a proportion of cells 78

Figure 25: Orf19.955p levels increase following treatment with methyl methanesulfate
(MMS)..... 79

List of Tables

Table 1: <i>Candida albicans</i> strains used in this study.....	16
Table 2: Oligonucleotides used in this study.....	18
Table 3: Plasmids used throughout the course of this study.....	21
Table 4: Comparison of separase homologues in various organisms.....	36
Table 5: Cell phenotype and position of nuclei in cells depleted of Esp1p or Orf19.955p for 5 h.....	46
Table 6: Cell phenotype and position of nuclei in cells depleted of Esp1p or Orf19.955p for 8 h.....	47
Table 7: Orbitrap LC/MS analysis of putative Esp1p-interacting proteins from exponential-growing yeast cells.....	56
Table 8: Orbitrap LC/MS analysis of putative Esp1p-interacting proteins from yeast cells blocked in mitosis.....	58
Table 9: Fungal Blast of Orf19.955p.....	64

List of Acronyms

ARM	Armadillo Repeats
bp	base pair(s)
cAMP	Cyclic adenosine monophosphate
CDC	Cell division cycle
CDK	Cyclin-dependent kinase
Co-IP	Co-immunoprecipitation
DAPI	4', 6' diamidino-2-phenylindole dihydrochloride
DNA	Deoxyribonucleic acid
DOX	Doxycycline
dNTP	Deoxyribonucleotide triphosphate
EDTA	Ethylenediaminetetraacetic acid
FEAR	Cdc14p early anaphase release factor
GEP	Guanine exchange factor
gDNA	Genomic DNA
HDAC	Histone deacetylase
HSG	Hyphal-specific gene
hr	Hour(s)
kb	kilo base pair(s)
L	Litre(s)
LiAc	Lithium acetate
MAP	Mitogen-activated protein
MEN	Mitotic Exit Network
MMS	Methyl Methanesulfate
MPF	Mitosis Promoting Factor
-MC	MM medium lacking methionine and cysteine.
+MC	MM medium supplemented with 2.5mM methionine and 0.5mM cysteine.
min	Minute(s)
ml	Milliliter(s)
nt	nucleotides
O.D.	Optical Density
PCR	Polymerase chain reaction
PEG	Polyethylene glycol
Rcf	Relative Centrifugal Force
RNA	Ribonucleic acid
rpm	Rotations per minute
MM	0.67% yeast nitrogen base without amino acids, 2% glucose
SAP	Secreted aspartyl proteinase
SDS	Sodium Dodecyl Sulfate
sec	Second(s)
ssDNA	Salmon Sperm DNA
TRIS	Tris(hydroxymethyl)aminomethane
YPD	1% yeast extract, 2% peptone, 2% dextrose

1.0 Introduction

1.1 Cell Cycle Regulation

1.1.1 Overview

The cell cycle is the process that governs duplication of DNA and subsequent division of the cell. In most eukaryotes it is composed of several phases, including G1, S, G2 and M phase, followed by cytokinesis. During G1 phase, many cell types will grow. S phase is characterized by duplication of genetic material and expression of histones required for DNA assembly. During G2 phase, growth can again occur in some cell types (1). Mitosis involves the alignment of duplicated chromosomes on a spindle, and their separation to opposite poles. Mitosis is then followed by cytokinesis, which results in the formation of daughter cells (1).

1.2 Mitosis

1.2.1 Overview of stages

Mitosis consists of various stages including prophase, metaphase, anaphase and telophase. In mammalian cells, during prophase, chromatin condenses into chromosomes and centrosomes nucleate microtubules. The nuclear envelope and nucleolus break down and the chromosomes are captured by the spindle microtubules. During metaphase, the chromosomes align at the cell equator. During anaphase, the chromosomes separate through degradation of the cohesin “glue” that held them together, and move to opposite poles of the cell. Finally, telophase is characterized by sister chromosomes reaching opposite poles of the spindle, and reformation of the nuclear envelope. Telophase is followed by cytokinesis, where the daughter cells separate. In the model yeast *Saccharomyces cerevisiae*, differences are seen with respect to the nuclear envelope, which does not break down but does form pores (2), as well as spindle assembly, which occurs earlier in S phase (3).

1.2.2 Regulation of the G2/M transition: Mitosis Promoting Factor (MPF)

A major regulator of many cell cycle transitions involves a Cyclin Dependent Kinase (CDK) interacting with a phase-specific cyclin. During the G2/M transition, a CDK interacts with a mitotic Cyclin B to form Mitosis Promoting Factor (MPF). In the model yeast *Saccharomyces*

cerevisiae, MPF consists of the CDK Cdc28p and the cyclin B Clb2p (4). The Cdc28p/Clb2p complex is held inactive at the G2/M transition by inhibitory phosphorylation from Swel1p kinase. The phosphatase Mih1p can activate Cdc28p/Clb2p by removing the inhibitory phosphate. In mammals, Cyclin B associates with Cdk1, which is also inactive due to phosphorylation by Wee1 and Myt1. Cdc25p dephosphorylates and activates CDK/Cyclin B to initiate the G2/M transition (5). Targets of MPF include proteins associated with the nuclear lamina and Golgi apparatus, for example, triggering their breakdown, factors required for spindle assembly, chromosome condensation, and activation of other processes required for mitotic progression. MPF activity must be down regulated in order for cells to exit mitosis, which occurs in part through targeted degradation of the B-type cyclin (6,7).

1.2.3 Regulation of the metaphase-to-anaphase transition

(a) Separase

The metaphase-to-anaphase transition is characterized by the separation of duplicated chromosomes to opposite poles of the spindle, and this requires the activity of separase, a cysteine-rich protease that helps cleave the glue holding chromosomes together. The « glue » consists of a cohesin complex, and this must be removed in order for the chromosomes to separate (8). The cohesin complex is composed of two core SMC proteins Smc1p and Smc3p, as well as two non-SMC kleisin proteins, Scc1p and Scc3p, which are highly conserved (8) (Fig. 1A). The alpha-kleisin subunit of the cohesin complex (Scc1p) is one of the main substrates of separase. Separases are highly conserved proteins, where conservation is found in the ARM repeat sequences at the N-terminus. Some common separases include Esp1p from *S. cerevisiae* (9), Cut1p from *Shizosaccharomyces pombe* (10), *bimB* from *A. nidulans* (11), *ESP1* from humans and mouse (12), and *Sep-1* from *C. elegans* (13), for example. They are composed of three main domains, the tail, trunk, and head. The head domain in the C-terminus is the most conserved and contains catalytic caspase-like domains, whereas the tail in the N-terminus consists of Armadillo (ARM) repeats that form a super helix of alpha helices that mediate protein-protein interactions (14, 15). In *S. cerevisiae*, *ESP1* is essential and its absence results in large-budded cells with unsegregated chromatin predominantly located in the daughter bud.

Spindles were abnormal in most cells, resembling discontinuous microtubule arrays that were often curved around the perimeter of the cell, or were very weak in staining, while a smaller proportion of cells contained a short G2 spindle (16). Long-term absence resulted in accumulation of extra spindle poles (17). Buds that did not receive DNA went on to form hypoploid cells that remained unbudded, whereas the daughter cells that acquired the DNA could undergo budding and at least one more round of DNA synthesis (16). In *S. cerevisiae*, when cells are depleted of Cdc20p and Esp1p is overexpressed simultaneously, levels of the Esp1p repressor Pds1p increase and fully elongated spindles form (18). The ability of separase to cleave Scc1p in mammals and *S. cerevisiae*, for example, is enhanced by previous phosphorylation of Scc1p by polo-like kinases such as Plk1p or Cdc5p (19, 20, 21, 22). Esp1p and Cut1p localize to the spindle pole bodies and spindles prior to and during anaphase, while human separase is associated with the centrosome (14).

Separases are linked to other functions. For example, in *S. cerevisiae*, Esp1p also cleaves Slk19p, a kinetochore and spindle-associated protein, which then functions in stabilizing the spindle during anaphase (23). Esp1p is also thought to play a role in the Cdc14 early anaphase release pathway (FEAR; see below) but in a non-proteolytic manner (24, 25), through down-regulating the phosphatase PP2A^{cdc55}, allowing phosphorylation of Net1p and initial release of Cdc14p from the nucleolus.

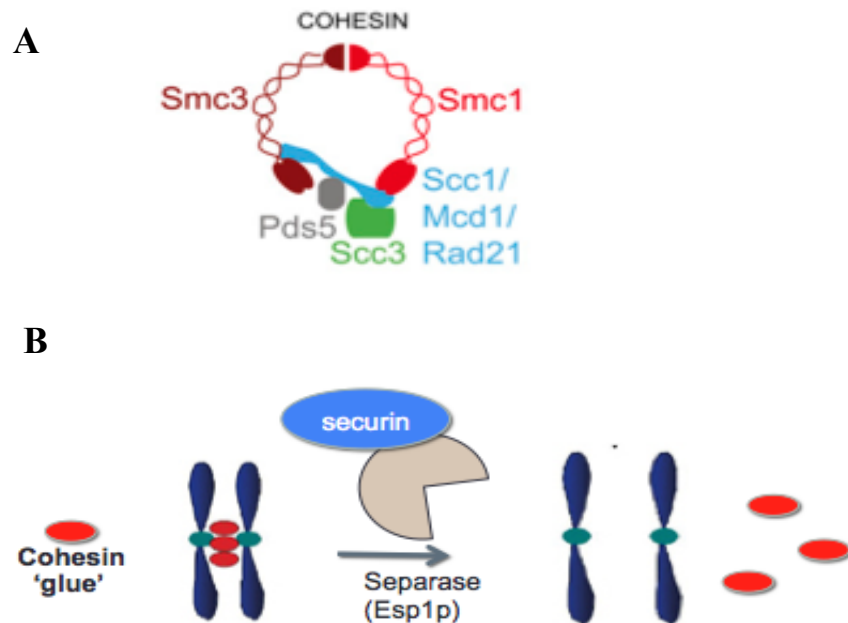


Fig 1: Cohesin complex and its role in sister chromatid separation.

(A) Cohesin complex subunits (6) (B) Key protein factors involved in sister chromatid separation during metaphase-to-anaphase transition.

(b) Securin

Esp1p is regulated in part by securin. Securin homologues are not well conserved at the sequence level, but some homology exists between Pds1p and Cut2p in *S. cerevisiae* or *S. pombe*, respectively (9, 10), as well as PTTG1p in humans (12) and Pimp in *Drosophila* (26). Securins have not been identified to date in other fungi and in plants (14). Of the known homologues, the proteins share regions of charged amino acids (27). Securins bind separase at specific binding sites, which slightly differ between organisms. For example, in fission yeast, the N-terminus of separase binds the C-terminus of securin, whereas in budding yeast, the C-terminus of Pds1p interacts with the first 156 amino acids of the N-terminus in separase as well as other amino acid sites (14).

In *S. cerevisiae*, Pds1p acts as both an inhibitor and activator of Esp1p (27). As a repressor, Pds1p, for example, binds Esp1p and inhibits it from cleaving the Scc1 subunit of the cohesin complex as previously described. Pds1p binding holds Esp1p inactive prior to anaphase

through preventing the N and C termini of Esp1p from interacting. As an activator it may assist in Esp1p folding (27) and promotes efficient nuclear localization of Esp1p from the cytoplasm (28).

In *S. cerevisiae*, Pds1p is not essential but important for growth at elevated temperatures. In *S. cerevisiae*, *PDS1* mutants displayed precocious separation of chromosomes in the presence of microtubule inhibitors. In the absence of the drugs, 75% of *PDS1* temperature-sensitive mutants grown at restrictive temperature were large-budded cells with a single chromosomal mass of DNA, while the remaining cells were unbudded aneuploid cells (9). This phenotype is due to the fact that Pds1p is both an activator and repressor of Esp1p. Pds1p mutants can form spindles, but were not fully elongated as most large-budded cells contained bar spindles characteristic of metaphase or were shorter in length (9). Cytokinesis was not impaired, as septa were observed bisecting DNA and aloid cells could form, and cells could enter the next cell cycle based on duplication of DNA and spindle pole bodies. At permissive temperature, some chromosome segregation defects were evident, resulting in only 40% of cells being able to form colonies, which were often very small and/or heterogeneous in size (9). Expression of a non-degradable version of Pds1p arrests cells in metaphase (18). In the absence of Pds1p, another protein, the phosphatase PP2A, becomes essential. PP2A prevents cohesin cleavage by antagonizing the promoting activity of Cdc5p phosphorylation of Scc1p (29). Human PTTG1p is also not essential (30) and has other mechanisms to compensate for loss of chromosome segregation genes (31). For example, a study has shown that Cdk1p binds phosphorylated separase in conjunction with its regulatory subunit Cyclin B1 (32). This in turn inhibits separase as well as the kinase (32). In other organisms, such as *S. pombe* and *D. melanogaster* securins are essential (33).

Securin is regulated in several ways. In *S. cerevisiae*, Pds1p is cyclic, where it is induced after G1 phase but degraded at anaphase onset (9). Securin can also be phosphorylated as a result of DNA or spindle damage, or by the mitotic Cdk regulator, Cdc28p (34). During DNA damage in *S. cerevisiae*, the kinase Chk1p acts on Pds1p to ensure anaphase does not proceed (35, 36). During a normal cell cycle, Cdc28p phosphorylates Pds1p during mitosis, which allows it to interact with Esp1p more efficiently as well as enhance its ability to influence the nuclear localization of Esp1p (34).

(c) Anaphase Promoting Complex/Cyclosome (APC/C)

Securin is bound to Esp1p during early stages of mitosis. In order for securin to be removed and thus liberate separase, the Anaphase Promoting Complex/Cyclosome (APC/C), another conserved regulatory network governing mitotic progression, must target it for degradation (Fig. 2). The APC/C is an ubiquitin ligase system that targets proteins for destruction through assembling a chain of ubiquitin tags on substrates. Such tags are recognized by the 26s proteasome and destroyed at the appropriate time. The APC/C is composed of 11 to 13 subunits and contains a core cullin subunit (Apc2p) as well as a RING subunit (Apc11p), which is responsible for binding the E2-ubiquitin conjugate (37).

APC/C activity is under control of two major co-factors, one of which is Cdc20p. One of the major targets of APC^{Cdc20} is securin, as well as B-type cyclins such as Clb2p and Clb5p in *S. cerevisiae*, for example (38, 39, 40, 41). In *S. cerevisiae*, *CDC20* mutants arrest in metaphase, but absence of *PDS1* in this background results in a telophase arrest, suggesting that Cdc20p is important for both the metaphase to anaphase transition as well as mitotic exit (42). Cdc20p is regulated at multiple levels. *CDC20* transcription is activated by Cks1p, a protein that interacts with CDK (43). Cdc20p protein levels are cell cycle regulated, where destruction in late mitosis/G₁ is initiated by activation of the APC via another co-factor, Cdh1p (38, 42, 43, 44, 45). Cdc20p is also a target of the spindle checkpoint; upon spindle damage, checkpoint factors such as Mad2p form an inhibitory complex with Cdc20p, thus preventing APC/C activation and anaphase (46, 47). Cdc20p may also be regulated by phosphorylation (48).

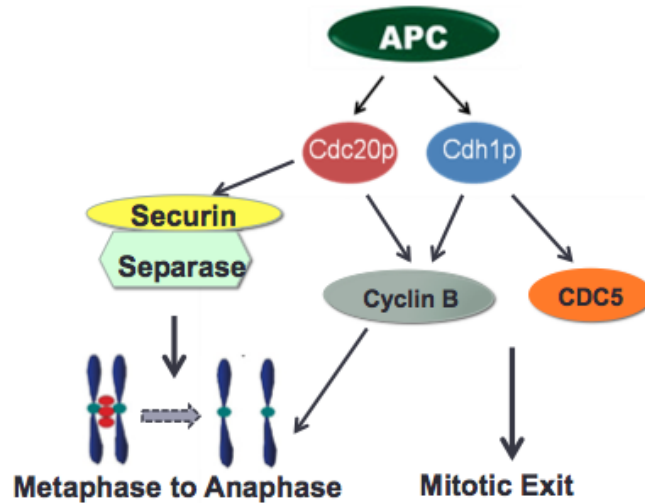


Fig 2: The Anaphase Promoting Complex/Cyclosome (APC/C), its targets and effect on mitotic progression.

A second APC/C co-activator is Cdh1p (Fig. 2). The APC/C falls under control of Cdh1p later in mitosis, and targets Cdc20p, the remainder of mitotic cyclins, other mitotic regulators such as the polo like kinase Cdc5p, and various proteins required for spindle function during degradation (49). *CDH1* is not essential in *S. cerevisiae*. Cells lacking the protein are very small, and grow slightly slower than the wild-type cells, and show a delay in telophase, indicating a role in mitotic exit (44, 50). Cdh1p levels are constant throughout the cell cycle, and its activity is negatively regulated by phosphorylation via CDK activity (45, 51, 52, 53). In order to be activated, it requires dephosphorylation by the phosphatase Cdc14p. Cdh1p activity is also negatively regulated by the spindle checkpoint pathway, since it is important for mitotic exit.

(c) Mitotic Exit Network (MEN) and Cdc14 Early Anaphase Release (FEAR) pathways

In *S. cerevisiae*, additional major regulatory circuits that control the metaphase to anaphase transition and eventual mitotic exit are the FEAR and MEN pathways (7). These pathways function to control release of the phosphatase Cdc14p from its inhibitor, Net1p, in the nucleolus, thereby allowing dephosphorylation of mitotic CDK targets, inactivation of CDK, and mitotic exit (7). The FEAR pathway functions during early anaphase to allow initial and transient release of Cdc14p. It consists of the separase Esp1p, Slk19p, and Spo12p, which inactivate the

phosphatase PP2A, resulting in enhanced phosphorylation of Net1p and initial release of Cdc14p. Cdc5p contributes to this process by interacting with Cdc14p and Esp1p (54, 55). Accumulation of Cdc14p results in the activation of the MEN at the spindle pole body by allowing for one spindle pole body to enter the bud at anaphase (56). The MEN pathway activation maintains Cdc14p release, allowing eventual mitotic exit. Here, Cdc5p negatively regulates the GTPase-activating protein (GAP) complex Bub2p-Bfa1p. This in turn negatively regulates the Ras-like Tem1p GTPase. Tem1p is localized to the daughter spindle pole bodies where it is activated by Lte1p, a guanine exchange factor (GEF) for Tem1p, only in the bud (Fig 3B) (57). The active form of Tem1p leads to a protein kinase signaling cascade including Cdc15p, Dbf2p and Mob1p, which function in releasing the remaining Cdc14p phosphatase from the nucleolus through phosphorylation (58). Released Cdc14p dephosphorylates Sic1p, a Cdk inhibitor, and Swi5p, a transcription factor for *SIC1*, resulting in down-regulation of Cdc28p/Clb2p activity. This is further enhanced by Cdc14p-mediated dephosphorylation of the APC/C cofactor Cdh1p, which in turn targets the remaining Clb2p for degradation, resulting in mitotic exit.

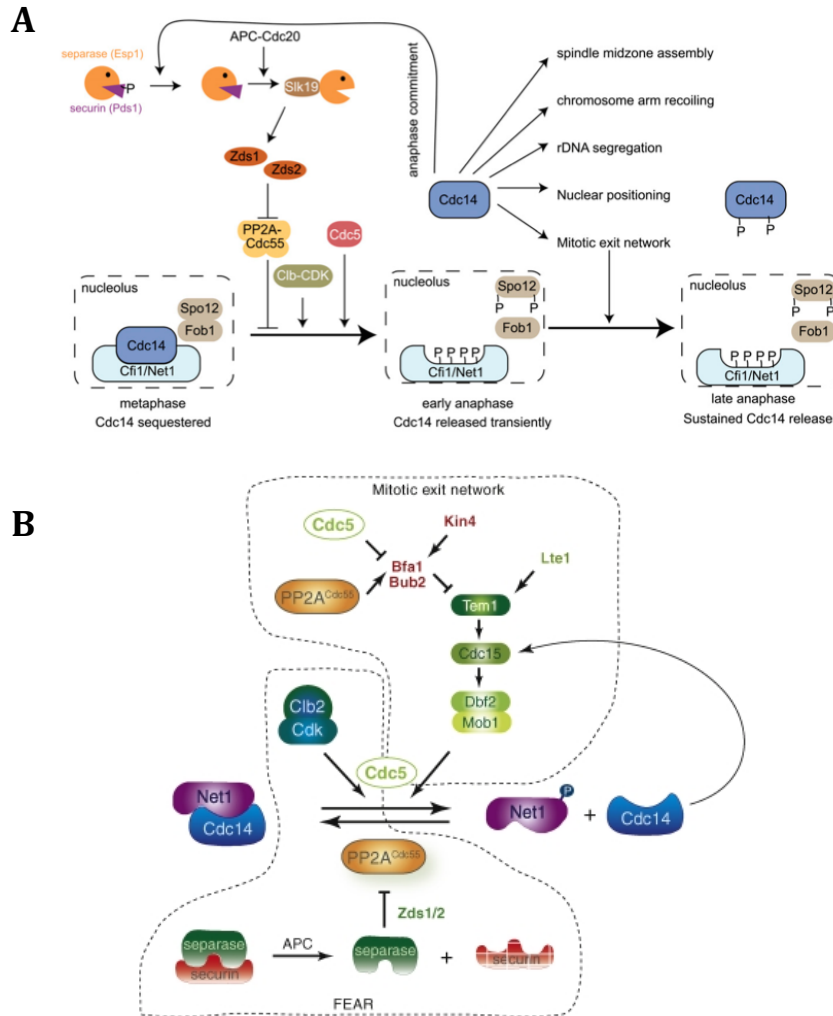


Fig 3: Mitotic regulatory pathways.

(A) Cdc14p early anaphase release pathway (FEAR) (6). (B) Mitotic exit network (MEN) (57).

1.3 *Candida albicans*

1.3.1 General overview

Candida albicans is an ascomycete fungus that is normally a commensal in human gastrointestinal and urogenital tracks (59). However, under conditions of immune suppression, such as in individuals suffering from HIV or undergoing chemotherapy treatments, it can be pathogenic, causing mucosal infections such as thrush or vaginitis, or more serious systemic infections that involve entry into the bloodstream and invasion of organs. Systemic infections are

associated with up to 50% mortality rates (60). In order to treat infection, several classes of antifungal drugs are currently in use. Azoles such as fluconazole affect cell membrane development through targeting ergosterol synthesis (61) and are fungistatic. On the other hand, the polyene Amphotericin B inserts within lipid bilayers and binds to sterols, resulting in the formation of small pores that disrupt membrane integrity and is thus fungicidal (61). Other drugs including the fluoropyrimidines and the echinocandins target nucleic acid synthesis and cell wall development, respectively, and are also fungistatic towards selective *Aspergillus* species (62). However, some antifungal drug targets have homologues in humans, resulting in toxic side effects (61), and *C. albicans* is showing increased resistance to some drug treatments (63). Thus, there is a need to identify additional drug targets and develop new anti-fungal therapies, which in turn requires a comprehensive understanding of the basic biology of *C. albicans*.

1.4 Virulence-determining trait: Morphogenesis

1.4.1 Cell types

Virulence in *C. albicans* is dependent on a number of processes and factors. For example, adherence to host cells is important and mediated by biomolecules termed adhesins, including those that belong to the ALS family. These aid *C. albicans* cells in colonizing endothelial and epithelial cells (64, 65). For host cell invasion, *C. albicans* cells utilize induced endocytosis and active penetration (65). Through the endocytosis pathway, specialized proteins called invasins line the cell surface, bind host cells and trigger them to engulf the virulent cells (65). Active penetration requires viable *C. albicans* hyphae as well as certain proteases including the SAPs and phospholipases (65).

Another process that is important for virulence is the ability of *C. albicans* to undergo morphological changes between yeast, pseudohyphal and hyphal forms under specific environmental conditions (Fig. 4). Yeast cells grow via budding that initiates at the G1/S transition of the cell cycle, and a ring of septins marks the future bud emergence site. Initial bud outgrowth is polar, and associated with a high concentration of actin patches and a polarisome, but switches to an isometric mode near mitosis, when the actin patches disperse evenly around the bud and polarisome components re-locate to the bud neck (66, 67, 68). Nuclear division takes

place across the mother-bud neck, followed by septation and cytokinesis (69). Yeast cells fall into two classes, white or opaque (70). White phase yeast cells are more round, grow into cream-colored colonies and are incapable of mating. The less frequent opaque cells are enlarged, bean-shaped yeast that are mating form of *C. albicans* by virtue of being homozygous at the mating type locus (71). White phase yeast cells can switch to filamentous cell forms, including pseudohyphae and hyphae. Pseudohyphae are chains of elongated yeast cells with an extended G2 phase that do not separate after cytokinesis, and show constrictions at septation sites (72). Hyphae are distinct in that they initiate and maintain polarized growth, and thus maintain a high concentration of actin patches at the tip. The first nuclear division takes place within the germ tube and not at the bud neck (72). Hyphae contain a polarisome but also a proposed vesicle supply center, called the Spitzenkörper, in the tips (68, 74). Spitzenkörper components such as the myosin light chain Mlc1p are maintained at the growing tip and simultaneously localize to subapical septation sites. Hyphae lack constrictions at septation sites, and do not have extended cell cycle phases like pseudohyphae, indicating that hyphal growth runs independently of the cell cycle (67, 72). This plasticity in form is crucial for survival in the host and virulence, because cells locked in one mutant form lose their pathogenicity (71). The yeast cells are thought to be optimal for dissemination in the bloodstream, whereas the filamentous forms are more adept at penetrating and invading tissue (73).

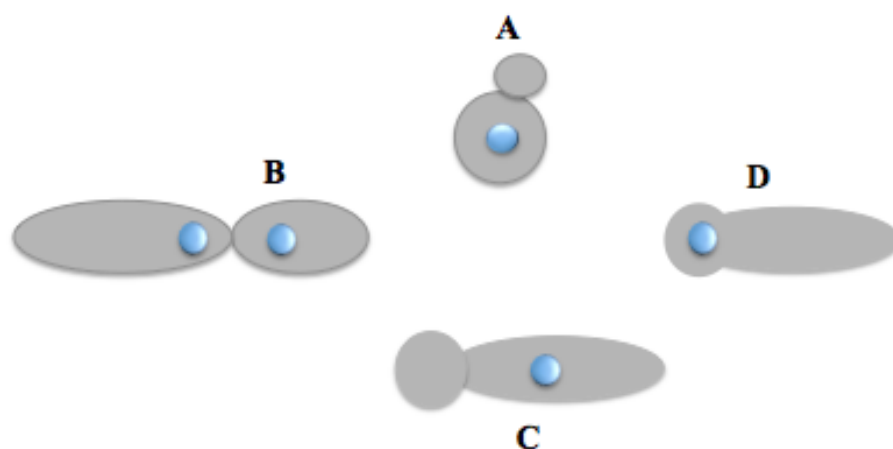


Fig 4: Cell types in *Candida albicans* produced from mitotic arrest.

(A) Yeast. (B) Pseudohyphal cell. (C) Elongated filaments produced from mitotic arrest with nucleus in daughter cell. (D) Hyphal cell.

1.4.2 Environmental Regulation of Morphogenesis

The regulation of morphogenesis involves environmental cues and associated signaling pathways. For example, yeast, pseudohyphae and hyphae grow at 30, 36 or 37°C, respectively. Hyphae additionally require factors such as serum, a pH between 6 and 7, or alternative carbon sources to form (72). The yeast-to-hyphal transition has been extensively investigated, where environmental cues are mediated by a diversity of signaling pathways, including the mitogen-activated protein kinase (MAPK) and cyclic AMP (cAMP) and others (75), for example. An important downstream transcription factor that many of the pathways converge on is Efg1p. Efg1p is a master regulator of hyphal growth and expression of hyphal-specific genes (HSGs), since cells lacking Efg1p can't form hyphae under most hyphal-inducing conditions (76) and Efg1p is required for expression of many HSGs, including adhesions, proteases and other factors required for virulence of hyphae (76). Another HSG that is a target of Efg1p is the transcription factor *UME6* (75,77). Yeast cells lacking Ume6p initiate but do not maintain hyphal growth, and *UME6* overexpression can drive hyphal formation under yeast growth conditions (78). Ume6p regulates expression of many genes, including *HGC1*. *HGC1* is expressed only in hyphae and is homologous to a G1 cyclin, yet is not required for the cell cycle (79). Hgc1p interacts with the cyclin-dependent kinase Cdc28p and phosphorylates the Cdc42p inhibitory GTPase activating protein (GAP) Rga2p, preventing it from localizing to hyphal tips and thus permitting hyphal growth (79). Cdc28p/Hgc1p also phosphorylates Efg1p, which targets it to promoters of genes that repress cell separation in hyphae (80) and Sec2p, a secretory vesicle-associated protein that is specifically localized to the Spitzenkörper (81). The yeast-to-hyphal transition can also be negatively regulated by other transcription factors, including Tup1p, Nrg1p and Rfg1p (76).

1.4.3 Virulence-determining trait: Cell proliferation

1.4.3.1 General

Cell proliferation is another biological process that is crucial for survival in the host and for virulence. However, cell cycle regulation has not been well characterized in *Candida albicans*. At a transcriptional level, there are similarities in cell cycle phase-specific modulated genes compared to other yeast systems including *S.cerevisiae* and *S. pombe* (82). However there

were also many differences, including modulation of *Candida*-specific and/or uncharacterized genes. Several putative cell cycle-associated and regulatory proteins remain to be characterized in *C. albicans*, of those that have been analyzed, many show variation in function compared to homologues in other systems, including yeast and mammals. This suggests the existence of novel features in the cell cycle circuitry in *C. albicans*, which may be exploited for the purpose of new drug target discovery.

1.4.3.2 Regulation of mitosis in *C. albicans*

(a) MPF, FEAR and MEN homologues

In *C. albicans*, little is known about the regulation of mitosis. Of the factors that have been characterized, several show variations or differences in function in *C. albicans* compared to orthologues in *S. cerevisiae*, suggesting re-wiring in the mitotic networks, or mechanisms of action remain unclear. For example, homologues of the CDK Cdc28p and the B-type cyclin Clb2p exist. Absence of either results in a mitotic arrest but Clb2p-depleted cells were arrested in telophase (83), while the arrest point for Cdc28p-depleted cells was not determined (84). Further, regulation of Cdc28p/Clb2p and targets remain elusive. With respect to MEN and FEAR pathways, *C. albicans* contains a homologue of *CDC14* but unlike the situation in *S. cerevisiae*, it is not essential and is required in late telophase (85, 52). *DBF2* in *C. albicans* is essential and required spindle formation, cytokinesis, septum formation, and exit from mitosis in *C. albicans* (86), while *S. cerevisiae DBF2* is not essential and is required for mitotic exit and cytokinesis (87). The GTPase Tem1p, however, is essential for mitotic exit, cytokinesis and cell separation in both *S. cerevisiae* and *C. albicans*, *C. albicans* also contains a homologue of the polo-like kinase, Cdc5p, but it is required earlier in the cell cycle in *C. albicans* compared to *S. cerevisiae* (88).

Intriguingly, many of the factors that are essential for mitosis in *C. albicans* result in a novel phenotype upon depletion, where the yeast cells grow into long filaments as opposed to arresting as large doublets (Fig. 4) (88). We recently demonstrated that the filaments associated with Cdc5p depletion were elongated buds that failed to switch from polar to isometric growth, and then adapted a hyphal fate over time. This required delayed activation of a core hyphal

regulator, the transcription factor Ume6p (89), but the mechanism linking mitotic arrest to changes in polar growth at the bud tip and subsequent activation of Ume6p remain unclear.

(b) APC/C cofactors Cdc20p and Cdh1p

With respect to the APC/C, orthologues of Cdc20p and Cdh1p were partially characterized in a previous report by conducting a series of biochemical and genetic analyses (90). In order to determine the function of Cdc20p, a strain was constructed where one copy of the gene was placed under control of a conditional promoter. DAPI staining and tubulin localization demonstrated that cells depleted of Cdc20p were arrested in metaphase or telophase. Further, the mitotic cyclin Clb2p as well as the polo-like kinase Cdc5p were enriched, suggesting that Cdc20p shows conservation in function as well as targets in regulating mitosis in *C. albicans*. In order to determine the function of Cdh1p, a deletion strain was created and the gene was not essential. DAPI staining and tubulin localization showed that a high proportion of *cdh1Δ/cdh1Δ* cells contained a telophase spindle, and enriched Clb2p and Cdc5p, suggesting a delay in telophase, similar to the situation in *S. cerevisiae*. Thus, *C. albicans* Cdh1p has some conserved function in regulating mitotic exit in *Candida albicans*.

However, other results suggest additional novel features or functions associated with *C. albicans* Cdc20p and Cdh1p. For example, cells depleted of Cdc20p formed elongated filaments, and did not arrest as large doublets as seen in *S. cerevisiae cdh1Δ* cells (90). Further, *C. albicans* lacks a sequence orthologue of the conserved Cdc20p target, securin. In addition, cells depleted of Cdh1p showed a pleiotropic phenotype, and of the yeast form cells, the size was significantly larger than control yeast cells. In contrast, *S. cerevisiae cdh1Δ* cells are one of the smallest cell size mutants in this system (90). Thus, Cdc20p and Cdh1p in *C. albicans* are important for mitosis and morphogenesis, and may have some novel functions and mechanisms of action. These results further underscore differences in the mitotic machinery in *C. albicans* relative to other systems, including mammals.

Thus, some key factors controlling mitosis have been identified in *C. albicans*, but a comprehensive picture of the mitotic regulatory networks and how arresting mitosis may lead to changes in bud growth pattern is lacking. Specifically, the mechanisms of action of Cdc20p and Cdh1p remain unclear, particularly in the context of governing the metaphase-to-anaphase

transition, due to the absence of a securin homologue and lack of characterization of other putative regulators, including separase, in this organism.

1.5 Objectives

The primary aim of this thesis is to determine the mechanisms of action of Cdc20p, and thereby gain insight on the regulation of mitosis and the metaphase-to-anaphase transition in *C. albicans*. We hypothesize that Cdc20p may function in part through targeting a divergent yet functional homologue of a securin, and that this may be identified through determining the interacting proteins of the conserved separase Esp1p. *C. albicans* contains a homologue of Esp1p, but to date it has not been fully characterized. Our specific objectives include: 1) Characterize the Esp1p homologue in *C. albicans* and determine whether it plays a conserved role in chromosome separation; 2) Identify the interacting factors of Esp1p in order to gain insight on its mechanisms of action and identify a putative Securin homologue; and 3) Validate the physical interaction between Esp1p and novel proteins, and further characterize these proteins to determine whether any may function as a securin.

2.0. Materials and Methods

2.1 Strains, oligonucleotides, and plasmids

Strains, oligonucleotides and plasmids used in this study are listed in Tables 1, 2 and 3, respectively.

Table 1: *Candida albicans* strains used in this study

Strain	Genotype	Source
BWP17	<i>ura3::imm434/ura3::imm434, his1::hisG/his1::hisG arg4::hisG/arg4::hisG</i>	Wilson <i>et al.</i> , 1999
BH440	BWP17 (pBS-CaHIS1, pBS-CaURA3)	Hussein <i>et al.</i> , 2011
AG153	<i>MET3::CDC20-ARG4/cdc20::URA3, CLB2-HA-HIS1</i>	Glory, 2014
AG636	<i>ESP1/ESP1-TAP-URA3</i>	Glory, 2014
HCCA1	<i>cdc20::URA3/CDC20</i>	Chou <i>et al.</i> , 2011
HCCA109	<i>cdc20::URA3/MET3::CDC20-HIS1</i>	Chou <i>et al.</i> , 2011
HCCA118	<i>MET3::CDC5-HIS1/cdc5::URA3</i>	Chou <i>et al.</i> , 2011
SS1, 5	<i>esp1::HIS1/ESP1-TAP-URA3</i>	This study
SS2-4	<i>ESP1/ESP1-TAP-ARG4, cdc20::URA3/MET3::CDC20-HIS1</i>	This study
SS10-15	<i>orf19.955::URA3/ORF19.955</i>	This study
SS16-19	<i>ESP1/ESP1-HA-URA3</i>	This study
SS20, 21	<i>esp1::URA3/ESP1</i>	This study

SS22	<i>orf19.955::URA3/ORF19.955-MYC-HIS1</i>	This study
SS23-28	<i>orf19.955::URA3/MET3::ORF19.955-HIS1</i>	This study
SS29, 30	<i>ORF19.955/ORF19.955-MYC-HIS1, ESP1/ESP1-HA-URA3</i>	This study
SS31-36	<i>esp1::URA3/MET3::ESP1-HIS1</i>	This study
SS37	<i>TUB2-GFP-ARG4/TUB2, esp1::URA3/MET3::ESP1-HIS1</i>	This study
SS38	<i>TUB2-GFP-ARG4/TUB2, orf19.955::URA3/MET3::ORF19.955-HIS1</i>	This study
GRACE Strain	<i>orf19.955::URA3/TET::ORF19.955</i>	Roemer <i>et al.</i> , 2003
GRACE Strain	<i>esp1::URA3/TET::ESP1</i>	Roemer <i>et al.</i> , 2003

Table 2: Oligonucleotides used in this study

Oligonucleotide	Sequence in 5'- 3' Direction	Source
SS1F	GTT ATT GCT AAA AGA CAA GCT TTG GAA CGT	This Study
SS1R	GC TGA ATC AAA CTG TAA TGA AAT ACA GAT	This Study
SS2F	TAA TGT TGG CAT TTT CTG ATG GAA TTG TTG	This Study
SS2R	TGC ACA GTA TGG ATT GCT AGT CCT AGA GAA	This Study
SS3F	ATC TGT ATT TCA TTA CAG TTT GAT TCA GCC/TAT AGG GCG AAT TGG AGC TC	This Study
SS3R	CAA CAA TTC CAT CAG AAA ATG CCA ACA TTA/GAC GGT ATC GAT AAG CTT GA	This Study
SS10F	GGA ACC ATT AAG AGA GCA TA	This Study
SS10R	TTG CTA GTT TGG GTG CTA AT	This Study
SS18F	AAT ACC AAT TAT TGA AGG TAT TGA TGA GGA AAT TGG TTT AAC TAG CGA TGA TTT GGA TAA TTT ATT AGG AGG TGG TGG TCG GAT CCC CGG GTT AAT TAA	This Study
SS18R	AGT ATG AAC AAC AGG GGT ACG AGC AAT CAT GTG CCC AAC AAT AAT ACC ATG TAA ATA CTC AAT ATA TGA AGA ATT CCG GAA TAT TTA TGA GAA AC	This Study
SS19F	GAA CCA TTA AGA GAG CAT AAA TTG GGT AAG	This Study
SS19R	AAC TCA TTG TAA GCT AAT GAA GGG AGT AA	This Study
SS20F	ATG GAT AAC TCG TTG GAT CAA AAA CTA TTG	This Study
SS20R	TGG AAA CAT ATT GGG CTA TCC ATT GTA AAA	This Study
SS21F	TTA CTC CCT TCA TTA GCT TAC AAT TGA GTT	This Study

	GGA TCC TGG AGG ATG AGG AG	
SS21R	CAA TAG TTT TTG ATC CAA CGA GTT ATC CAT CAT GTT TTC TGG GGA GGG TA	This Study
SS25F	GGG GGC TTC ATT ATC TAT TT	This Study
SS25R	GAG AAT CCG ATC AAT TTC CA	This Study
SS26F	CGA TGG AGA CAT AAG TTT CT	This Study
SS27F	GTC GAC CAC CAA GTG GTG ACA CTT TAA ATG	This Study
SS27R	TTC CTC ATT TCT CCT TTT AGT GGT TCA ACC	This Study
SS28F	ATG TCA AGT CAT ATA TTC AAA GAT ATT CAA	This Study
SS28R	TTG AGT TGG CTT AGT TAA TGA ATC CGT AAA	This Study
SS29F	GGT TGA ACC ACT AAA AGG AGA AAT GAG GAA GGA TCC TGG AGG ATG AGG AG	This Study
SS29R	TTG AAT ATC TTT GAA TAT ATG ACT TGA CAT CAT GTT TTC TGG GGA GGG TA	This Study
AG3R	GCG GTT GGC TGC TGA GAC GG	Glory, 2014
AG 67F	TGC TGG TGA TGA GAC CTT ACG ATT TTG GAA TGT ATT TGA AAA AAA TAG GCA TAA CGA ATC ACC TG CTT CGG TTT TGT TAG GAG CAT TTC TGC AGT TGC GCG GTC GAC GGA TCC CCG GGTT	Glory, 2014
AG 67R	ACT TGA ATA CAT GCA GAT ACT AGT TAC AGA TGA TTT GGG AAA TGT GAC ACT TTC ACT TGA ACG ACT TGA AAA TTG GTG CTC ACA AAA CAA GGT TGT TCC CTC GAT GAA TTC GAG CTC GTT	Glory, 2014
AG 68F	CTA TAA TAC CCC TAC AGT CT	Glory, 2014
AG68R	CAA GGA AGT CTT ATC GTA CG	Glory, 2014

AG 103F	GGA TTT GAC TAA TTG TGT TGT TCA AAG TCG AAG TAA ATG TAC TTT GAA ATA CTT GAA TGG ATC AGC ACC TGT GGT TTA TGG TCT ACC AAT GTA TTT AAA AGG TCG ACG GAT CCC CGG GTT	Glory, 2014
AG 103R	AGT GAT TGG GTG CAA AAT TTG TTC ATA ACA AAC CAA ACA ATA CAA AAT CAA GAT CCA AAT TAT GCT CTT TTT CTT ATT ATT AAA ATA TAT AAA CTT ATA TTC GAT GAA TTC GAG CTC GTT	Glory, 2014
CB 135F	CAA TAC CAA GAA GCT AGT ATT GAT GAA GAA GAA TTA GAA TAT GCC GAT GAA ATC CCA TTA GAA GAT GCC GCC ATG GAA GGT GCT GGC GCA GGT GCT TC	Bachewich <i>et al.</i> 2003
CB 135R	ATA TTG TGC CGA TAA ATA ATA AAA GGG TAT AAT CAT TAA CTA AAC CAA AAA AAA CCA TAA TTA TAT TAG AAG TGA ACA AAG ATA TCA TCG ATG AAT TCG A	Bachewich <i>et al.</i> 2003
caURA3F	GGT AAT ACC GTG AAG AAA CA	Glory, 2014
caHIS1F	CCT GCA GCT GAT ATC CCA GT	Glory, 2014
caHIS1R	ACT GGG ATA TCA GCT GCA GG	Glory, 2014
caARGF	ACT ATG GAT ATG TTG GCT ACT	Glory, 2014
caARGR	AGT AGC CAA CAT ATC CAT AGT	Glory, 2014

Table 3: Plasmids used throughout the course of this study

Plasmid	Description	Source
pBS-Ca <i>URA3</i>	pBluescript-Ca <i>URA3</i>	A.J.P Brown
pBS-Ca <i>HIS1</i>	pBluescript-Ca <i>HIS1</i>	C. Bachewich
pFA-TAP-Ca <i>ARG4</i>	pFunctional Analysis Cassette-TAP- <i>ARG4</i>	Lavoie <i>et al.</i> , 2008
pFA-TAP-Ca <i>HIS1</i>	pFunctional Analysis Cassette-TAP- <i>HIS1</i>	Lavoie <i>et al.</i> , 2008
pFA-HA-Ca <i>URA3</i>	pFunctional Analysis Cassette-HA- <i>URA3</i>	Lavoie. <i>et al.</i> , 2008
pMG2093	pFA6a-13myc-TRP1 ligated into pFA-GFP- <i>HIS1</i>	Bensen, E. <i>et al.</i> , 2005
pFA- <i>MET3</i> -Ca <i>HIS1</i>	<i>MET3</i> promotor-Ca <i>HIS1</i>	Gola, S. <i>et al.</i> , 2003

2.2 Medium and growth conditions

Most strains were grown at 30°C in YPD medium containing 1% yeast extract, 2% peptone and 2% glucose. Conditional strains were grown in synthetic complete minimal medium (MM) containing 0.67% of yeast nitrogen base, 2% dextrose and amino acid supplements with or without the addition of 2.5 mM methionine and 0.5 mM cysteine for repression and induction of the *MET3* promoter, respectively (91). MM media was supplemented with 100 mg/L uridine, histidine or arginine to allow for growth of *URA3*⁺, *HIS1*⁺ or *ARG4*⁺ auxotrophs with the exception of selective conditions. For growth assays and collection of cells for protein extraction, strains were incubated overnight in medium at 30°C, diluted into fresh medium to an O.D_{600nm} of 0.1, and incubated until the O.D_{600nm} reached 0.8-1.0 or for specific time points.

2.3 Strain Construction

2.3.1 *esp1::HIS1/ESP1-TAP-URA3*

In order to tag the C-terminus of *ESP1* with the TAP epitope (Protein A and Calmodulin-binding protein separated by a tobacco etch virus (TEV) protease cleavage site) (92), the 3.0 kb *TAP-URA3* cassette was amplified from plasmid pFA-TAP-*URA3* (92) with oligonucleotides

AG103F and AG103R, which contained 100bp of homology to either side of the *STOP* codon of *ESPI* and 20 bp homology to the plasmid. The PCR reaction mixture consisted of 0.4 mM dNTPs, 100 ng of DNA template, 0.6 μ M oligonucleotides, 10X Buffer and 3.75U of Expand Long Template Polymerase (Roche). The reaction conditions were as follows: 94°C for 4 min, followed by 25 cycles of 94°C for 1 min, 40°C for 1 min, 68°C for 2 min, 59 sec, 68°C followed by a 7 min extension, and storage at 4°C. The PCR product was cleaned (Omega PCR purification kit) and 8.0 μ g of the product was transformed into strain BWP17, resulting in strain AG636.

Next, the second copy of *ESPI* was knocked out using a two-step PCR reaction. First, a 500 bp fragment corresponding to the 5' flank of *ESPI*, located just before the START codon, was PCR amplified from gDNA with oligonucleotides SS1F and SS1R. The thermocycling conditions included: 94°C for 3 min, followed by 25 cycles of 94°C for 30 sec, 46°C for 30 sec, 68°C for 30 sec, and a final elongation at 68°C for 7 min. The reaction mix was composed of a final concentration of 0.6 μ M of oligonucleotides, 0.4 mM dNTPs, 100 ng of gDNA as template, 3.75U of Expand Long Template Polymerase, and 1X Buffer 3. A 545 bp fragment corresponding to the 3' flank of *ESPI*, starting 545 bp after the stop codon, was similarly amplified using oligonucleotides SS2F and SS2R and the following thermo-cycling conditions: 94°C for 3 min, followed by 25 cycles of 94°C for 30 sec, 46°C for 30 sec, 68°C for 35 sec, and a final elongation at 68°C for 7 min. The reaction mix composition was similar to that used for the 5' flank. In order to amplify the 1348 bp *HIS1* cassette fragment from plasmid pBS-Ca*HIS1*, oligonucleotides SS3F and SS3R were used, which contain homology to the plasmid plus additional 30 bp sequences bearing homology to oligonucleotides SS1R and SS2F, respectively. The following thermocycling conditions were used: 94°C for 3 min, followed by 25 cycles of 94°C for 30 sec, 40°C for 30 sec, 68°C for 1 min 25 sec, and a final elongation at 68°C for 7 min. The reaction mix was composed of a final concentration of 0.6 μ M of oligonucleotides, 0.4 mM dNTPs, 100 ng of pBS-Ca*HIS1* as template, 3.75U of Expand Long Template Polymerase, and 1X Buffer 3. In order to create the final construct for transformation, oligonucleotides SS1F and SS2R were used at a concentration of 0.6 μ M with a 1:2:1 (50ng:100ng:50ng) amount of 5' fragment, marker and 3' fragment, in a reaction including 0.4 mM of dNTPs, 3.75U of Expand

Long Template Polymerase, and 1X Buffer 3. The following thermocycling conditions were used: 94°C for 3 min, followed by 25 cycles of 94°C for 30 sec, 50°C for 30 sec, and 68°C for 2 min 24 sec, and a final elongation at 68°C for 7 min. The cleaned construct was transformed into strain AG636 (*ESP1/ESP1-TAP-URA3*), resulting in strains SS1 and SS5 (*esp1::HIS1/ESP1-TAP-URA3*).

2.3.2 *ESP1/ESP1-TAP-ARG4, cdc20::URA3/MET3::CDC20-HIS1*

In order to TAP tag *ESP1* in a strain carrying a single copy of *CDC20* under control of the *MET3* promoter, strain HCCA109 (*cdc20::URA3/MET3::CDC20-HIS1*), the strategy described above was followed with the exception of using plasmid pFA-TAP-ARG4 with oligonucleotides AG103F and AG103R. Purified product (7.1 µg) was transformed into strain HCCA109, resulting in strains SS2, SS3 and SS4 (*ESP1/ESP1-TAP-ARG4, cdc20::URA3/MET3::CDC20-HIS1*).

2.3.3 *ESP1/ESP1-HA-URA3*

In order to tag the C-terminus of *ESP1* with the hemagglutinin (HA) epitope (92), the 1.9 kb *HA-URA3* cassette was amplified from plasmid pFA-HA-URA3 (92) with oligonucleotides AG103F and AG103R, which contained 100 bp of homology to either side of the *STOP* codon of *ESP1* and 20 bp homology to the plasmid. The PCR reaction mixture consisted of 0.4 mM dNTPs, 100 ng worth of the DNA template, 0.6 µM oligonucleotides, 10X Buffer and 3.75U of Expand Long Template Polymerase (Roche). The reaction conditions were as follows: 94°C for 4 min, followed by 25 cycles of 94°C for 1 min, 40°C for 1 min, 68°C for 1 min 57 sec, 68°C followed by a 7 min extension, and storage at 4°C. The PCR product was cleaned and 7.1 µg was transformed into strain BWP17, resulting in strains SS16, SS17, SS18 and SS19 (*ESP1/ESP1-HA-URA3*).

2.3.4 *esp1::URA3/MET3::ESP1-HIS1*

In order to construct a strain carrying a single copy of *ESP1* under control of the *MET3* promoter, one copy of *ESP1* was deleted from strain BWP17 using a two-step PCR reaction as

described previously, with the exception of utilizing pBS-Ca*URA3* in place of pBsCa*HIS1*. In order to amplify the 1481 bp *URA3* cassette fragment from plasmid pBS-Ca*URA3*, oligonucleotides SS3F and SS3R were used, which contain homology to the plasmid plus additional 30 bp sequences bearing homology to oligonucleotides SS1R and SS2F, respectively. The following thermocycling conditions were used: 94°C for 3 min, followed by 25 cycles of 94°C for 30 sec, 40°C for 30 sec, 68°C for 1 min 28 sec, and a final elongation at 68°C for 7 min. The reaction mix was composed of a final concentration of 0.6 μM of oligonucleotides, 0.4 mM dNTPs, 100 ng of pBS-Ca*HIS1* as template, 3.75U of Expand Long Template Polymerase, and 1X Buffer 3. In order to create the 2.5kb final construct for transformation, oligonucleotides SS1F and SS2R were used at a concentration of 0.6 μM with a 1:2:1 (50ng:100ng:50ng) amount of these three PCR fragments (5' fragment, pBS-Ca*URA3*, and 3' fragment), in a reaction including 0.4 mM of dNTPs, 3.75U of Expand Long Template Polymerase, and 1X Buffer 3. The following thermocycling conditions were used: 94°C for 3 min, followed by 25 cycles of 94°C for 30 sec, 50°C for 30 sec, and 68°C for 2 min 32 sec, and a final elongation at 68°C for 7 min. The cleaned construct was transformed into strain BWP17 resulting in strains SS20 and SS21 (*esp1::URA3/ESPI*).

Next, the remaining copy of *ESPI* was placed under the control of the *MET3* promotor using a two-step PCR reaction. First, a 522 bp fragment corresponding to the 5' flank of *ESPI*, located just before the *START* codon, was PCR amplified from gDNA with oligonucleotides SS19F and SS19R. The thermocycling conditions included: 94°C for 3 min, followed by 25 cycles of 94°C for 30 sec, 46°C for 30 sec, 68°C for 31 sec, and a final elongation at 68°C for 7 min. The reaction mix was composed of a final concentration of 0.6 μM of oligonucleotides, 0.4 mM dNTPs, 100 ng of gDNA as template, 3.75U of Expand Long Template Polymerase, and 1X Buffer 3. A 549 bp fragment corresponding to 549bp downstream of the *START* codon, was similarly amplified using oligonucleotides SS20F and SS20R and the following thermo-cycling conditions: 94°C for 3 min, followed by 25 cycles of 94°C for 30 sec, 46°C for 30 sec, 68°C for 33 sec, and a final elongation at 68°C for 7 min. The reaction mix composition was similar to that used for the 5' flank. In order to amplify the 2776 bp *HIS1-MET3* cassette fragment from plasmid pFA-*MET*-Ca*HIS1*, oligonucleotides SS21F and SS21R were used. The following thermocycling

conditions were used: 94°C for 3 min, followed by 25 cycles of 94°C for 30 sec, 41°C for 30 sec, 68°C for 2 min 47 sec, and a final elongation at 68°C for 7 min. The reaction mix was composed of a final concentration of 0.6 µM of oligonucleotides, 0.4 mM dNTPs, 100 ng of pFA-MET-CaHIS1 as template, 3.75U of Expand Long Template Polymerase, and 1X Buffer 3. In order to create the final construct for transformation, oligonucleotides SS19F and SS20R were used at a concentration of 0.6 µM with a 1:2:1 (50ng:100ng:50ng) amount of these three PCR fragments as previously described, in a reaction including 0.4 mM of dNTPs, 3.75U of Expand Long Template Polymerase, and 1X Buffer 3. The following thermocycling conditions were used: 94°C for 3 min, followed by 25 cycles of 94°C for 30 sec, 46°C for 30 sec, and 68°C for 3 min 51 sec, and a final elongation at 68°C for 7 min. The cleaned construct was transformed into strain SS20 (*esp1::URA3/ESP1*), resulting in strains SS31 to SS35 (*esp1::URA3/MET3::ESP1-HIS1*).

2.3.5 *orf19.955::URA3/ORF19.955-MYC-HIS1*

In order to tag the C-terminus of *ORF19.955* with the MYC epitope, one copy of *ORF19.955* was first deleted using a two-step PCR reaction. First, a 526 bp fragment corresponding to the 5' flank of *ORF19.955*, located just before the *START* codon, was PCR amplified from gDNA with oligonucleotides SS22F and SS22R. The thermocycling conditions included: 94°C for 3 min, followed by 25 cycles of 94°C for 30 sec, 46°C for 30 sec, 68°C for 32 sec, and a final elongation at 68°C for 7 min. The reaction mix was composed of a final concentration of 0.6 µM of oligonucleotides, 0.4 mM dNTPs, 100 ng of gDNA as template, 3.75U of Expand Long Template Polymerase, and 1X Buffer 3. A 529 bp fragment corresponding to the 3' flank of *ORF19.955*, starting 529 bp after the *STOP* codon, was similarly amplified using oligonucleotides SS23F and SS23R and the following thermo-cycling conditions: 94°C for 3 min, followed by 25 cycles of 94°C for 30 sec, 45°C for 30 sec, 68°C for 35 sec, and a final elongation at 68°C for 7 min. The reaction mix composition was similar to that used for the 5' flank. In order to amplify the 1481 bp *URA3* cassette fragment from plasmid pBS-CaURA3, oligonucleotides SS24F and SS24R were used, which contain homology to the plasmid plus additional 30 bp sequences bearing homology to oligonucleotides SS22F and SS23R, respectively. The following thermocycling conditions were used: 94°C for 3 min, followed by 25

cycles of 94°C for 30 sec, 40°C for 30 sec, 68°C for 1 min 28 sec, and a final elongation at 68°C for 7 min. The reaction mix was composed of a final concentration of 0.6 μM of oligonucleotides, 0.4 mM dNTPs, 100 ng of pBS-Ca*URA3* as template, 3.75U of Expand Long Template Polymerase, and 1X Buffer 3. In order to create the 2.5kb final construct for transformation, oligonucleotides SS22F and SS23R were used at a concentration of 0.6 μM with a 1:2:1 (50ng:100ng:50ng) amount of these three PCR fragments, in a reaction including 0.4 mM of dNTPs, 3.75U of Expand Long Template Polymerase, and 1X Buffer 3. The following thermocycling conditions were used: 94°C for 3 min, followed by 25 cycles of 94°C for 30 sec, 45°C for 30 sec, and 68°C for 2 min 32 sec, and a final elongation at 68°C for 7 min. The cleaned construct was transformed into strain BWP17 resulting in strains SS10 to SS15 (*orf19.955::URA3/ORF19.955*).

Next, the 3.8 kb *MYC-HIS1* cassette was amplified from plasmid pMG2093 (83) with oligonucleotides SS18F and SS18R, which contained 100bp of homology to either side of the *STOP* codon of *ORF19.955* and 20 bp homology to the plasmid. The PCR reaction mixture consisted of 0.4 mM dNTPs, 100 ng worth of the DNA template, 0.6μM oligonucleotides, 10X Buffer and 3.75U of Expand Long Template Polymerase (Roche). The reaction conditions were as follows: 94°C for 4 min, followed by 25 cycles of 94°C for 1 min., 41°C for 1 min., 68°C for 3 min, 50 sec, 68°C followed by a 7 min extension, and storage at 4°C. The PCR product was cleaned and 7.2 μg was transformed into strain SS10 (*orf19.955::URA3/ORF19.955*), resulting in strain SS22 (*orf19.955::URA3/ORF19.955-MYC-HIS1*).

2.3.6 *ORF19.955/ORF19.955-MYC-HIS1, ESP1/ESP1-HA-URA3*

The strain was created as described above with the exception of transforming 7.2μg product into strain SS17 (*ESP1/ESP1-HA-URA3*), resulting in strains SS29 and SS30 (*ORF19.955/ORF19.955-MYC-HIS1, ESP1/ESP1-HA-URA3*).

2.3.7 *orf19.955::URA3/MET3::orf19.955-HIS1*

In order to construct a strain carrying a single copy of *ORF19.955* under control of the *MET3* promoter, a two-step PCR reaction was conducted. First, a 472 bp fragment corresponding

to the 5' flank of *ORF19.955*, located just before the *START* codon, was PCR amplified from gDNA with oligonucleotides SS27F and SS27R. The thermocycling conditions included: 94°C for 3 min, followed by 25 cycles of 94°C for 30 sec, 49°C for 30 sec, 68°C for 28 sec, and a final elongation at 68°C for 7 min. The reaction mix was composed of a final concentration of 0.6 µM of oligonucleotides, 0.4 mM dNTPs, 100 ng of gDNA as template, 3.75U of Expand Long Template Polymerase, and 1X Buffer 3. A 539 bp fragment corresponding to 539bp downstream of the *START* codon, was similarly amplified using oligonucleotides SS28F and SS28R and the following thermocycling conditions: 94°C for 3 min, followed by 25 cycles of 94°C for 30 sec, 42°C for 30 sec, 68°C for 32 sec, and a final elongation at 68°C for 7 min. The reaction mix composition was similar to that used for the 5' flank. In order to amplify the 2776 bp *HIS1-MET3* cassette fragment from plasmid pFA-*MET3*-Ca*HIS1*, oligonucleotides SS29F and SS29R were used. The following thermocycling conditions were used: 94°C for 3 min, followed by 25 cycles of 94°C for 30 sec, 41°C for 30 sec, 68°C for 2 min 47 sec, and a final elongation at 68°C for 7 min. The reaction mix was composed of a final concentration of 0.6 µM of oligonucleotides, 0.4 mM dNTPs, 100 ng of pFA-*MET3*-Ca*HIS1* as template, 3.75U of Expand Long Template Polymerase, and 1X Buffer 3. In order to create the final construct for transformation, oligonucleotides SS27F and SS28R were used at a concentration of 0.6 µM with a 1:2:1 (50ng:100ng:50ng) amount of these three PCR fragments, as previously described, in a reaction including 0.4 mM of dNTPs, 3.75U of Expand Long Template Polymerase, and 1X Buffer 3. The following thermocycling conditions were used: 94°C for 3 min, followed by 25 cycles of 94°C for 30 sec, 46°C for 30 sec, and 68°C for 3 min 47 sec, and a final elongation at 68°C for 7 min. The cleaned construct was transformed into strain SS14 (*orf19.955::URA3/ORF19.955*), resulting in strains SS23 to SS28 (*orf19.955::URA3/MET3::ORF19.955-HIS1*).

2.3.8 *TUB2-GFP-ARG4/TUB2, orf19.955::URA3/MET3::ORF19.955-HIS1*

In order to tag the C-terminus of *TUB2* with the green fluorescent protein (GFP) epitope (100) a 3.2 kb *GFP-ARG4* cassette was amplified from plasmid pFA-GFP-ARG4 (100) with oligonucleotides CB135F and CB135R, which contained 100bp homology to either side of the *STOP* codon of *ORF19.955* and 20 bp homology to the plasmid. The PCR reaction mixture

consisted of 0.4mM dNTPs, 100ng of DNA template, 0.6µM oligonucleotides, 10X Buffer and 3.75U of Expand Long Template Polymerase. The reaction conditions were as follows: 94°C for 4 min, followed by 25 cycles of 94°C for 1 min, 36°C for 1 min, 68°C for 3 min 8 sec, 68°C followed by a 7 min extension, and storage at 4°C. The PCR product was cleaned and 7.0µg was transformed into strain SS25 (*orf19.955::URA3/MET3::ORF19.955-HIS1*), resulting in strain SS38 (*TUB2-GFP-ARG4/TUB2, orf19.955::URA3/MET3::ORF19.955-HIS1*).

2.3.9 *TUB2-GFP-ARG4/TUB2, esp1::URA3/MET3::ESP1-HIS1*

In order to tag the C-terminus of *TUB2* with the green fluorescent protein (GFP) epitope (100) a 3.2 kb *GFP-ARG4* cassette was amplified from plasmid pFA-GFP-ARG4 (100) with oligonucleotides CB135F and CB135R, which contained 100bp homology to either side of the *STOP* codon of *ORF19.955* and 20 bp homology to the plasmid. The PCR reaction mixture consisted of 0.4mM dNTPs, 100ng of DNA template, 0.6µM oligonucleotides, 10X Buffer and 3.75U of Expand Long Template Polymerase. The reaction conditions were as follows: 94°C for 4 min, followed by 25 cycles of 94°C for 1 min, 36°C for 1 min, 68°C for 3 min, 08 sec, 68°C followed by a 7 min extension, and storage at 4°C. The PCR product was cleaned and 7.3 µg was transformed into strain SS35 (*esp1::URA3/MET3::ESP1-HIS1*), resulting in strain SS37 (*TUB2-GFP-ARG4/TUB2, esp1::URA3/MET3::ESP1-HIS1*).

2.4 Transformation of *C. albicans*

C. albicans cells were transformed using a lithium acetate one-step transformation protocol (93, 94, 95). To prepare the One-Step-Buffer (OSB), 25 µl of salmon sperm DNA (10 mg/ml stock, Invitrogen) was first boiled for 10 min, cooled on ice for 5 min, then added to 200 µl of sterilized 1 M Lithium Acetate. Subsequently, 25 µl of 4.0 M DTT was added, followed by 800 µl of 50% PEG 4000 (Sigma). The mixture was vortexed for 1 min, and 100 µl of OSB solution was combined with 200-300 µl of washed, stationary phase cells that had been centrifuged from culture. Approximately 5-7 µg of transforming DNA in a maximum volume of 10 µl was added. The reaction mix was vortexed for 1 min and incubated overnight at 30°C. The following day, the mixture was heat-shocked for 1 h at 43°C and plated on selective solid

medium. After 2-3 days, transformants were streaked to single colony three times on fresh selective medium prior to screening. For increased transformation efficiency in the conditional strains, cells were grown overnight in minimal media (MM) lacking methionine and cysteine, and then transferred into rich YPD medium for 2 h prior to collection.

2.5: Genomic DNA (gDNA) extraction

In order to extract gDNA, (96) cells were inoculated in 5.0 mls of YPD medium or minimal media (MM) lacking methionine and cysteine, incubated at 30°C overnight and then centrifuged for 5 min at 3000 rpm. The supernatant was discarded and the pellet was washed once with 0.5 ml sterile distilled water. The pellet was then re-suspended in 1.0 ml of sorbitol buffer (1M sorbitol, 0.1M EDTA) mixed with 10.0 µl of lyticase (10U/µl) (Sigma) and 2.0 µl of 4.0 M DTT. The mixture was incubated at 37°C for 1.5 h, centrifuged for 1 min at 13 500 rpm, and the supernatant was discarded. The pellet was re-suspended in 200 µl Tris-EDTA solution (50 mM Tris, 20 mM EDTA), 1% final SDS and incubated at 65°C for 30 min. After this incubation, 100 µl of 5.0 M potassium acetate (KAc) was added and the solution was gently mixed. The mixture was incubated on ice for 40 min, centrifuged for 10 min at 13 500 rpm, and the supernatant transferred to new Eppendorf tubes. An equal volume of 100% isopropanol was added to the supernatant, and after mixing for 1 min, the DNA pellet was collected by centrifuging at 13 500 rpm for 1 min. The DNA pellet was then washed with 70% ethanol, and re-suspended into 100 µl of TE buffer (1 mM EDTA, 10 mM Tris-HCl pH 8.0) with 2 µl of RNaseA (10 mg/ml, Molecular Bioproducts). DNA was incubated at 37°C for 30 min and stored at 4°C. Genomic DNA was quantified with a fluorometer (Hoefer DQ300) using Hoechst Dye (Invitrogen).

2.6 PCR Screening

PCR screening reaction mixes were composed of 0.6 µM of oligonucleotides, 0.4 mM of dNTPs, 100 ng of gDNA as template, 3 mM of MgCl₂, 1X Taq Buffer with (NH₄)₂SO₄ and 1U Taq DNA Polymerase (Fermentas). In order to confirm strains SS1 and SS5 (*esp1::HIS1/ESP1-TAP-URA3*), oligonucleotide SS10F, which is located 593 bp upstream of the *START* codon of

ESP1 and CaHISR, which is nested in the *HIS1* marker of plasmid pBS-Ca*HIS1*, were utilized to amplify a 1130 bp DNA fragment. The reaction conditions were as follows: 95°C for 3min, 30 cycles of 95°C for 30 sec, 43°C for 30 sec, 72°C for 1 min 8 sec, followed by a 7 min extension at 72 °C and storage at 4°C. Strains SS2, SS3 and SS4 (*ESP1/ESP1-TAP-ARG4, cdc20::URA3/MET3::CDC20-HIS1*) were confirmed using oligonucleotides AG104F, which lies 594bp upstream of the STOP codon of *ESP1*, and AG3R, which is nested in the *TAP* sequence of pFA-TAP-ARG in order to amplify a fragment of 675bp. The PCR conditions were as follows: 95°C for 3 min, 30 cycles of 95°C for 30 sec, 40°C for 30 sec, 72°C for 41 sec, followed by a 7 min extension at 72 °C and storage at 4°C. In order to confirm strains SS16 to SS19 (*ESP1-HA-URA3/ESP1*), oligonucleotides AG104R, which lies 385bp downstream of the *STOP* codon of *ESP1*, and CaURA3R, which is nested in the *URA3* marker of plasmid pFA-HA-URA3, were used. The PCR conditions were as follows: 95°C for 3 minutes, 30 cycles of 95°C for 30 seconds, 38°C for 30 seconds, 72°C for 1 min 2 sec, followed by a 7 min extension at 72 °C and storage at 4°C. In order to confirm strains SS31 to SS36 (*esp1::URA3/MET3::ESP1-HIS1*) oligonucleotides SS10F and CaURA3R amplified a 1802 bp band using the following conditions: 95°C for 3 min, 30 cycles of 95°C for 30 sec, 36°C for 30 sec, 72°C for 1 min 48 seconds, followed by a 7 min extension at 72°C and storage at 4°C. Next, the *MET3::ESP1* integration was confirmed using oligonucleotides SS26F, which lies 623 bp upstream of the *ESP1* START codon, and CaHIS1R, were used with the following conditions: 95°C for 3 min, 30 cycles of 95°C for 30 sec, 39°C for 30 sec, 72°C for 34 sec, followed by a 7 min extension at 72 °C and storage at 4°C.

In order to confirm strains SS22 (*orf19.955::URA3/orf19.955-MYC-HIS1*), oligonucleotides SS25F, which lies 720 bp upstream of the *START* codon of *ORF19.955*, and CaURA3R, which is nested in the *URA3* marker of plasmid pBS-CaURA3, were used to amplify a 1028 bp DNA fragment. The following PCR conditions were used: 95°C for 3 min, 30 cycles of 95°C for 30 sec, 38°C for 30 sec, 72°C for 1 min 37 sec, followed by a 7 min extension at 72 °C and storage at 4°C. Next, the *MYC-HIS1* integration was confirmed with oligonucleotides SS25R and CaHIS1F, which lie 672bp downstream of the *STOP* codon of *ORF19.955*, and nested in CaHIS1F, respectively. The oligonucleotides amplify a 1341bp DNA fragment. The following

PCR conditions were used: 95°C for 3 min, 30 cycles of 95°C for 30 sec, 38°C for 30 sec, 72°C for 1 min 20 sec, followed by a 7 min extension at 72 °C and storage at 4°C. The same oligos were used in part to confirm strains SS29 and SS30 (*ORF19.955/orf19.955-MYC-HIS1*, *ESP1/ESP1-HA-URA3*). In order to confirm strains SS23 to SS28 (*orf19.955::URA3/MET3::orf19.955-HIS1*), oligonucleotides SS25F and CaHISR were used to amplify a 1141bp DNA fragment. The following PCR conditions were used: 95°C for 3 min, 30 cycles of 95°C for 30 sec, 38°C for 30 sec, 72°C for 1 min 8 seconds, followed by a 7 min extension at 72 °C and storage at 4°C. Oligonucleotides SS25F and CaURA3R were also used as described above to ensure the proper integration of *orf19.955::URA3*.

2.7 Protein Extraction

2.7.1 Bead-beating method

In order to extract protein using the bead-beating method (83) cells were first inoculated in 2.0 ml of either YPD or minimal inducing medium without methionine and cysteine (-MC) and incubated overnight at 30°C. The culture was then diluted into 20 ml of YPD or -MC medium to an OD_{600nm} of 0.1, and incubated at 30°C until the culture reached an OD_{600nm} of 0.8-1.0. After centrifuging for 5 min at 3000 rpm and removing the supernatant, the pellet was placed in dry ice and stored at -80°C. The pellets were thawed on ice, re-suspended in 50 µl of RIPA buffer (10 mM sodium phosphate, 1% Triton X-100, 0.1% SDS, 10 mM EDTA, 150 mM NaCl, pH 7.0, 5 µg/ml Leupeptin, 5 µg/ml Aprotinin and 1mM AEBSF) and 200 µl of glass beads (Sigma, 425-600) were added. Cells were homogenized in a bead-beater (Biospec, mini bead-beater-8) for 30 seconds followed by 3 min incubation on ice five times. An additional 200 µl of RIPA buffer was added, and the extracts were centrifuged at 13 500 rpm for 10 min at 4°C. The supernatant was centrifuged at 13 500 rpm for 1 hour at 4°C, transferred to a new Eppendorf tube, and frozen at -80°C.

2.7.2 Lyophilization method

Protein was alternatively extracted using lyophilization (97). Briefly, cell pellets were lyophilized in a freeze dryer for 24-48 hours (ThermoSavant, Modulyo D), ground to a fine powder using a mortar and pestle, and extracted with HK buffer (0.08g dry material per 1.0 ml of

HK buffer (25 mM TRIS pH7.5, 0.5% NP40, 300 mM NaCl, 5 mM EDTA pH 8.0, 15 mM EGTA pH8.0, 60 mM Beta Gly.PO₄, 500 μM Na Vanadate, 10 mM Na Fluoride, 15 mM pNPP, 1 μg/ml Pepsatin A, 10 μg/ml Leupeptin, 10 μg/ml Trypsin ChymoT inhibitor, 10 μg/ml Aprotinin, 10 μg/ml TPCK, 2 mM TAME, 5.0 mM Benzamidine, 250 μg/ml PMSF, and 1 mM DTT). Samples were vortexed for 10 sec, placed on ice for 3 min, a total of 5 trials. Extracts were then centrifuged at 13 500 rpm for 10 min at 4°C. The supernatant was centrifuged for 1 h at 13 500 rpm at 4°C, and protein concentration was measured using the Bradford assay (Bio-Rad).

2.8 Western Blotting

For Western blots, 30μg of protein was loaded onto 7.5 or 10% SDS-PAGE gels. Proteins were transferred to a polyvinyl difluoride (PVDF) membrane using 30 V overnight at 4°C. The membrane was dried and placed in a blocking solution consisting of Tris-buffered saline–Tween (TBST; 1.5M Tris , 137 mM NaCl, 0.1% Tween 20) containing 5.0 % skim milk for 90 min, followed by incubation in primary antibody solution consisting of either 0.4 μg/ml anti-HA antibody (12CA5; Roche) for 1.5 h, 0.2 μg/ml anti-TAP antibody (Thermo Scientific) for 1.5 h, or 1.0 μg/ml of anti-MYC(Santa Cruz) diluted in TBST supplemented with 2 % milk overnight at 4°C. Blots were washed three times for 15 min in 1% TBST and incubated for 1 h in a 0.04 μg/ml of horseradish peroxidase-conjugated secondary antibody anti-mouse (KPL) or anti-rabbit (Santa Cruz). After washing, blots were developed using ECL (GE Healthcare; Amersham ECL Western blotting analysis system). Blots were stripped and incubated with 0.2 μg/ml of anti-PSTAIRE (Santa Cruz Biotechnology) as a loading control. Western blots were quantified using ImageJ as described previously (90).

2.9 Co-Immunoprecipitation

Overnight cultures were diluted into 1.0 L of YPD medium and incubated at 30°C until an OD_{600nm} of 0.8-1.0. The culture was centrifuged for 5 min at 3000 rpm, and the remaining pellet was immersed in dry ice and stored at - 80°C. Protein was extracted using the lyophilization method described above. For Co-immunoprecipitation, Mono HA 11 Affinity beads (Covance) were used. A bead volume of 40 μl was centrifuged at 1500g for 2 min at 4°C

and bead buffer was removed. The beads were then washed 3 times with 500 μ l of HK buffer by inverting 10 times to mix and further centrifuging for 2 min, 1500g at 4°C. Following the final wash, beads were added to protein extract containing 40 mg of protein, and samples were incubated overnight at 4°C with rocking. After centrifugation to pellet the beads, the supernatant was transferred to fresh Eppendorf tubes. Beads were washed five times with 1.0 mL of HK buffer, centrifuged, and resuspended in 500 μ l of HK buffer. The contents were transferred to fresh Eppendorf tubes and centrifuged to pellet the beads. The supernatant was removed and protein was eluted by boiling in 50 μ l of 1X SDS sample buffer (50 mM Tris pH 6.8, 2% SDS, 0.01% Bromophenol blue, 10% Glycerol, 100mM DTT) for 10 min. After centrifuging, the supernatant was removed and beads were boiled in 40 μ l of 1X SDS sample buffer for 10 min. Eluted samples were loaded on 7.5 or 10% SDS PAGE gels for Western blotting.

3.0 Affinity Purification

Affinity purification was carried out according to Rigaut *et al.* 1999 and Liu *et al.* 2010. Strains BH440 (ESP1/ESP1, *URA3+ HIS1+*) and SS1 (*esp1::HIS1/ESP1-TAP-URA3*) were inoculated into 20 ml of YPD medium and grown overnight at 30°C. The overnight culture was diluted into 2 L of YPD and incubated in 30°C until the OD_{600nm} reached 0.8-1.0. The culture was centrifuged for 5 min at 3000 rpm and the pellet stored at -80°C. Protein was extracted using the lyophilization method as described. The 2 L culture resulted in 235mg of input protein. Protein was pre-cleared by adding 500 μ l of prewashed Sepharose 6B beads (Sigma) (1:1 slurry in HK buffer) and rocking at 4°C for 30 min. The beads were removed by centrifugation, and the protein extract was incubated with prewashed IgG Sepharose 6 Fast Flow (GE Healthcare) (1:1 slurry in HK buffer; 250 μ l bead volume) for 4 h or overnight at 4°C. The extract and beads were poured into a Poly-Prep Chromatography Column (BIO-RAD). The eluate was discarded and beads were washed twice with 10 ml ice cold IPP300 buffer (25 mM Tris-HCl pH 8.0, 300 mM NaCl, 0.1% NP-40), twice with 10 ml IPP150 buffer (25 mM Tris-HCl pH 8.0, 150 mM NaCl, 0.1% NP-40) and once with 10 ml TEV-CB (25 mM Tris-HCl pH 8.0, 150 mM NaCl, 0.1% NP40, 0.5 mM EDTA and 1 mM DTT). 1 ml TEV CB buffer containing 10 U of Ac-TEV protease (Intrivogen) was then added, the column was rocked overnight at 4°C. The eluate was then collected and beads were washed with another 1.0 ml TEV CB buffer. To the final 2.0 ml

eluate, 3.0 ml of CBB (25 mM Tris-HCl pH 8.0, 150 mM NaCl, 1 mM Mg acetate, 1 mM Imidazole, 2 mM CaCl₂), 24.0 µl of 1.0 M CaCl₂ and 300 µl of Calmodulin Sepharose 4B (GE Healthcare) was added. The mixture was rocked for 1 h at 4°C. After centrifugation, beads were washed twice with 1.0 ml CBB (0.1% NP-40), and once with 1.0 ml CBB (0.02% NP-40). Protein was eluted from the beads by two subsequent additions of 1.0 ml CEB (25 mM Tris-HCl pH 8.0, 150 mM NaCl, 0.02% NP-40, 1 mM Mg acetate, 1 mM Imidazole, 20 mM EGTA, 10 mM β-mercaptoethanol). The elutions were combined and protein was precipitated by adding 25% volume of 50% Trichloroacetic acid (TCA). The samples were kept on ice for 30 min, then centrifuged at 13 500 rpm for 10 min at 4°C. The supernatant was removed, and 1.0 ml of 80% acetone was added to wash the precipitate. The contents were then centrifuged at 13 500 rpm for 10 min at 4°C to remove the acetone, the sample was dried on ice for 60 min. The pellet was re-suspended in 30µl 1 X SDS sample buffer, and boiled for 10 min. Samples were loaded on an SDS-PAGE gel for staining with either Silver Stain (BioRad) or Coomassie blue (BioRad). For Coomassie Blue-staining, samples were run on gels until just entering the resolving gel (97). Stained gel pieces from tagged and untagged strains were cut and sent for processing and analysis via Orbitrap LC/MS (IRIC, University of Montreal).

For affinity purification of the *CDC20* conditional control strain AG153 (*cdc20::URA3/MET3::CDC20-ARG4, CLB2-HA-HIS1*) and experimental strain SS3 (*ESP1/ESP1-TAP-ARG4, cdc20::URA3/MET3::CDC20-HIS1*), strains were inoculated into 20 ml of minimal inducing medium (-MC) and grown overnight at 30°C. The overnight cultures were centrifuged to remove media and diluted to an O.D._{600nm} of 0.1 into 4 L of minimal repressing medium containing methionine and cysteine (+MC) and incubated at 30°C for 4 h. The cultures were centrifuged for 5 min at 3000 rpm, and the pellet stored at -80°C. Protein was extracted using the lyophilization method as described. A 4 L culture resulted in 330mg of input protein. The affinity purification was conducted as described above.

4.0 Cell staining and imaging

For Differential Interference Contrast (DIC) microscopy, cells were fixed in 70% ethanol for at least 1.0 h, washed twice with sterile water, and mounted on slides. To visualize nuclei, cells fixed in 70% ethanol were stained with 1.0 µg/ml of 4', 6'-diamidino-2-phenylindole

dihydrochloride (DAPI; Sigma-Aldrich) for 20 min, and washed with sterile water (90). For Propidium iodide staining (88), 24h cultures were incubated in 10 μ g/ μ l propidium iodide (Sigma) for 5 min, rinsed in dH₂O, and mounted on slides. For visualization of β -tubulin, live cultures were first centrifuged at 3000 rpm for 3 min, washed once in water and mounted on slides. Cells were imaged on a LeicaDM6000B microscope (Leica Microsystems Canada Inc., Richmond Hill, ON, Canada) equipped with a Hamamatsu-ORCA ER camera (Hamamatsu Photonics, Hamamatsu City, Japan) using either HCX PL APO 63x NA 1.40-0 oil or HCX PLFLUO TAR 100x NA 1.30-0.6 oil objectives and the DAPI (460nm), FITC (500nm) or Texas Red (615nm) filters. Images were captured with Volocity software (Improvision Inc., Perkin-Elmer, Waltham, MA).

3.0 Results

3.1 Characterization of the *C. albicans* Separase homologue Esp1p

The regulation of the metaphase-to-anaphase transition in *C. albicans* is not well understood. We previously characterized the *C. albicans* APC/C cofactor Cdc20p and showed that it is important for this process and for mitotic exit (90). In order to determine its mechanisms of action, we sought Cdc20p targets by first searching the *C. albicans* genome for homologues of factors that bind Cdc20p in other systems. Through this approach, we found that *C. albicans* lacks the conserved Cdc20p target, securin. Blasting the *C. albicans* genome with securin sequences from *S. cerevisiae*, *S. pombe*, or *A. nidulans*, including Pds1p, Cut2p, or Bim1, respectively, or securin sequences from mammals, did not reveal any close homologues (<http://www.candidagenome.org>). We hypothesize that *C. albicans* may alternatively contain a functional securin homologue of divergent sequence, which may be revealed through determining the interacting proteins of Cdc20p. However, attempts to tag Cdc20p with a TAP tag were not successful. Alternatively, *C. albicans* contains an orthologue of a conserved securin-binding protein, the separase *ESP1/ORF19.3356*. Esp1p is 23.2% identical and 40.5% similar to Esp1p from *S. cerevisiae* (Table 4). *C. albicans* Esp1p has not been extensively characterized, although a recent large-scale screen of mutant strains suggested that it may be essential, and repression via the *TET* promoter resulted in filamentous growth (63).

Table 4: Comparison of separase homologues in various organisms¹

First Sequence	Second Sequence	% AA Alignment Identity	% AA Alignment Similarity
<i>C. albicans</i>	<i>S. cerevisiae</i>	23.2	40.5
<i>C. albicans</i>	<i>S. pombe</i>	19.5	32.0
<i>C. albicans</i>	<i>Homo sapiens</i>	15.3	29.0
<i>S. cerevisiae</i>	<i>S. pombe</i>	22.7	35.7
<i>S. cerevisiae</i>	<i>Homo sapiens</i>	16.3	28.4
<i>S.pombe</i>	<i>Homo sapiens</i>	17.2	27.0

¹Sequences obtained for *C. albicans*, *Homo sapiens*, *S. cerevisiae*, and *S.pombe* were obtained from Candida Genome Database (<http://www.candidagenome.org>), Uniprot Database (<http://www.uniprot.org>), Saccharomyces Genome Database (<http://www.yeastgenome.org>) and PomBase (<http://www.pombase.org>) respectively. Sequences were aligned using ClustalW (<http://www.ebi.ac.uk>) to obtain percent identity and similarity in amino acid sequence.

In order to characterize *C. albicans* Esp1p, one copy was deleted from strain BWP17, and the other was placed under control of the *MET3* promoter (Figs. 5, 7), resulting in strains SS31 to SS36 (Fig. 8). When plated on solid inducing medium (-MC) at 30°C for 48 h, colonies from strain SS35 (*esp1::URA3/MET3::ESP1-HIS1*) appeared normal compared to control strain BH440 (*ESP1/ESP, URA3+, HIS1+*) (Fig. 9A). However, on repressing medium (+MC), strains lacking Esp1p showed little growth (Fig. 9A). In liquid inducing medium, strain SS35 grew as normal yeast cells that were indistinguishable from those of control strain BH440 (Fig. 9B). However, by 5-8 h in repressing medium, cells of strain SS35 were predominantly large budded or multi-budded cells (Fig. 9B, Tables 5, 6). By 24 h, the majority of cells depleted of Esp1p were enlarged and filamentous (Fig. 9B). Similar results were obtained when strain *esp1::URA3/TET::ESP1-HIS1* was incubated in doxycycline (Figs. S1, S2, Tables S1, S2).

In order to investigate the effects of long-term depletion on growth, strains BH440 and SS35 were incubated on solid inducing or repressing medium for several days. Strains HCCA118 (*cdc5::URA3/MET3::CDC5-HIS1*) and SS25 (*orf19.955::URA3/MET3::ORF19.955-HIS1*), which regulates an essential or non-essential gene, respectively, were included for comparison. Little growth was observed in strain SS35 (Fig. 10), similar to depletion of the essential gene *CDC5* and in contrast to strains BH440 and SS25. Thus, the data suggest that *ESP1* is an essential gene, as previously reported for the *TET*-regulated strain (63), and its absence results in large-budded yeast cells that subsequently develop filamentous growth.

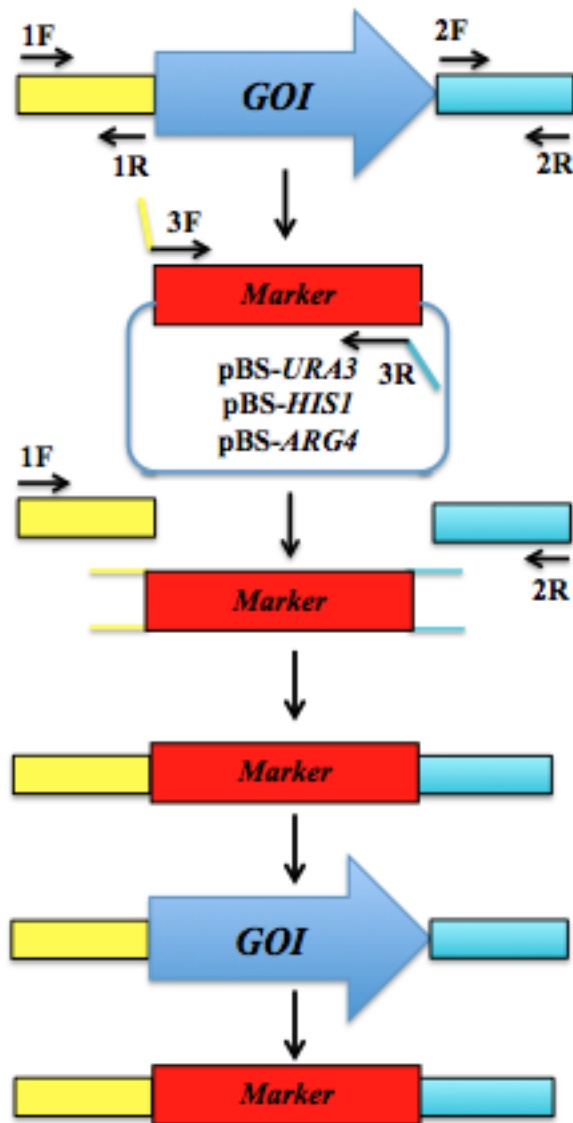


Fig 5: Strategy for replacing a single copy of a Gene of Interest (GOI) with a marker. Fragments corresponding to the 5' flank region, 3' flank region and a selectable marker were amplified from gDNA or plasmid pBS-*URA3*, *HIS1* or *ARG4* respectively using oligonucleotide pairs 1F/1R, 2F/2R, and 3F/3R respectively. The three products were combined with oligonucleotides 1F and 2R in a fusion PCR to create the final product for transformation.

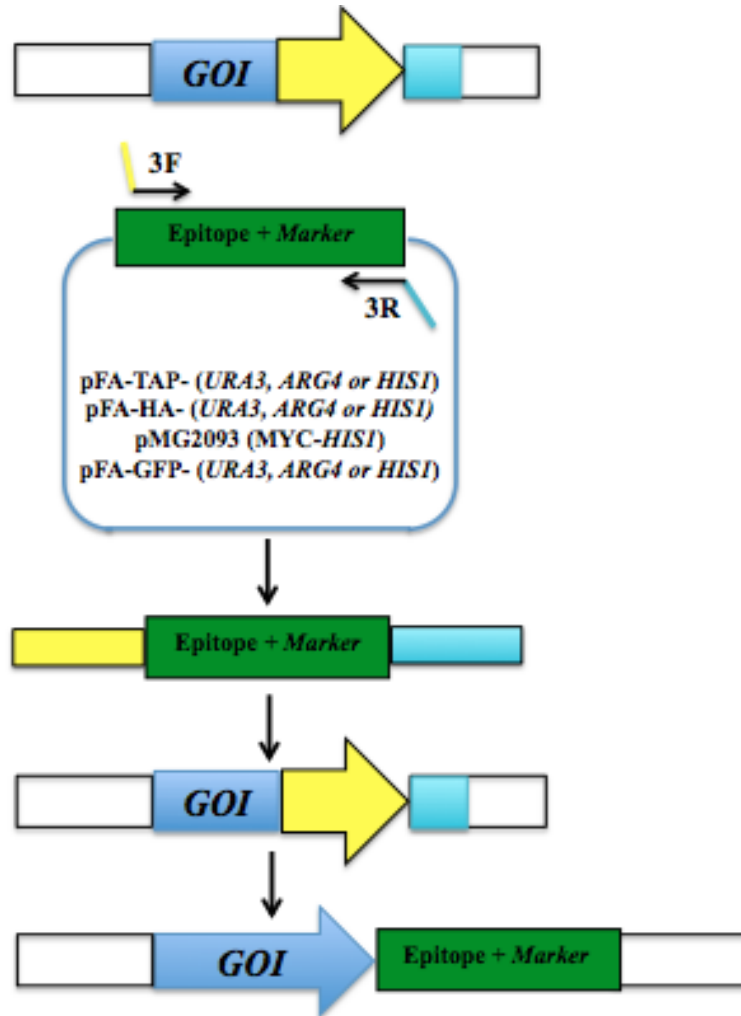


Fig 6: One-step PCR strategy for tagging a gene with TAP, HA, MYC or GFP epitopes. Oligonucleotides 3F and 3R containing 100 bp homology to a gene of interest (GOI) and 20bp homology to a cassette containing a tag and marker were used to amplify a construct that would tag a gene at the 3' terminus. The construct was transformed into strains for direct integration.

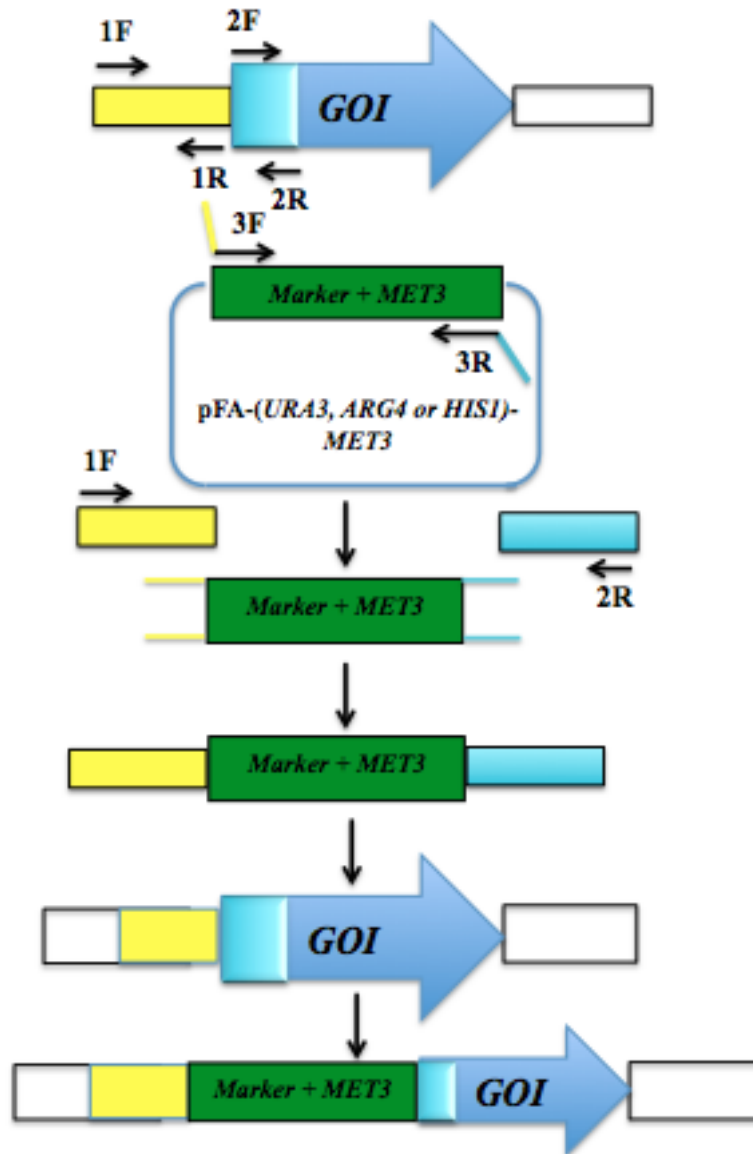


Fig 7: Strategy for creating a strain containing a single copy of a Gene of Interest (GOI) under control of the *MET3* promoter.

Fragments corresponding to 500 bp of 5' flank region and 700 bp starting from the Start codon were amplified from gDNA using oligonucleotide pairs 1F/1R and 2F/2R respectively. Oligonucleotides 3F/3R were used to amplify a marker and *MET3* promoter cassette from plasmid pFA-*Marker-MET3* (Gola *et al.* 2003). The three products were combined in a fusion PCR using oligonucleotides 3F and 3R to create the final product for transformation.

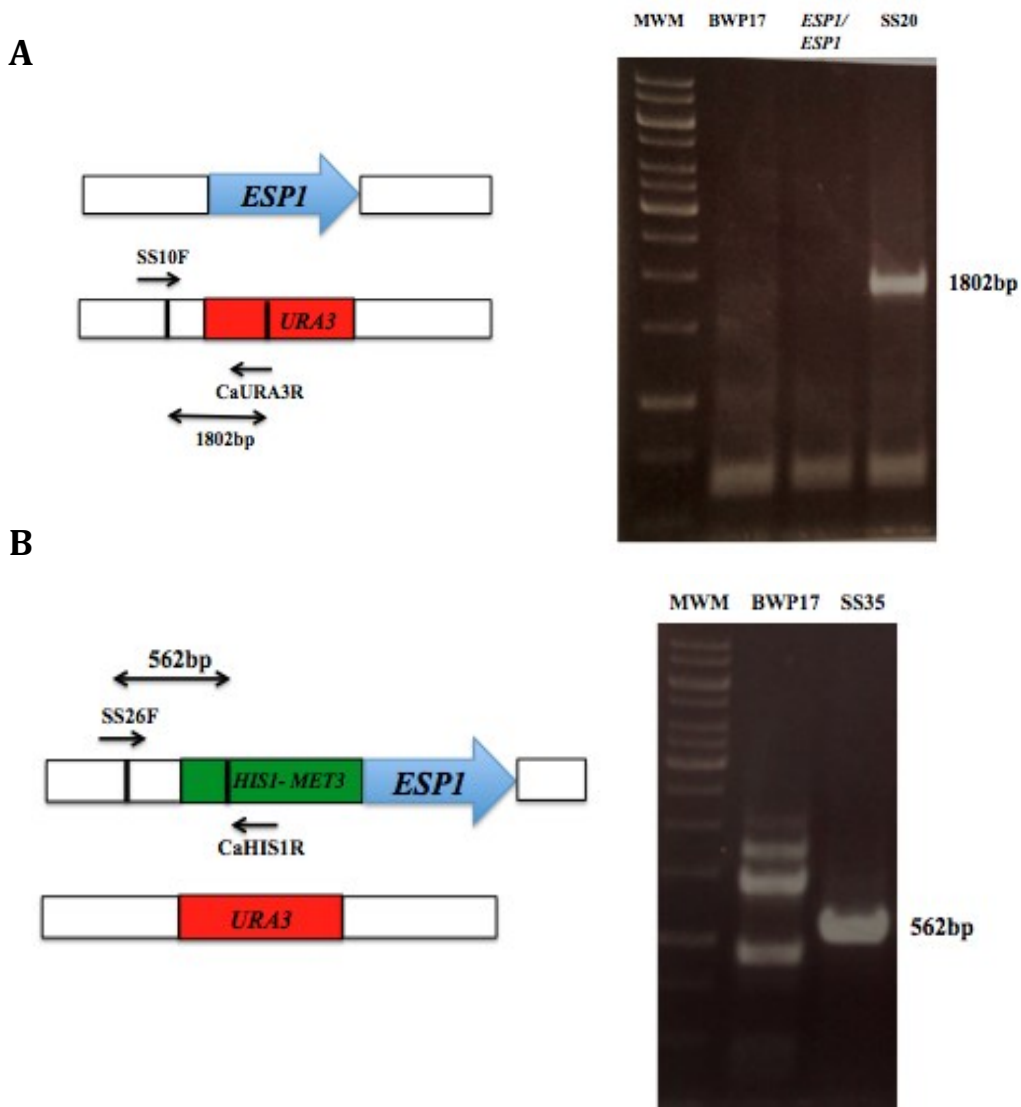


Fig 8: Confirmation of An *esp1::URA3/MET3::ESP1-HIS1* strain.

(A) Map and DNA gel showing the PCR screening strategy to confirm correct integration of the *URA3*-containing construct. Oligonucleotides SS10F and CaURA3R generate a 1802 bp band for the *URA3* replacement. Positive strain SS20 and the negative control strain BWP17 are demonstrated. (B) Map and DNA gel showing the PCR screening strategy to confirm correct integration of the *MET3*-containing construct. Oligonucleotides SS26F and CaHIS1R generate a 562 bp band for the *MET3* integration. Positive strain SS35 and the negative control strain BWP17 are demonstrated. Vertical bars delineate the length of the transforming construct.

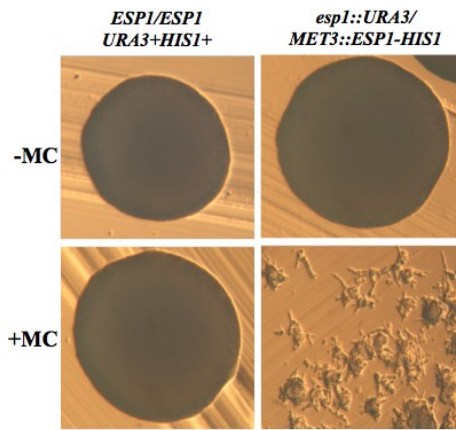
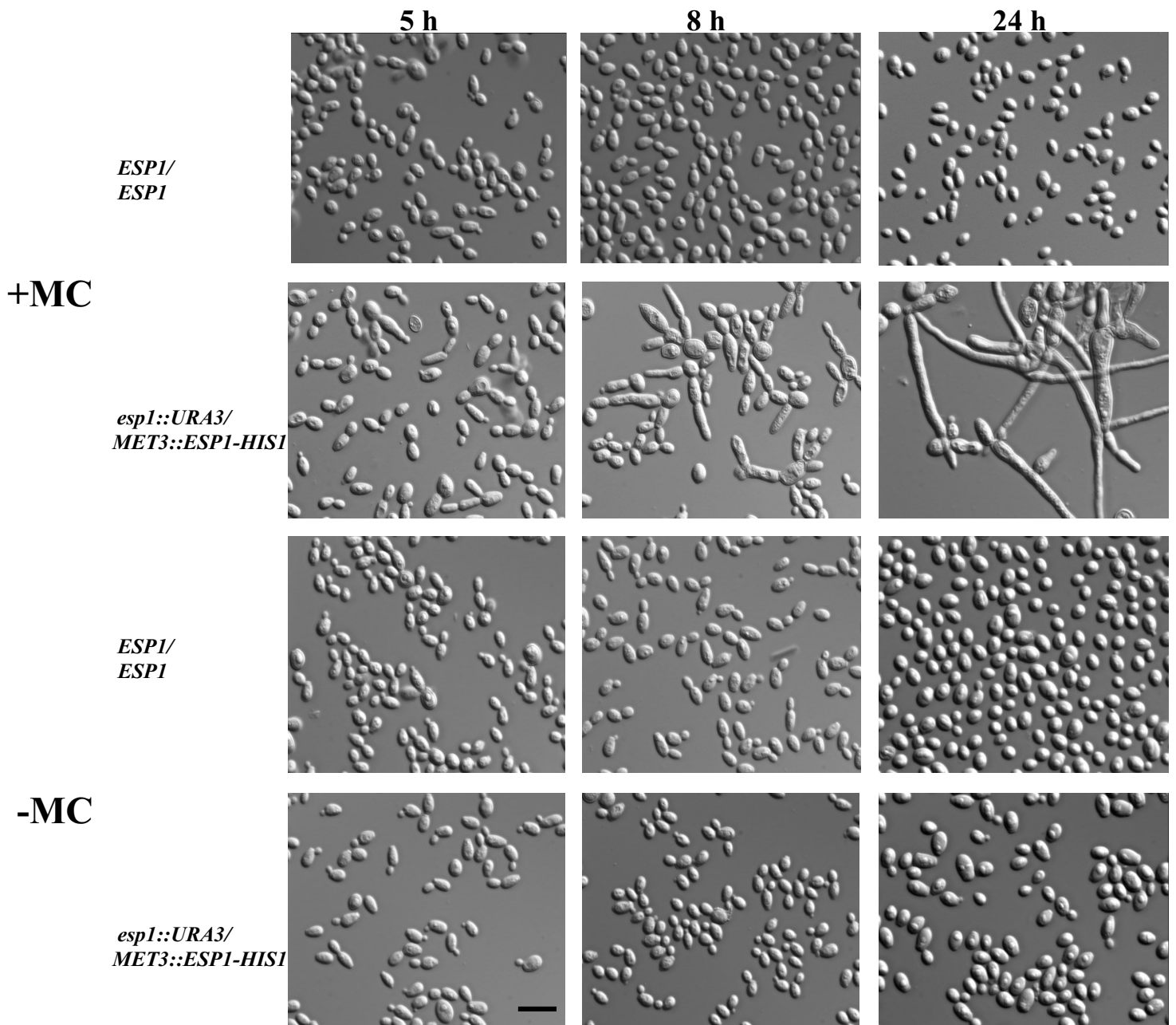
A**B**

Fig 9: Depletion of Esp1p results in poor growth and yeast cells forming large buds followed by filaments.

(A) Strains BH440 (*ESP1/ESP1*, *URA+HIS+*) and SS35 (*esp1::URA3/MET3::ESP1-HIS1*) were streaked onto solid repressing (+MC) or inducing (-MC) medium and incubated at 30°C for 24 h.
B) Overnight cultures of strains BH440 or SS35 were diluted into liquid -MC or +MC medium and incubated at 30°C for the indicated time periods. Bar: 10 μm.

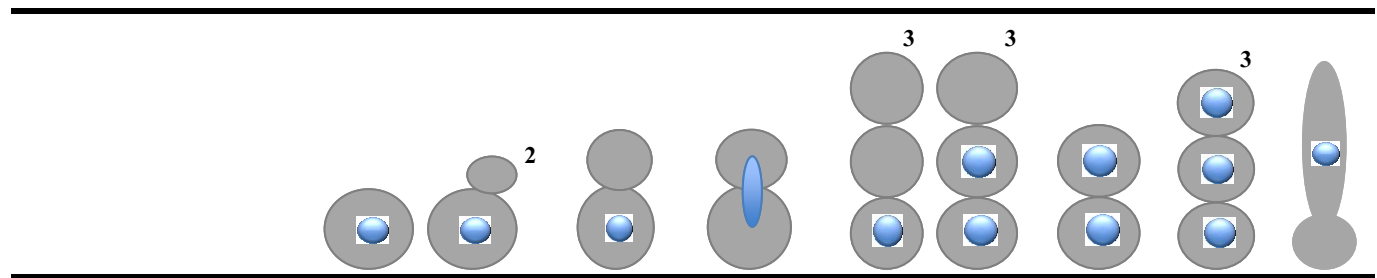
3.2 *C. albicans* Esp1p is required for separation of chromosomes

In *S. cerevisiae*, *esp1* mutants arrest as large-budded cells with unsegregated chromatin, predominantly in the daughter cell. Spindles are either short or difficult to observe due to weak staining and/or microtubules being in disarray, due to a role for Esp1p in spindle stability (16, 18). If *C. albicans* Esp1p functions as a separase, its absence should also result in a defect in chromosome separation. In order to test this, cells of strains BH440 (*ESP1/ESP1*, *URA3+HIS1+*) and SS35 (*esp1::URA3/MET3::ESP1-HIS1*) were incubated in inducing or repressing medium for 5 or 8 h, fixed and stained with DAPI. After 5 h in repressing medium, 18.7 % of control strain BH440 cells were in mitosis, where DAPI-stained chromatin was predominantly located as a single mass within one half of a large-budded cell, or through the bud neck and was not fully separated. The remainder were unbudded or small-budded (Fig. 11; Table 5). In contrast, approximately 43.9% of cells depleted of Esp1p were large-budded with a single mass of chromatin that was located in one half of the majority of cells, or at the bud neck in a smaller proportion of large-budded cells, consistent with a defect in metaphase (Fig. 11; Table 5). By 8 h, 51% of cells from strain SS35 contained a single mass of unsegregated chromosomes and were either large-budded or multi-budded, the latter suggesting an uncoupling of nuclear division and budding. Only 10% of cells were capable of separating chromosomes, where every cell compartment of large-budded or multi-budded cells contained DAPI-stained DNA (Table 6). Similar results were obtained with strain *esp1::URA3/TET::ESP1-HIS1* incubated in YPD medium containing doxycycline, with the exception that more cells were filamentous at 8 h (Fig. S2, Tables S1, S2).

In order to confirm the mitotic stage at which Esp1p may function, spindles were analyzed by tagging β -tubulin with GFP in strain SS35, resulting in strain SS37 (Fig. 6). After incubation in inducing medium for 7 h, 27% (n=62) of cells contained short bar spindles characteristic of metaphase and early anaphase, while 14.5% contained telophase spindles (Fig. 12). In contrast, in repressing medium, 42.8 % (n=63) of cells contained short bar spindles, while only 4.7% contained a telophase spindle (Fig. 12). The remaining cells were either filamentous and contained extensive cytoplasmic microtubules that could interfere with visualization of spindles, or were in the yeast form where spindles were either not visible or appeared disorganized (Fig.

12). Notably, the strain showed transient filamentation when transferred to fresh medium, irrespective of composition. However, by 7 h, the majority of cells in inducing medium had recovered and were in a yeast form. Although tagging β -tubulin results in a minor transient phenotype, precluding analysis of microtubule organization during earlier time points, a notable difference was observed in inducing vs repressing medium by 7 h, consistent with a role for Esp1p in early mitotic progression. Thus, absence of Esp1p impairs the segregation of chromosomes and subsequent progression to telophase, suggesting that it may be functioning as a separase.

Table 5: Cell phenotype and position of nuclei in cells depleted of Esp1p or Orf19.955p for 5 h¹.



<u>+MC</u>								
<i>HIS1</i> ⁺ <i>URA3</i> ⁺ (n=151)	42.4	12.1	6.6	-	-	25.8	10.6	-
<i>ESP1::URA3/</i> <i>MET3::ESP1-HIS1</i> (n=161)	37.8	32.3	10.4	1.2	2.5	11.0	4.3	-
<i>ORF19.955::URA3/</i> <i>MET3::ORF19.955-</i> <i>HIS1</i> (n=106)	46.5	14.9	4.4	4.4	6.1	13.2	9.6	1.0
<u>-MC</u>								
<i>HIS1</i> ⁺ <i>URA3</i> ⁺ (n=87)	44.5	26.4	3.4	-	-	19.5	5.7	-
<i>ESP1::URA3/</i> <i>MET3::ESP1-HIS1</i> (n=120)	82.5	7.5	2.5	-	-	6.6	-	-
<i>ORF19.955::URA3/</i> <i>MET3::ORF19.955-</i> <i>HIS1</i> (n=117)	72.0	10.3	3.7	-	-	13.1	1.0	-

¹Percentage of cells showing the indicated patterns. Strains BH440 (*URA3*⁺*HIS1*⁺), SS35 (*esp1::URA3/MET3::ESP1-HIS1*), SS25 (*orf19.955::URA3/MET3::ORF19.955-HIS1*) were incubated in +MC or -MC medium for 5 h, fixed, and stained with DAPI.

²Includes unbudded and small-budded cells.

³Pattern includes multibudded and pseudohyphal cells.

Table 6: Cell phenotype and position of nuclei in cells depleted of Esp1p or Orf19.955p for 8 h¹.

	1	2	3	4	5	6	7	8	9
<u>+MC</u>									
<i>HIS1</i> ⁺ <i>URA3</i> ⁺ (n=155)	63.0	15.5	5.2	-	1.0	15.4	-	-	-
<i>ESP1::URA3/</i> <i>MET3::ESP1-HIS1</i> (n=161)	19.3	22.4	6.2	22.4	15.5	6.8	3.1	4.3	-
<i>ORF19.955::URA3/</i> <i>MET3::ORF19.955-</i> <i>HIS1</i> (n=120)	23.3	5.0	2.5	1.0	8.3	19.2	40.0	1.0	-
<u>-MC</u>									
<i>HIS1</i> ⁺ <i>URA3</i> ⁺ (n=98)	57.0	20.4	3.1	-	-	19.4	-	-	-
<i>ESP1::URA3/</i> <i>MET3::ESP1-HIS1</i> (n=117)	70.9	12.0	2.6	-	-	14.5	-	-	-
<i>ORF19.955::URA3/</i> <i>MET3::ORF19.955-</i> <i>HIS1</i> (n=114)	78.0	9.6	1.0	-	-	11.4	-	-	-

¹Percentage of cells showing the indicated patterns. Strains BH440 (*URA3*+*HIS1*+), SS35 (*esp1::URA3/MET3::ESP1-HIS1*), SS25 (*orf19.955::URA3/MET3::ORF19.955-HIS1*) were incubated in +MC or -MC medium for 8 h, fixed, and stained with DAPI.

²Includes unbudded and small-budded cells.

³Pattern includes multibudded and pseudohyphal cells.

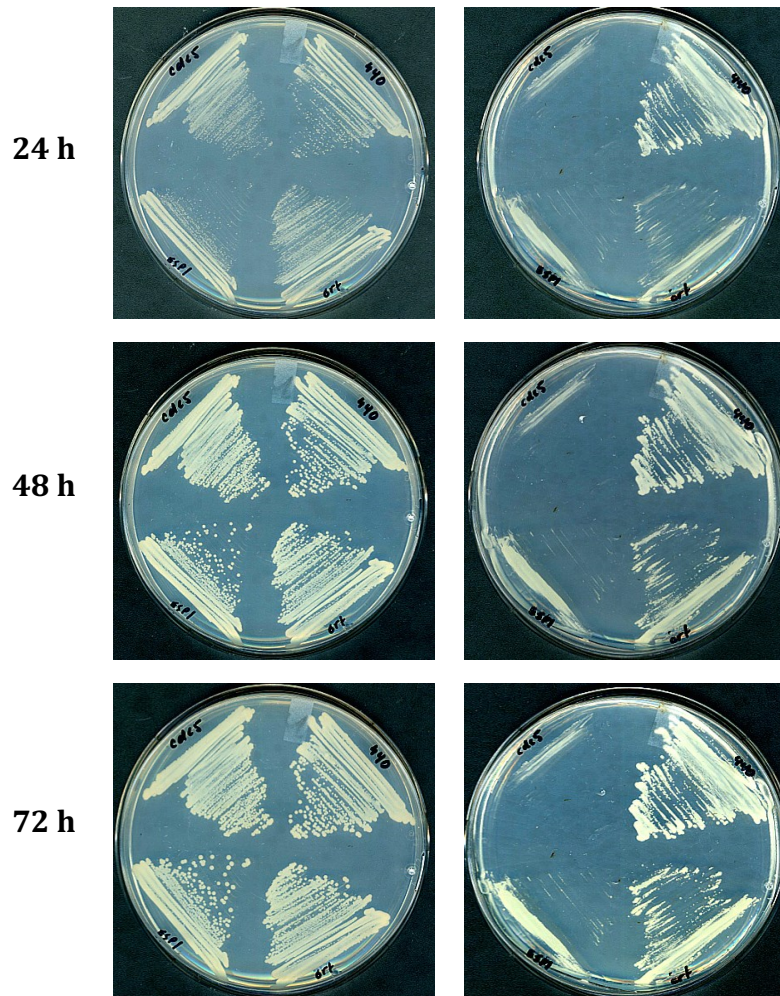
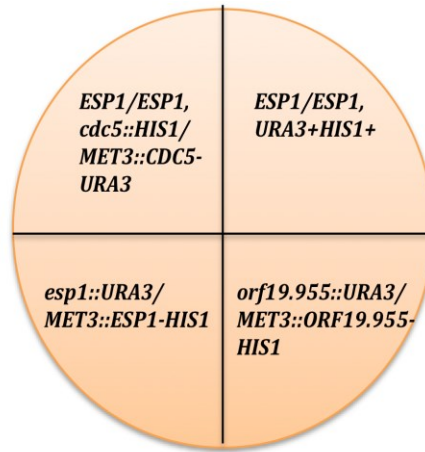


Fig 10: *ESP1* is essential while *ORF19.955* is not.

Strains BH440 (*ESP1/ESP1*, URA⁺HIS1⁺), SS35 (*esp1::URA3/MET3::ESP1-HIS1*), HCCA108 (*cdc5::HIS1/MET3::CDC5-URA3*) and SS25 (*orf19.955::URA3/MET3::ORF19.955-HIS1*) were plated on solid inducing (-MC) or repressing (+MC) medium and incubated at 30°C for select times.

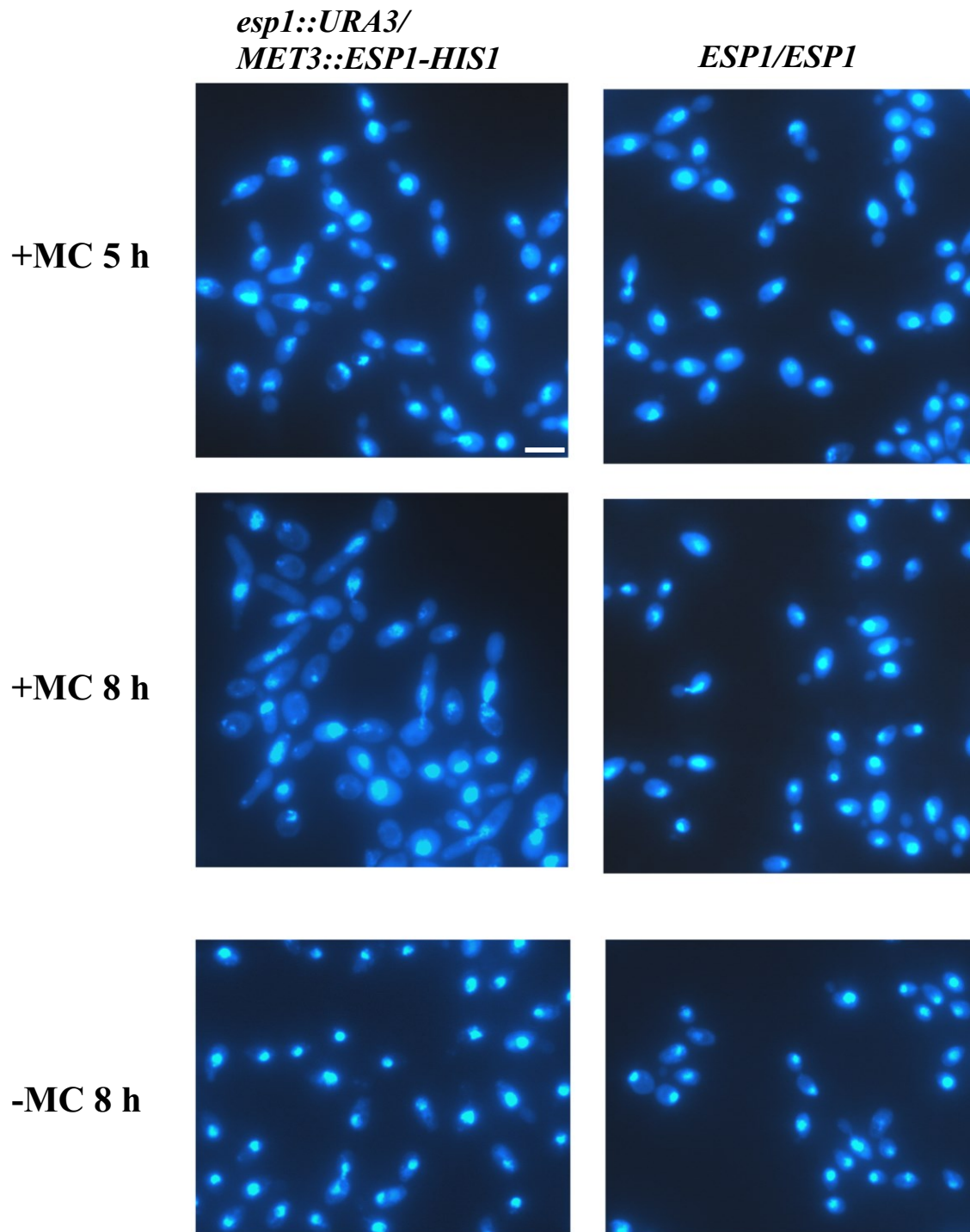


Fig 11: Cells depleted of Esp1p impair chromatin separation.

Strains BH440 (*ESP1/ESP1*, *URA3+HIS1+*) and SS35 (*esp1::URA3/MET3::ESP1-HIS1*) were incubated in inducing (-MC) or repressing (+MC) medium for 5 or 8 h, fixed and stained with DAPI. Bar: 10 μ m.

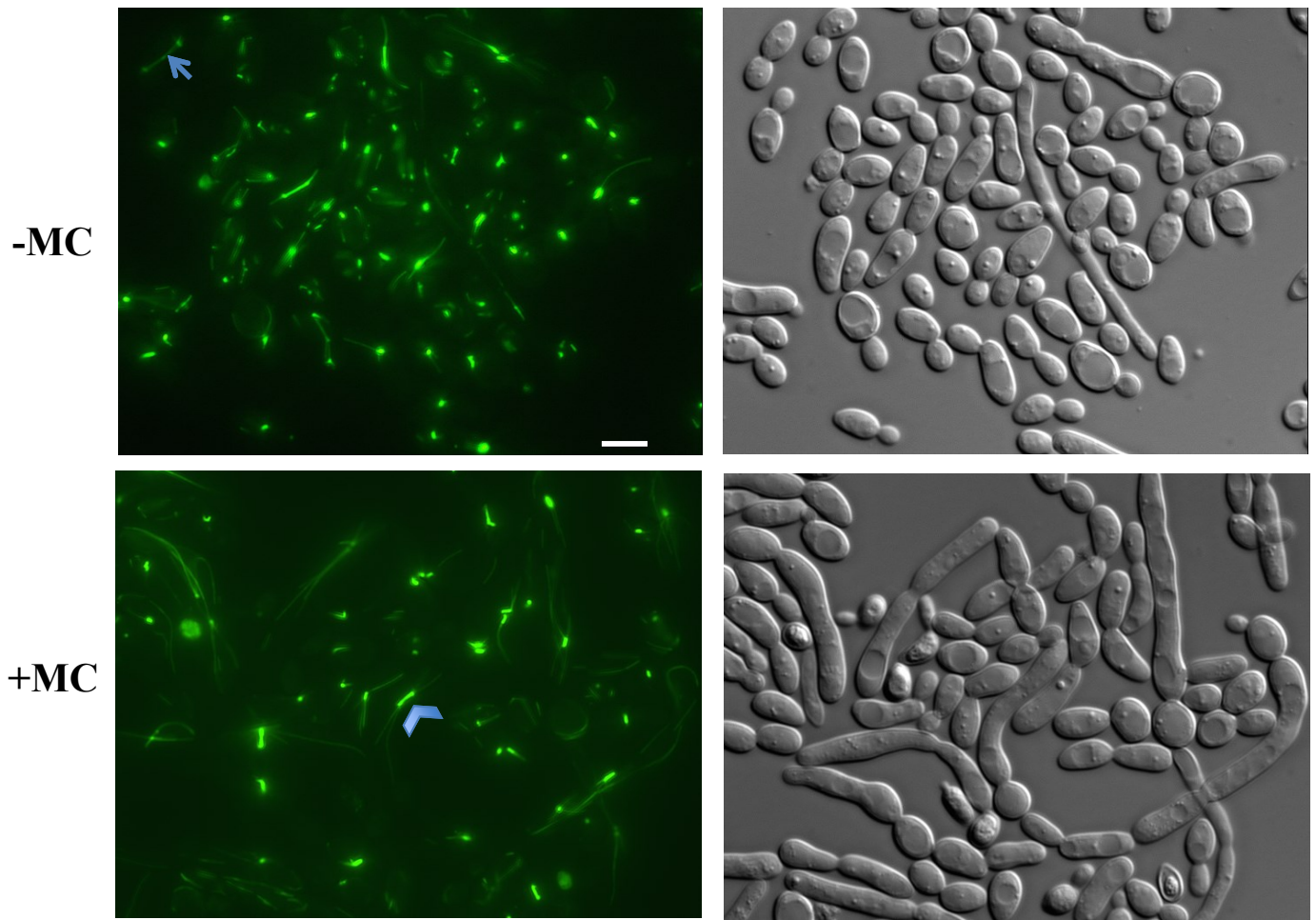


Fig. 12: Cells depleted of Esp1p impair progression to telophase and microtubule organization in a proportion of cells.

Strain SS35 (*esp1::URA3/MET3::ESP1-HIS1*) was incubated in inducing (-MC) or repressing (+MC) medium for 7 h, and imaged live on a LeicaDM6000B microscope. Bar: 10 μ m. An arrow denotes a telophase spindle and an arrowhead denotes a metaphase or early anaphase spindle.

3.3 Identification of Esp1p-interacting proteins reveals strong enrichment of a novel, previously uncharacterized protein, Orf19.955p

Since Esp1p of *C. albicans* may function as separase, we reasoned that one of its interacting proteins may be a functional homologue of a securin. In order to test this hypothesis, strains carrying a single copy of *ESP1* tagged at the C-terminus with the Tandem Affinity Purification (TAP) tag composed of Protein A and calmodulin-binding peptide, separated by a tobacco etch virus (TEV) protease cleavage site, were created (Fig. 13A). Strains SS1 and SS5 (*esp1::HIS1/ESP1-TAP-URA3*) grew at rates similar to control strain AG636 (*ESP1/ESP1-TAP-URA3*), and expressed the protein, indicating that Esp1p-TAP was functional (Fig. 13B, C). Next, strains BH440 (*ESP1/ESP1, URA3+HIS1+*) and SS1 (*esp1::HIS1/ESP1-TAP-URA3*) were incubated in YPD medium to an O.D_{600nm} of 0.8, collected and subjected to affinity purification. Since a silver-stained gel revealed a higher abundance of precipitated protein from strain SS1 vs. BH440 (Fig. S5), the affinity purification was repeated. Precipitated samples were run on an SDS PAGE gel until the sample just entered the resolving gel, and a single gel piece of compacted bands from each strain was sent for analysis via Orbitrap LC/MC (IRIC, University of Montreal) (97). The results demonstrate that few proteins co-precipitated with Esp1p, and Esp1p itself was not greatly enriched (Table 7). Of notable interest was the phosphatase Cdc14p, histones H2B, H4, and Orf19.6506p, which has a putative role in histone deacetylation. Of these factors, none were reported to physically interact with Esp1p in *S. cerevisiae* (<http://www.yeastgenome.org>). However, there may be an indirect interaction between Cdc14p and Esp1p in *S. cerevisiae*, through Cdc55p and Net1p intermediates (7).

In order to enhance detection of Esp1p and its interacting partners, *ESP1* was next tagged with TAP in a *CDC20* conditional strain, to allow for a synchronized block in mitosis (Fig. 14), resulting in strains SS2-4 (*ESP1/ESP1-TAP-ARG4, MET3::CDC20-ARG4/cdc20::URA3*). In order to investigate whether Esp1p expression levels were modulated under conditions of Cdc20p depletion, strain SS2 was incubated in inducing or repressing medium for 3 or 6 h, then processed for Western blotting. Since Esp1p-TAP was still expressed when Cdc20p was depleted (Fig. 15), we proceeded with the affinity purification and mass spectrometry analysis. Strains SS2 and control AG153 (*MET3::CDC20-ARG4/cdc20::URA3, CLB2-HA-HIS1*) were diluted into +MC

medium for 4 h prior to collection and processing. The results reveal significant enrichment of Esp1p compared to previous data obtained from exponential-phase cells (Table 8). Intriguingly, Cdc14p was also enriched, as well as a previously uncharacterized protein, Orf19.955p. Additional co-purifying peptides corresponded to proteins of varying function, including the heat shock protein *HSP70*, the filamentation regulator *DEF1*, as well as *CTA3*, which plays a role in endocytosis. Of these proteins, only the Cta3p, Ede1p interacts with Esp1p in *S. cerevisiae* (<http://www.yeastgenome.org>). Notably, homologues of other known interacting proteins of Esp1p in *S. cerevisiae*, including the protein kinase Cdc5p, the regulatory subunit of the protein phosphatase Cdc55p, the alpha-kleisin subunit of the cohesin complex Scc1p, kinetochore-associated protein Slk19p and any securin, did not co-precipitate with *C. albicans* Esp1p. Further, histone-related proteins as identified under exponential growth conditions were not present. Thus, we identified some conserved but also novel interacting proteins of Esp1p in *C. albicans*, including the protein of unknown function Orf19.955p.

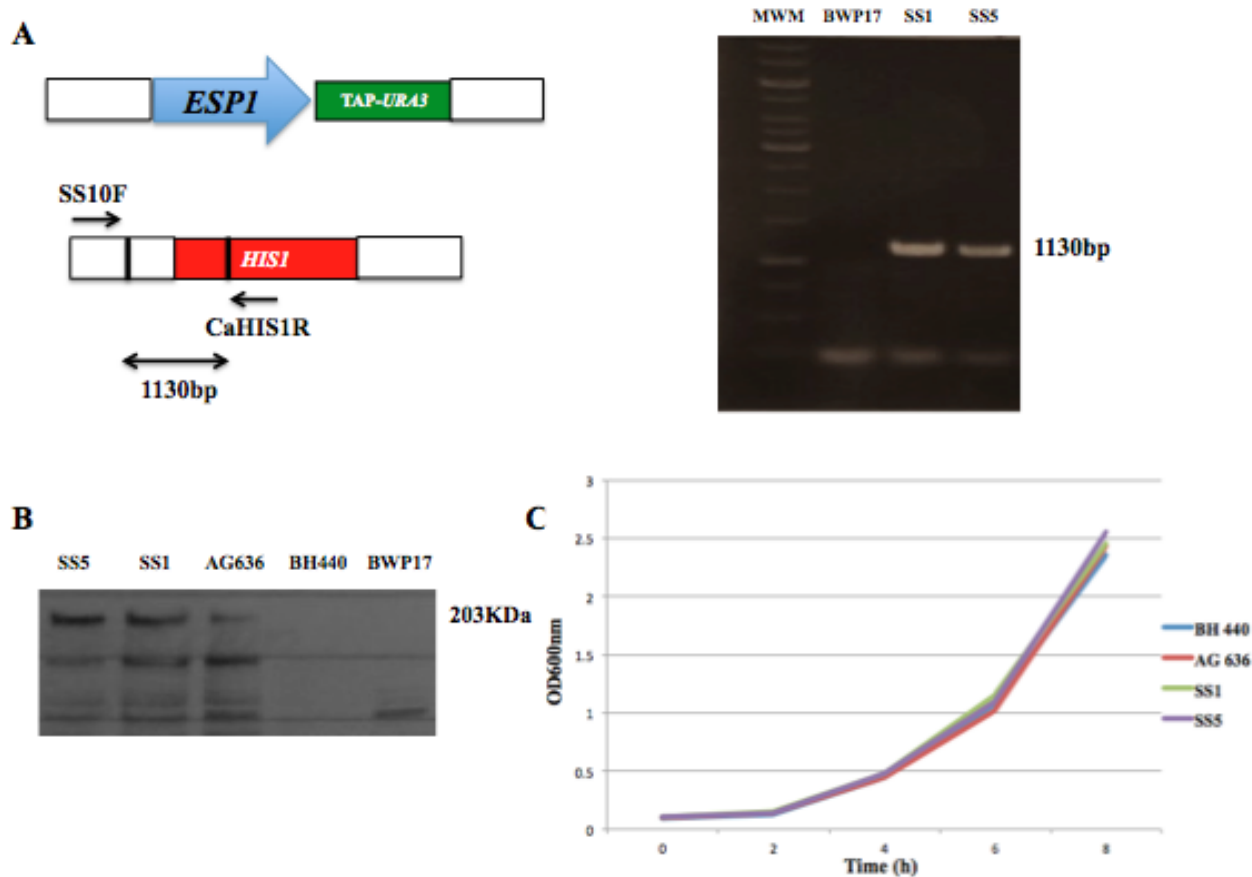


Fig 13: Confirmation of strain *esp1::HIS1/ESP1-TAP-URA3*.

(A) Map showing PCR screening strategy to confirm proper integration of the knockout gene construct. Oligonucleotides SS10F and CaHIS1R generate a 1130 bp band for the *HIS1*-containing knockout construct. Positive strains SS1 and SS2, and the negative control strain BWP17 are demonstrated. Vertical bars delineate the length of the transforming construct.

(B) Western blot showing confirmation of *ESP1-TAP*. (C) Strains BH440 (*ESP1/ESP1, URA3+HIS1+*), AG636 (*ESP1/ESP1-TAP-URA3*), SS1 and SS2 (*esp1::HIS1/ESP1-TAP-URA3*) were incubated in YPD medium at 30°C and the O.D._{600nm} was recorded at set times.

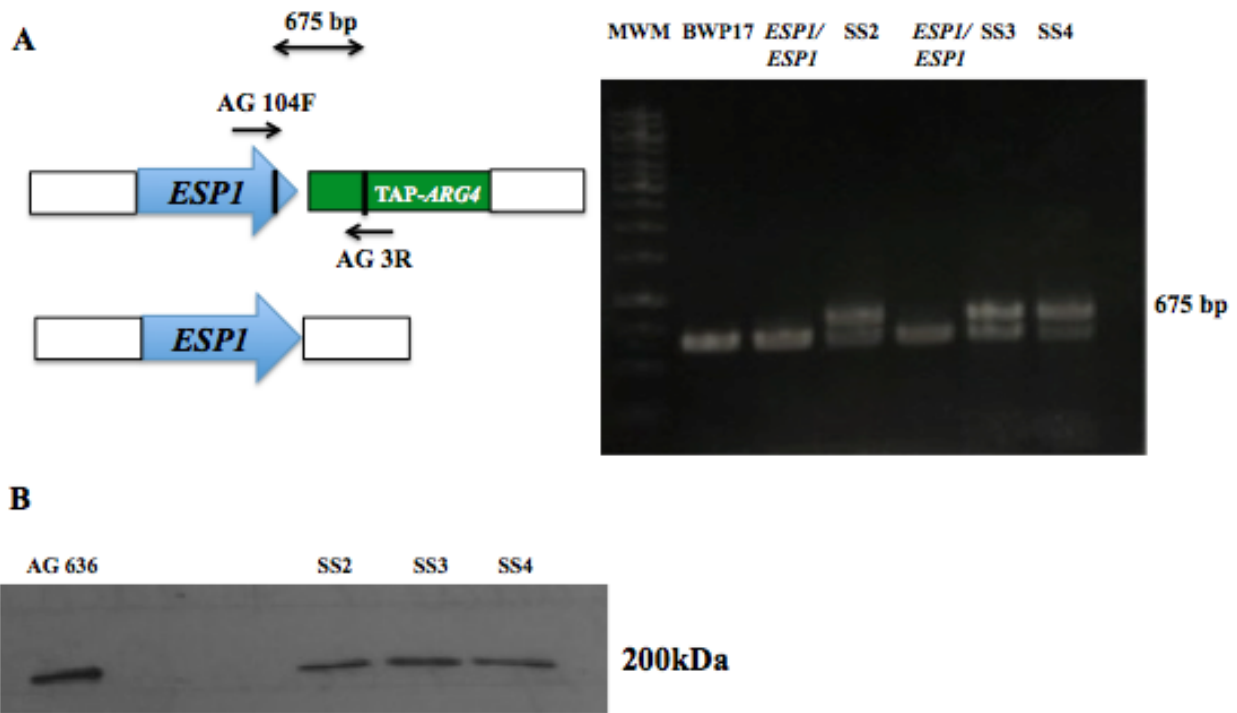


Fig 14: Confirmation of strain *ESP1/ESP1-TAP-ARG4* in *Cdc20p*-conditional background. (A) Map and ethidium-bromide stained DNA gel showing PCR screening strategy to confirm proper integration of *ESP1-TAP* gene construct. Oligonucleotides AG104F and AG3R generate a 675 bp band for the *ESP1-TAP*-containing construct. Positive strains SS2, SS3 and SS4 (*ESP1/ESP1-TAP-ARG4, cdc20::URA3/MET3::CDC20-HIS1*) and the negative control strain BWP17 (*ESP1/ESP1*) are demonstrated. Vertical bars delineate the length of the transforming construct. (B) Western blot showing confirmation of Esp1p-TAP expression.

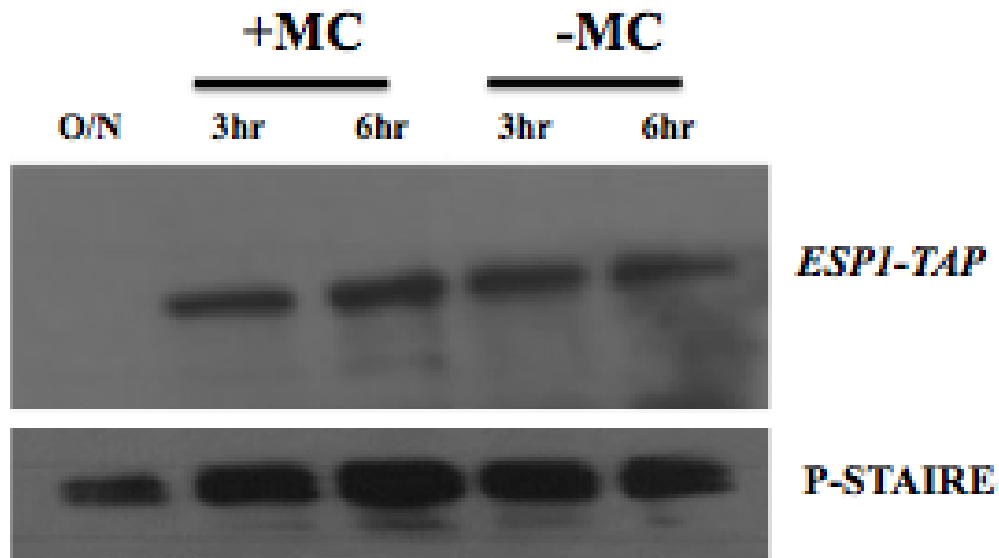


Fig 15: Esp1p-TAP expression is not significantly modulated in the presence vs. absence of Cdc20p.

Strains AG636 (*ESP1/ESP1-TAP-URA3*) and SS2 (*ESP1/ESP1-TAP-ARG4, cdc20::URA3/MET3::CDC20-HIS1*) were incubated in +MC or -MC medium for set times, collected and processed for Western blotting. Blots were incubated with anti-TAP antibody, stripped and incubated with anti-p-STAIRES antibody as a loading control.

Table 7: Orbitrap LC/MS analysis of putative Esp1p-interacting proteins from exponential-growing yeast cells¹.

Protein ID	Number of Peptides²	ORF Name	Present in Control³	Description
CAL0004160	4	<i>Orf19.3356/ESP1</i>	N	Putative caspase-like cysteine protease; mutation confers increased sensitivity to nocodazole; periodic mRNA expression, peak at cell-cycle S/G2 phase; mRNA binds She3
CAL0005886	3	<i>Orf19.4192/CDC14</i>	N	Protein involved in exit from mitosis and morphogenesis; ortholog of <i>S. cerevisiae</i> Cdc14p, which is a dual-specificity phosphatase and cell-cycle regulator;
CAL0001185	3	<i>Orf19.1052</i>	N	Predicted histone H2B; Hap43-induced gene; Spider biofilm repressed
CAL0003208	2	<i>Orf19.173</i>	N	C2H2 transcription factor; induced by Mnl1 under weak acid stress
CAL0003038	2	<i>Orf19.6506</i>	N	Ortholog(s) have role in histone deacetylation, negative regulation of antisense RNA transcription, regulation of DNA-dependent DNA replication initiation, transcription
CAL0001194	2	<i>Orf19.1059/HHF1</i>	N	Putative histone H4; repressed in fkh2 mutant; regulated by Efg1; fluconazole induced; amphotericin B repressed; farnesol regulated; colony morphology-related gene
CAL0002693	2	<i>Orf19.5182/POL3</i>	N	Large subunit of DNA polymerase III; partially complements defects of an

				S. cerevisiae cdc2 mutant; differing reports about periodic (G1/S) or non-periodic mRNA
CAL0005112	2	<i>Orf19.3490/FGR6-4</i>	N	Protein lacking an ortholog in S. cerevisiae; member of a family encoded by FGR6-related genes in the RB2 repeat sequence; transposon mutation affects filamentous growth

¹Approximately 235 mg protein extracts from 2 L cultures of strains SS1 (*esp1::HIS1/ESP1-TAP-URA3*) and BH440 (*ESP1/ESP1*) incubated in YPD medium until reaching an O.D._{600nm} of 0.8 were subjected to tandem affinity purification (Rigaut *et al.* 1999 ; Liu *et al.* 2010). Elutions were TCA-precipitated and run just into the resolving portion of an SDS PAGE gel. The compressed bands were stained with Coomassie blue, cut from the gel, and analysed using an LTQ-OrbitrapElite with nano-ESI.

²Peptides less than 2 were excluded from the results.

³Peptides identified in both the tagged strain and the untagged control strains were excluded from the results.

Table 8: Orbitrap LC/MS analysis of putative Esp1p-interacting proteins from yeast cells blocked in mitosis¹.

Protein ID	Number of Peptide²	ORF Name	Present in Control³	Description
CAL0004160	63	<i>Orf19.3356/ESP1</i>	N	Putative caspase-like cysteine protease; mutation confers increased sensitivity to nocodazole; periodic mRNA expression, peak at cell-cycle S/G2 phase; mRNA binds She3
CAL0005886	24	<i>Orf19.4192/CDC14</i>	N	Protein involved in exit from mitosis and morphogenesis; ortholog of <i>S. cerevisiae</i> Cdc14p, which is a dual-specificity phosphatase and cell-cycle regulator;
CAL000194	11	<i>Orf19.955</i>	N	Uncharacterized, protein of unknown function
CAL0000006	8	<i>Orf19.4980/HSP70</i>	N	Putative hsp70 chaperone; role in entry into host cells; heat-shock, amphotericin B, cadmium, ketoconazole-induced; surface localized in yeast and hyphae; antigenic in host; farnesol-downregulated in biofilm; Spider biofilm induced
CAL0005977	6	<i>Orf19.3575/CDC19</i>	N	Pyruvate kinase at yeast cell surface; Gcn4/Hog1/GlcNAc regulated; Hap43/polystyrene adherence induced; repressed by phagocytosis/farnesol; hyphal growth role; stationary phase enriched; flow model biofilm induced; Spider biofilm repressed
CAL0000121	4	<i>Orf19.7561/DEF1</i>	N	RNA polymerase II regulator; role in filamentation, epithelial cell escape, dissemination in RHE model; induced by fluconazole, high cell density; Efg1/hyphal regulated; role in adhesion, hyphal growth on solid media;
CAL0001571	4	<i>Orf19.5007/ACT1</i>	N	Actin; starvation; at polarized growth site in budding and hyphal cells; required for wild-type Cdc42 localization; Hap43-induced; Spider biofilm repressed

CAL0004558	4	<i>Orf19.1445/TEF1</i>	N	Translation elongation factor 1-alpha; at cell surface; binds human plasminogen; macrophage/pseudohyphal-induced; induced in RHE model of oral candidiasis, in clinical oral candidiasis isolates; possibly essential; Spider biofilm repressed
CAL0003655	3	<i>Orf19.930/PET9</i>	N	Mitochondrial ADP/ATP carrier protein involved in ATP biosynthesis; possible lipid raft component; 3 predicted transmembrane helices; flucytosine induced; ketoconazole-induced; downregulated by Efg1p
CAL0001672	3	<i>Orf19.1840</i>	N	Predicted lipid-binding ER protein; involved in ER-plasma membrane tethering; Spider biofilm induced
CAL0003176	3	<i>Orf19.3997/ADH1</i>	N	Alcohol dehydrogenase; oxidizes ethanol to acetaldehyde; at yeast cell surface; immunogenic in humans/mice; complements <i>S. cerevisiae</i> adh1 adh2 adh3 mutant; fluconazole, farnesol-induced; flow model biofilm induced; Spider biofilm repressed
CAL0002073	2	<i>Orf19.1126/CTA3</i>	N	Protein similar to <i>S. cerevisiae</i> Ede1p, which is involved in endocytosis; activates transcription in 1-hybrid assay in <i>S. cerevisiae</i>
CAL0006292	2	<i>Orf19.5597/POL5</i>	N	Putative DNA Polymerase phi; F-12/CO2 early biofilm induced
CAL0005797	2	<i>Orf19.6854/ATP1</i>	N	ATP synthase alpha subunit; antigenic in human/mouse; at hyphal surface; ciclopirox, ketoconazole, flucytosine induced; Efg1, caspofungin repressed; may be essential; sumoylation target; stationary phase-enriched; Spider biofilm repressed

CAL0003729	2	<i>Orf19.4657</i>	N	Ortholog(s) have phosphoprotein phosphatase activity, role in negative regulation of phospholipid biosynthetic process, nuclear envelope organization and Nem1-Spo7 phosphatase complex, integral to membrane, mitochondrion localization
CAL0000595	2	<i>Orf19.6285/GLC70</i>	N	Putative catalytic subunit of type 1 serine/threonine protein phosphatase; regulated by Shp1; induced in high iron; alternatively spliced intron in 5' UTR
CAL0002714	2	<i>Orf19.834</i>	N	Ortholog(s) have carbohydrate binding, mannosyl-oligosaccharide 1,2-alpha-mannosidase activity, role in ER-associated ubiquitin-dependent protein catabolic process and endoplasmic reticulum lumen localization
CAL0005867	2	<i>Orf19.6873/RPS8A</i>	N	Small 40S ribosomal subunit protein; induced by ciclopirox olamine; repressed upon phagocytosis by murine macrophage; 5'-UTR intron; Hap43-induced; Spider biofilm repressed
CAL0004607	2	<i>Orf19.7339/BGL22</i>	N	Putative glucanase; induced during cell wall regeneration
CAL0006245	2	<i>Orf19.5579</i>	N	Protein with a predicted double-strand break repair domain; Hap43-repressed gene
CAL0001878	2	<i>Orf19.4457/BNI4</i>	N	Protein required for wild-type cell wall chitin distribution, morphology, hyphal growth; not essential; similar to <i>S. cerevisiae</i> Bni4p (targeting subunit for Glc7p phosphatase, involved in bud-neck localization of chitin synthase III)

CAL0004511	2	<i>Orf19.7308/TUB1</i>	N	Alpha-tubulin; complements cold-sensitivity of <i>S. cerevisiae</i> tub1 mutant; <i>C. albicans</i> has single alpha-tubulin gene, whereas <i>S. cerevisiae</i> has two (TUB1, TUB3)
------------	---	------------------------	---	--

¹Approximately 330 mg protein extracts from 4 L cultures of strains SS2 (*ESP1/ESP1-TAP-ARG4, cdc20::URA3/MET3::CDC20-HIS1*) and AG 153 (*ESP1/ESP1*) incubated in +MC medium for 4 h were subjected to tandem affinity purification (Rigaut *et al.* 1999 ; Liu *et al.* 2010). Elutions were TCA-precipitated and run just into the resolving portion of an SDS PAGE gel. The compressed bands were stained with Coomassie blue, cut from the gel, and analysed using an LTQ-OrbitrapElite with nano-ESI.

²Peptides less than 2 were excluded from the results.

³Peptides identified in both the tagged strain and the untagged control strains were excluded from the results.

3.4 Orf19.955p is a *Candida*-specific protein with KEN and putative Destruction boxes

Since Orf19.955p was the most enriched interacting protein of Esp1p following Cdc14p, we focussed the remainder of our study on characterizing this factor and its function. *ORF19.955* contains a 978 bp open reading frame (ORF) encoding a potential protein of 325 amino acids and a predicted molecular weight of 36.4 kDa (Fig. 16). In a large-scale screen of *TET*-regulated strains, *ORF19.955* was reported to be essential (63), and yeast cells depleted of the protein showed mild filamentous growth and were impaired in their ability to form hyphae in response to serum. However, the function of Orf19.955p remains elusive. In performing a BLAST of the sequence against all known organisms (<http://blast.ncbi.nlm.nih.gov/Blast.cgi>) or against fungi only using the BLAST tool at the SGD data base (<http://www.yeastgenome.org>) (Table 9), no close homologues were identified except for several *Candida* species.

If Orf19.955p were a functional homologue of a securin, we predict that it may contain Destruction and/or a KEN box to mediate Cdc20p-dependent degradation, as well as CDK consensus phosphorylation sites, as do other securins (9). In agreement with this, one KEN box and several putative Destruction boxes were located within Orf19.955p (Fig. 16). While Pds1p from *S. cerevisiae* has several CDK phosphorylation sites (102), Orf19.955p contains one minimal consensus site (Fig. 16). Although securin homologues are not well conserved at the sequence level, they are charged proteins (99). Consistent with this, Orf19.955p is acidic, with a predicted PI of 4.79, and a hydropathy index of -0.96 (<http://www.candidagenome.org>). Thus, Orf19.955p is a *Candida*-specific protein with some features that are consistent with other securins.

```

1  MSSHIFKDIQ DKENELKTSG IRRKGIISNE NAGPLLSKDS NSRQVQQPQQ
51  TQQQQQQSKF TNKRIPLGGK NHNSNKLLLN RSQSSLNTPK TTQGITNVKP
101 PSLPKSNSSL GFSVVDQPT EQQKQLPQPF VVHNEQVLPV KRKLLQDTKD
151 ELSQNSKRVK LEKKESNANT FTDSLTKPTQ NVLAHVDDLQ TTISSKTDQL
201 NSSNLTHNDI NRNNVDPVKR NSRLKAIDDL VESHWQDPIE TIPETVGAEN
251 NNGEQLEELD IKFFSTPNES FDIGLDLENH LANNEQKLSL ELDFEDESNV
301 GEIPIIEGID EEIGLTSDDL DNLLG

```

Fig 16: Amino acid sequence of Orf19.955p.

Orf19.955p sequence obtained from the Candida Genome Data base (CGD; <http://www.candidagenome.org>), encoding a 36.4 kDa protein. Underlined are potential Destruction Box sequences (RXXLXXXXXX). A KEN box is highlighted in yellow. Minimal CDK consensus motif (S/T-P-X-R/K) is highlighted in purple.

Table 9: Fungal Blast of Orf19.955p¹.

Sequences with Significant Alignment	Score (bits)	E Value
ref XP_002420343.1 conserved hypothetical protein [Candida dubliniensis]	418.7	1.9e-118
gb EER30804.1 predicted protein [Candida tropicalis MYA-3404]	214.5	5.4e-57
gb EMG46289.1 hypothetical protein G210_3472 [Candida maltosa Xu316]	209.9	1.3e-55
ref XP_001548576.1 predicted protein [Botryotinia fuckeliana B05.10]	42.7	0.044
gb EMG50647.1 Activator 1 95 kDa subunit [Candida maltosa Xu316]	41.3	0.32
emb CCH40513.1 putative kinetochore protein [Wickerhamomyces ciferrii]	38.5	0.15
emb CAX45018.1 protein kinase, putative [Candida dubliniensis CD36]	36.7	1

¹ The amino acid sequence of *C. albicans Orf19.955p* was retrieved from the Candida Genome Database (<http://www.candidagenome.org>) and a fungal protein BLAST was conducted within the Saccharomyces Genome Database (<http://www.yeastgenome.org>).

3.5 Co-immunoprecipitation confirms a physical interaction between Orf19.955p and Esp1p.

In order to confirm the interaction between Esp1p and Orf19.955p, strains SS16 (*ESP1/ESP1-HA-URA3*), SS22 (*ORF19.955/ORF19.955-MYC-HIS1*) and SS29 and SS30 (*ORF19.955/ORF19.955-MYC-HIS1, ESP1/ESP1-HA-URA3*) were created (Figs. 17, 18, and 19). When Esp1p-*HA* was pulled down with anti-*HA* beads, Orf19.955p-*MYC* co-precipitated (Fig 20). However, Orf19.955p was not identified when control strain SS22 (*orf19.955::URA3/ORF19.955-MYC-HIS1*) was incubated with anti-*HA* beads. Thus, Esp1p and Orf19.955p physically interact.

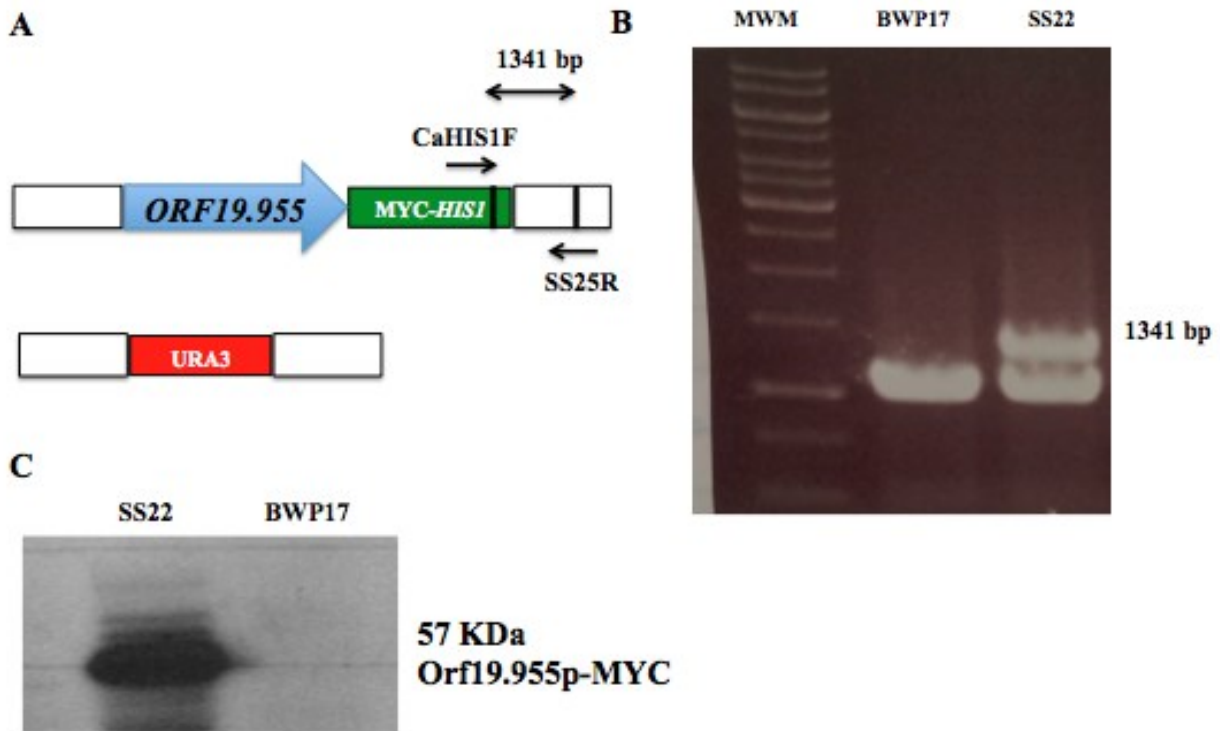


Fig 17: Confirmation of strain *orf19.955::URA3/ORF19.955-MYC-HIS1*.

(A, B) Map and ethidium bromide DNA gel showing PCR screening strategy to confirm proper integration of *ORF19.955-MYC* gene construct. Non specific bands are observed in the DNA gel in addition to the *ORF19.955-MYC* gene construct. Oligonucleotides *SS25R* and *CaHIS1F* generate a 1341 bp band for the *ORF19.955-MYC*-containing construct. Positive strains *SS22* (*orf19.955::URA3/ORF19.955-MYC-HIS1*) and the negative control strain *BWP17* (*ORF19.955/ORF19.955*) are demonstrated. Vertical bars delineate the length of the transforming construct. (C) Western blot showing confirmation of Orf19.955p-MYC expression.

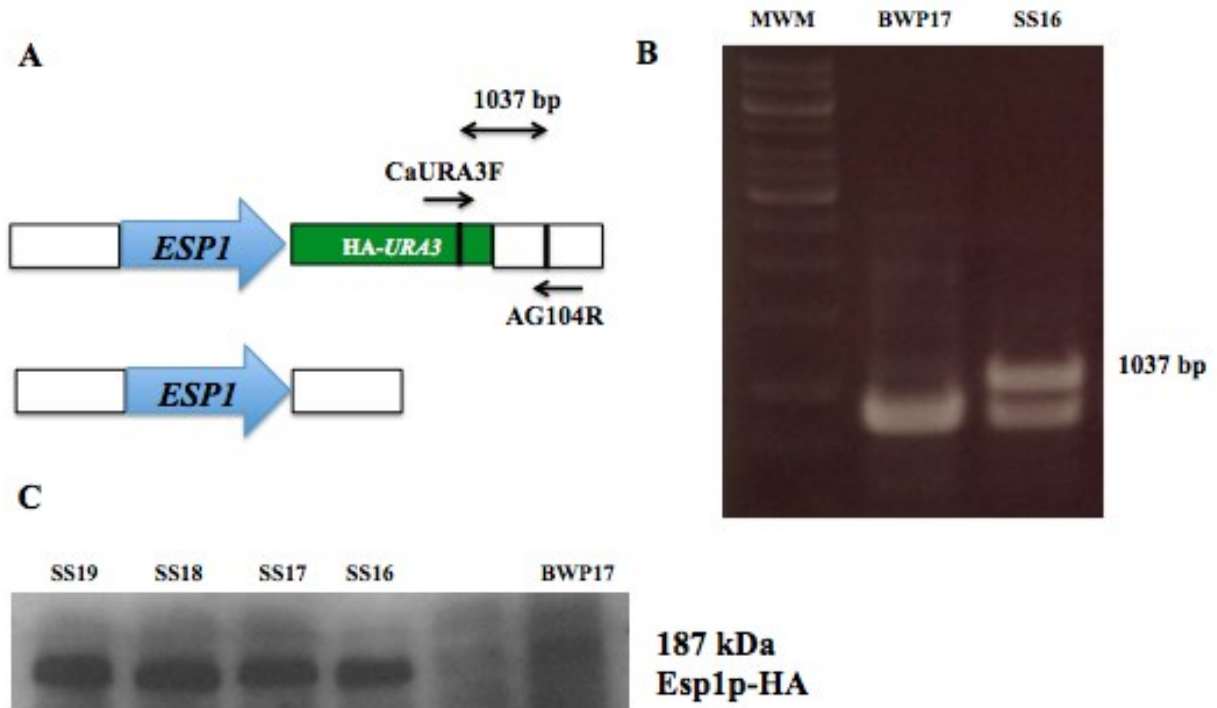


Fig 18: Confirmation of strain *ESP1/ESP1-HA-URA3*.

(A, B) Map and ethidium bromide DNA gel showing PCR screening strategy to confirm proper integration of *ESP1-HA* gene construct. Oligonucleotides AG104F and CaURA3R generate a 1037 bp band for the *ESP1-HA*-containing construct. Positive strains SS16-19 (*ESP1/ESP1-HA-URA3*) and the negative control strain BWP17 (*ESP1/ESP1*) are demonstrated. Vertical bars delineate the length of the transforming construct. (C) Western blot showing confirmation of Esp1p-HA expression.

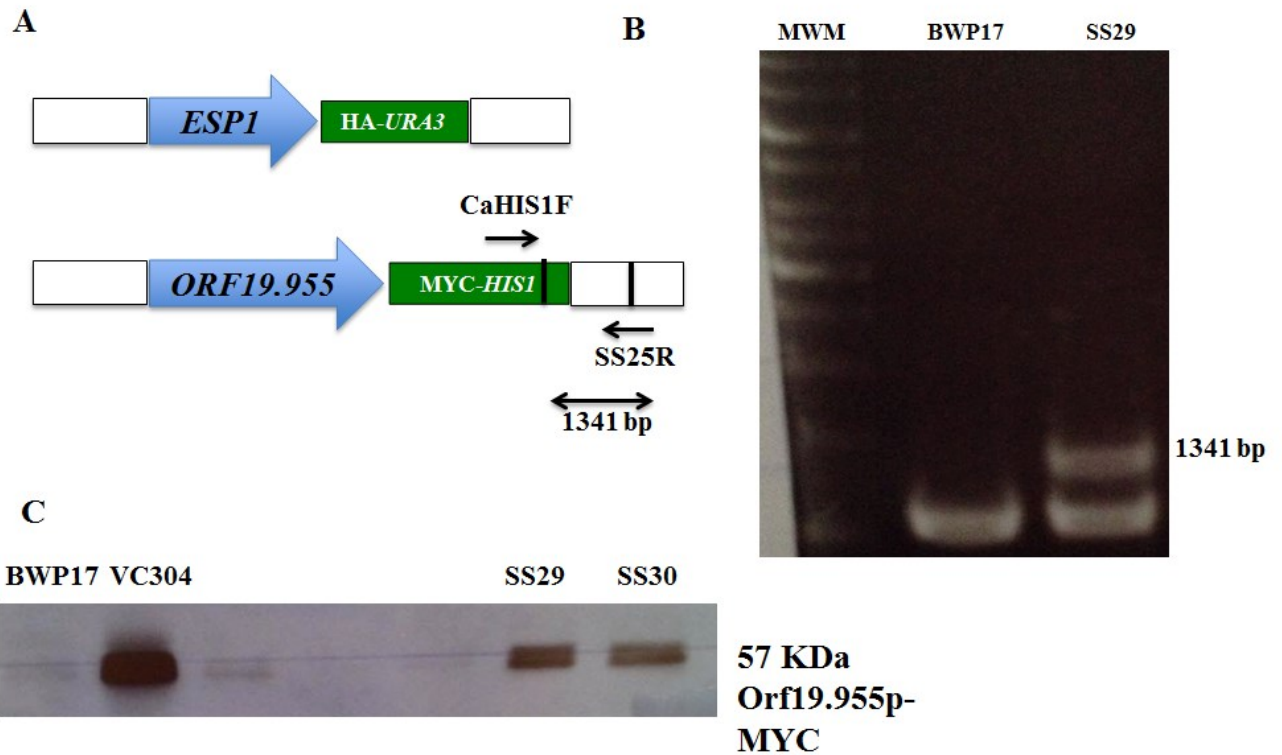


Fig 19: Confirmation of strain *ESP1/ESP1-HA-URA3*, *ORF19.955/ORF19.955-MYC-HIS1*. (A, B) Map and ethidium bromide DNA gel showing PCR screening strategy to confirm proper integration of *ORF19.955-MYC* gene construct into strain SS16 (*ESP1/ESP1-HA-URA3*). Oligonucleotides SS25R and CaHIS1F generate a 1341 bp band for the *ORF19.955-MYC*-containing construct. Positive strains SS29 and SS30 (*ESP1/ESP1-HA-URA3*, *ORF19.955/ORF19.955-MYC-HIS1*), positive control VC304 (*MBP1/MBP1-MYC-HIS1*), and the negative control strain BWP17 (*ESP1/ESP1*, *ORF19.955/ORF19.955*) are demonstrated. Vertical bars delineate the length of the transforming construct. (C) Western blot showing confirmation of Orf19.955p-MYC expression.

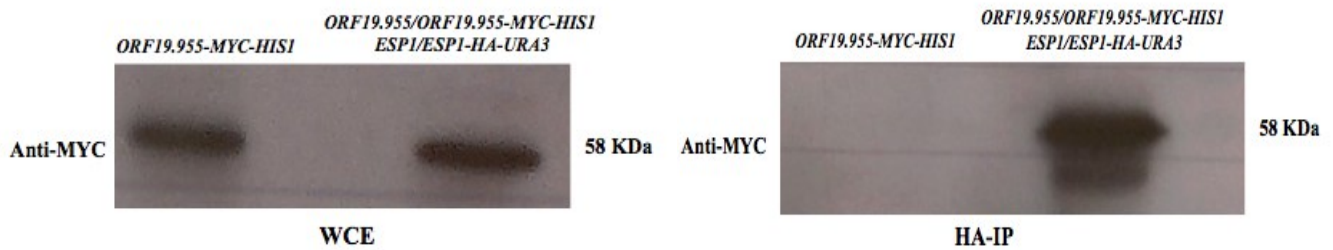


Fig 20: Co-immunoprecipitation demonstrates an interaction between Esp1p and Orf19.955p.

Western blots of whole cell extracts (WCE) and immune-precipitates of strains SS22 (*orf19.955::URA3/ORF19.955-MYC-HIS1*) and SS29 (*ORF19.955/ORF19.955-MYC-HIS1, ESP1/ESP1-HA-URA3*), using IgG sepharose (IgG-IP) or anti-HA agarose (HA-IP). 20 μ l of beads were incubated with 20 mg of protein overnight, washed, and boiled in SDS sample buffer to elute interacting proteins. Blots were incubated with anti-MYC antibody.

3.6 Depletion of Orf19.955p results in a pleiotropic phenotype including cells that are enlarged, multi-budded or in chains, or pseudohyphal

In *S. cerevisiae* cells depleted of Pds1 show single body of chromatin lying within large budded cells. In order to address the function of Orf19.955p, we created a strain (SS25; *orf19.955::URA3/MET3::ORF19.955-HIS1*) containing a single copy of the gene under control of the *MET3* promoter (Fig. 21). When plated on solid inducing medium (-MC) at 30°C for 48 h, colonies grew normally and appeared similar to those of control strain BH440 (*ORF19.955/ORF19.955, URA3+, HIS1+*) (Fig. 22A). However, on repressing medium (+MC), strain SS25 showed less growth, where colonies were small with some filamentation (Fig. 22A). After incubating in liquid- inducing or repressing medium for 5 h, strain SS25 resembled cells from control strain BH440 and were in various stages of yeast cell budding (Fig. 22B, Table 5). However, after 8 h in repressing medium, cells of strain SS25 appeared enlarged compared to control cells, and showed a pleiotropic phenotype, where 40% were multi-budded, pseudohyphal or in the form of chains of yeast cells (Table 6, Fig 22B). These phenotypes, including cell enlargement, were more prevalent after 24 h of repression (Fig. 22B). Similar results were obtained when Orf19.955p was down-regulated with doxycycline from the *TET* promoter (Figs. S3, S4, Tables S1, S2).

In order to investigate the effects of long-term depletion on growth, strains BH440 and SS25 were incubated on solid inducing or repressing medium for several days. Strains SS35 (*esp1::URA3/MET3::ESP1-HIS1*) and HCCA118 (*cdc5::URA3/MET3::CDC5-HIS1*) were included for comparison. In contrast to depletion of Cdc5p or Esp1p, which results in little to no growth, depletion of Orf19.955p resulted in some colony growth, although not as abundant as with control strain BH440 (Fig. 10). Similar results were obtained when Orf19.955p was depleted with doxycycline from the TET promoter (Fig. S3). In comparison, cells lacking Pds1p in *S. cerevisiae* are still viable but conditionally important for growth at elevated temperature (9, 22), and most mutants grown at restrictive temperature were large-budded cells with a single chromosomal mass of DNA, while the remaining cells were unbudded aneuploid cells (9). At permissive temperature, only 40% of cells could form colonies, which were often very small and/or heterogeneous in size (9). Thus, *ORF19.955* is important for growth and proper yeast

morphology, but it may not be an essential gene, in contrast to that reported for the *TET*-regulated strain (63). Further, its absence does not phenocopy absence of Esp1p in *C. albicans*, or absence of Pds1p in *S. cerevisiae*.

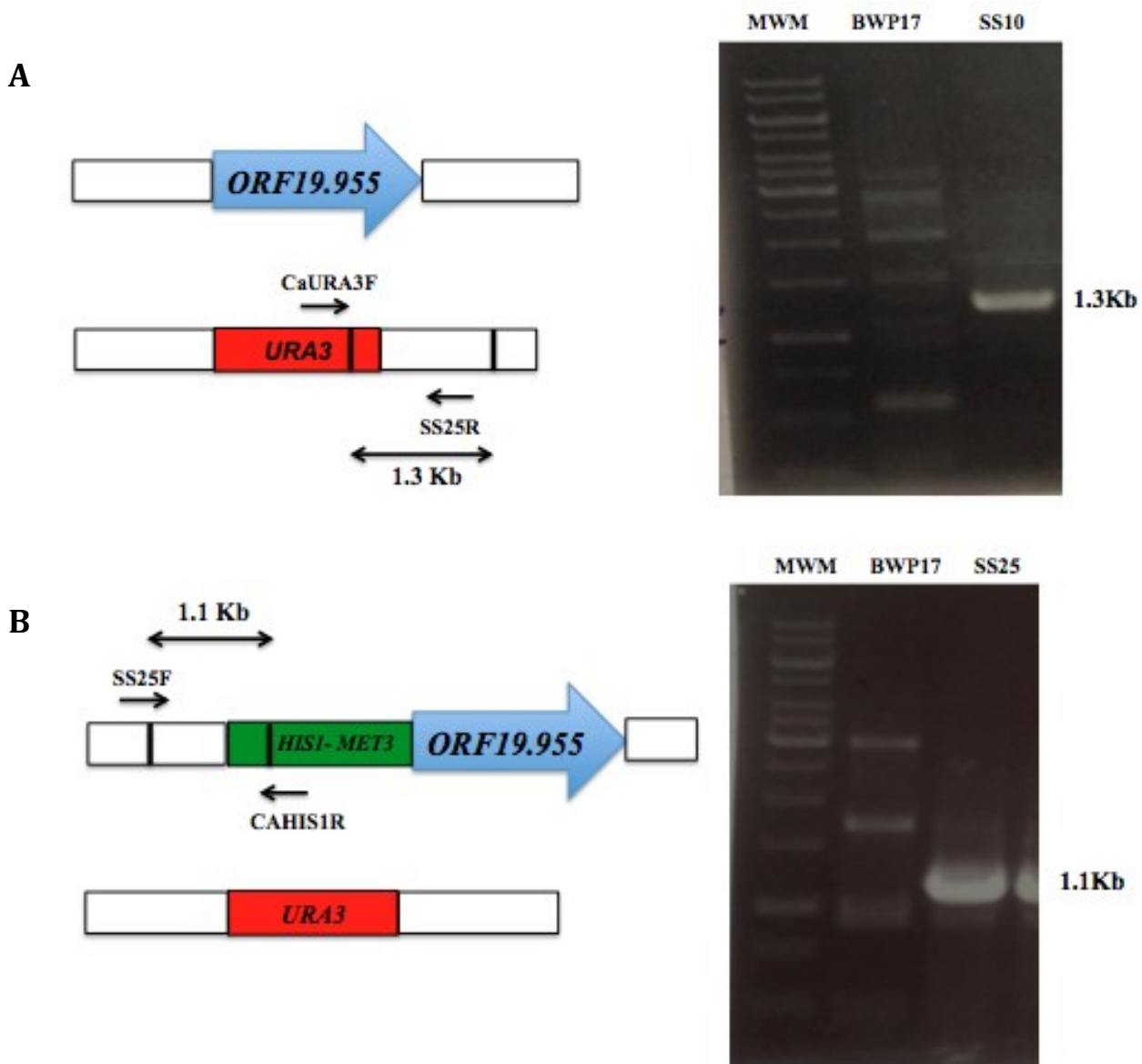


Fig 21: Confirmation of a *MET3::ORF19.955-HIS1/orf19.955::URA3* strain.

(A) Map and DNA gel showing the PCR screening strategy to confirm correct integration of the *URA3*-containing construct. Oligonucleotides SS25R and CaURA3F generate a 1.3 kb band for the *URA3* replacement. Positive strain SS10 and the negative control strain BWP17 are demonstrated. (B) Map and DNA gel showing the PCR screening strategy to confirm correct integration of the *MET3*-containing construct. Oligonucleotides SS25F and CaHIS1R generate a 1.1 kb band for the *MET3* integration. Positive strain SS25 and the negative control strain BWP17 are demonstrated. Vertical bars delineate the length of the transforming construct.

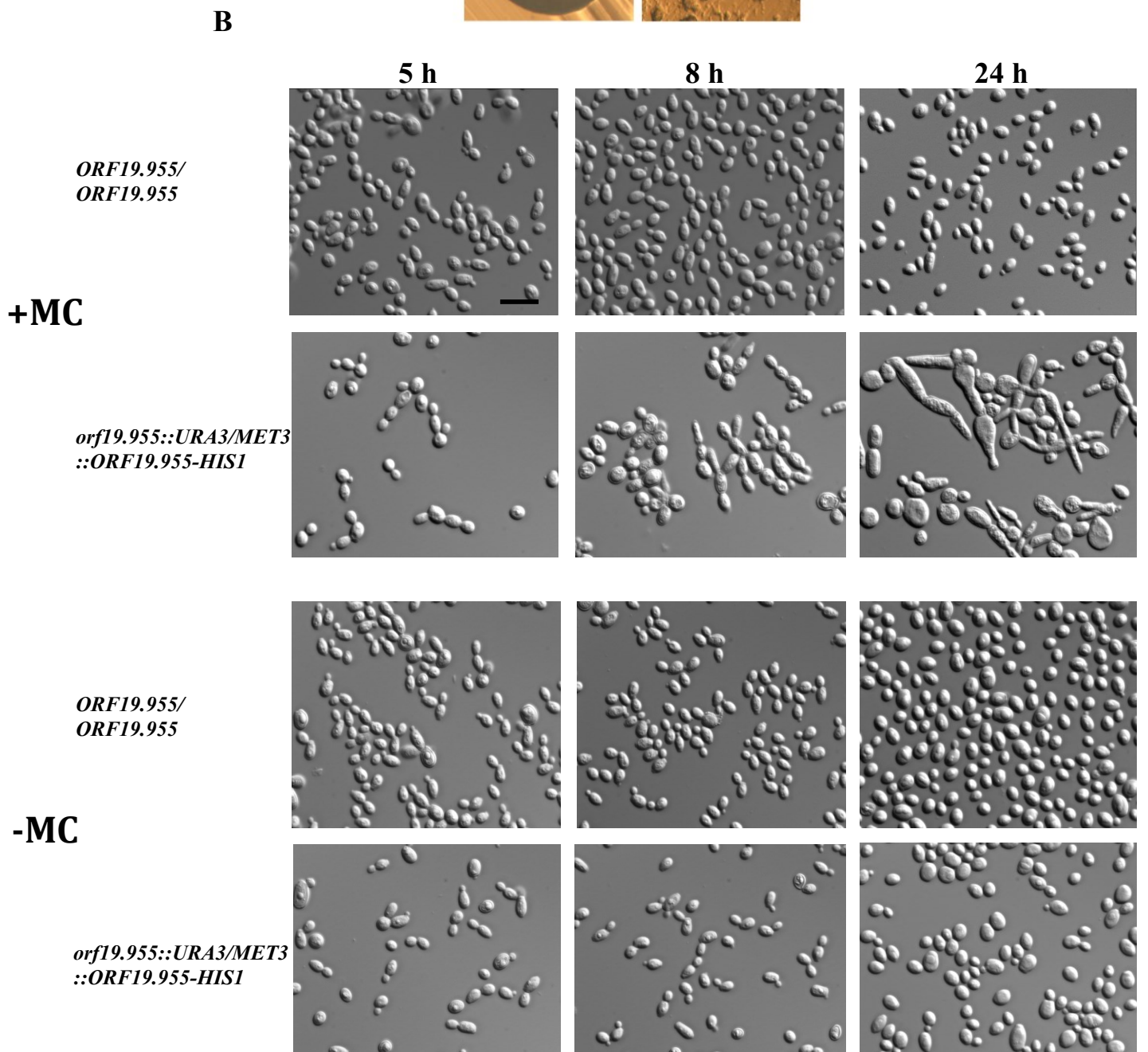
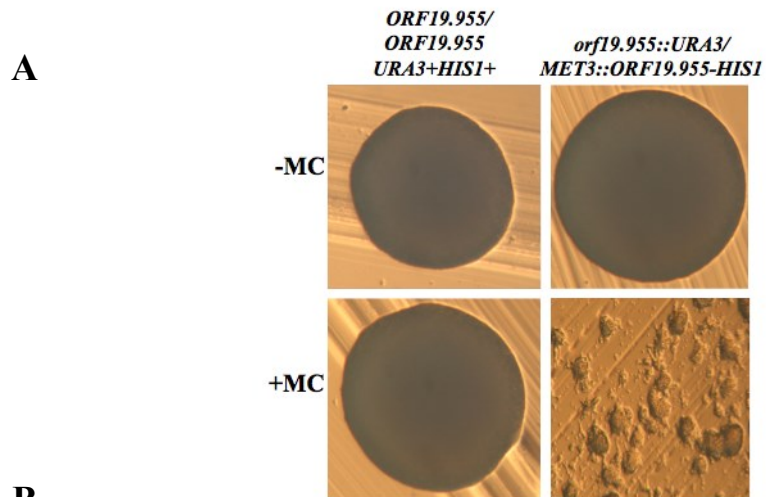


Fig 22: Yeast cells depleted of Orf19.955p demonstrate a pleiotropic phenotype including cell enlargement, multi-budding and pseudohyphal growth.

(A) Strains BH440 (*ORF19.955/ORF19.955*, *URA3+HIS1+*) and SS25 (*orf19.955::URA3/MET3::ORF19.955-HIS1*) were streaked onto repressing (+MC) or inducing (-MC) solid medium and incubated at 30°C for 24 h. (B) Overnight cultures of strains BH440 and SS25 were incubated at 30°C, diluted into inducing (-MC) or repressing (+MC) medium and incubated for the indicated time periods. Bar: 10 µm.

3.7 Absence of *Orf19.955* results in abnormalities in chromosome organization

In *S. cerevisiae*, *pds1* mutants displayed precocious separation of chromosomes in the presence of microtubule inhibitors. In the absence of the drugs, 75% of *PDS1* temperature-sensitive mutants grown at restrictive temperature were large-budded cells with a single chromosomal mass of DNA, while the remaining cells were unbudded aneuploid cells (9, 18). Spindles could form, but were not fully elongated as most large-budded cells contained bar spindles characteristic of metaphase or were shorter in length, and cytokinesis was not impaired. If *Orf19.955p* functions as a securin in a similar manner as *Pds1p*, its absence should influence chromosome separation. In order to test this, cells of strains SS25 (*orf19.955::URA3/MET3::ORF19.955-HIS1*) and BH440 (*ORF19.955/ORF19.955, URA3+HIS1+*) were incubated in inducing or repressing medium for 5 h or 8 h, fixed and stained with DAPI. After 5 h in repressing medium, strains BH440 and SS25 were similar in that 18.7 and 23.7% of cells, respectively, were in mitosis, where DAPI-stained chromatin was predominantly located as a single mass within one half of a large-budded cell, or through the bud neck and was not fully separated (Fig. 23, Table 5). By 8 h, fewer cells appeared to be in mitosis in strain SS25 vs BH440 (Table 6). Rather, 40% were multi-budded or chains of yeast cells, in which all compartments contained a mass of chromosomal DNA (Table 6, Fig. 23), suggesting that chromosome separation was not impaired. However, 59% (n=114) of cells of strain SS25 showed diffuse or fragmented DAPI staining, and some cells showed no staining at all, compared to 3.0% (n=100) of cells of strain BH440, suggesting abnormalities in chromosome organization and possibly separation. In comparison, 16.8 (n=119) or 24.5 (n=106) % of cells from strains SS25 and BH440, respectively, showed these defects in –MC inducing medium. Similar results were obtained with strain *orf19.955::URA3/TET::ORF19.955-HIS1* incubated in YPD medium containing doxycycline (+DOX: 61.8% (n=123) vs. –DOX: 22.8% (n=127) (Fig S4).

In order to further determine whether absence of *Orf19.955p* influences a specific stage of mitosis, spindles were analyzed by tagging β -tubulin with GFP in strain SS25, resulting in strain SS38 (Fig. 6). After incubation in inducing medium for 7 h, 22.7% of cells (n=110) contained short bar spindles characteristic of metaphase and early anaphase, while 11.8% contained telophase spindles (Fig. 24). Similar results were obtained in repressing medium, where 18.8%

(n=85) of cells contained short bar spindles, while 10.6% contained a telophase spindle (Fig. 24). However, many spindles and cytoplasmic microtubules appeared mispositioned, disrupted or disorganized. Although this remains to be quantified. Thus, although absence of Orf19.955p does not prevent separation of chromosomes, in contrast to presence of Pds1p, it does influence chromosome organization, raising the possibility that it could function as a securin in *C. albicans*, albeit with some mechanisms different from that of Pds1p.

3.8 Orf19.955p levels increase in response to MMS-mediated DNA damage

Pds1p in *S. cerevisiae* is required to prevent anaphase initiation and mitotic exit in response to DNA damage (9). Under these conditions, it becomes phosphorylated in a Mec1p and Chk1p-dependent manner (35, 36). In order to determine whether Orf19.955p is functioning in a similar manner in *C. albicans*, strain SS22 (*ORF19.955/ORF19.955-MYC-HIS1*) was incubated in the presence or absence of the DNA-damage inducing drug methyl methanesulfate (MMS) for 5 h, collected and processed for Western blotting to detect possible phosphorylation-dependent band shifts (Fig. 25). The mobility of Orf19.955p-MYC was similar in the presence vs. absence of MMS. However, the levels of the protein were higher in the presence vs. absence of the drug (Fig. 25). MMS treatment arrests mitosis and causes *C. albicans* yeast cells to switch to filamentous growth (103). It is thus possible that the increase in Orf19.955p levels is due to a higher proportion of cells being in mitosis in the presence of MMS. However, we cannot rule out the possibility of an induction of Pds1p levels, and thus a possible link between Orf19.955p and the cellular response to DNA damage.

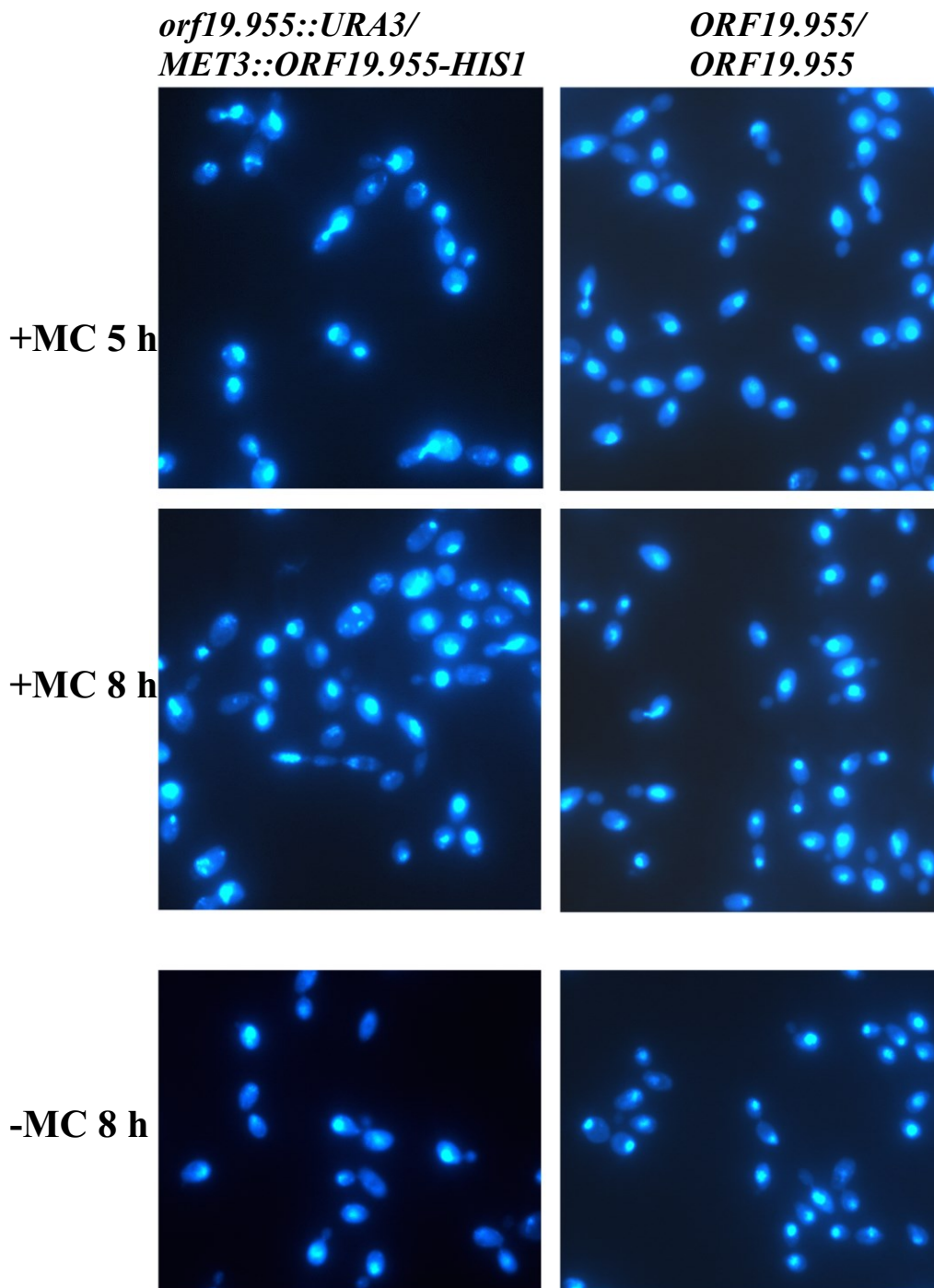


Fig 23: Cells depleted of Orf19.955p demonstrate abnormal chromosomal segregation including fragmentation.

Strains BH440 (*ORF19.955/ORF19.955*, *URA3+HIS1+*) and SS25 (*orf19.955::URA3/MET3::ORF19.955-HIS1*) were incubated in inducing (-MC) or repressing (+MC) medium for 5 or 8 h, fixed and stained with DAPI. Bar: 10 μ m.

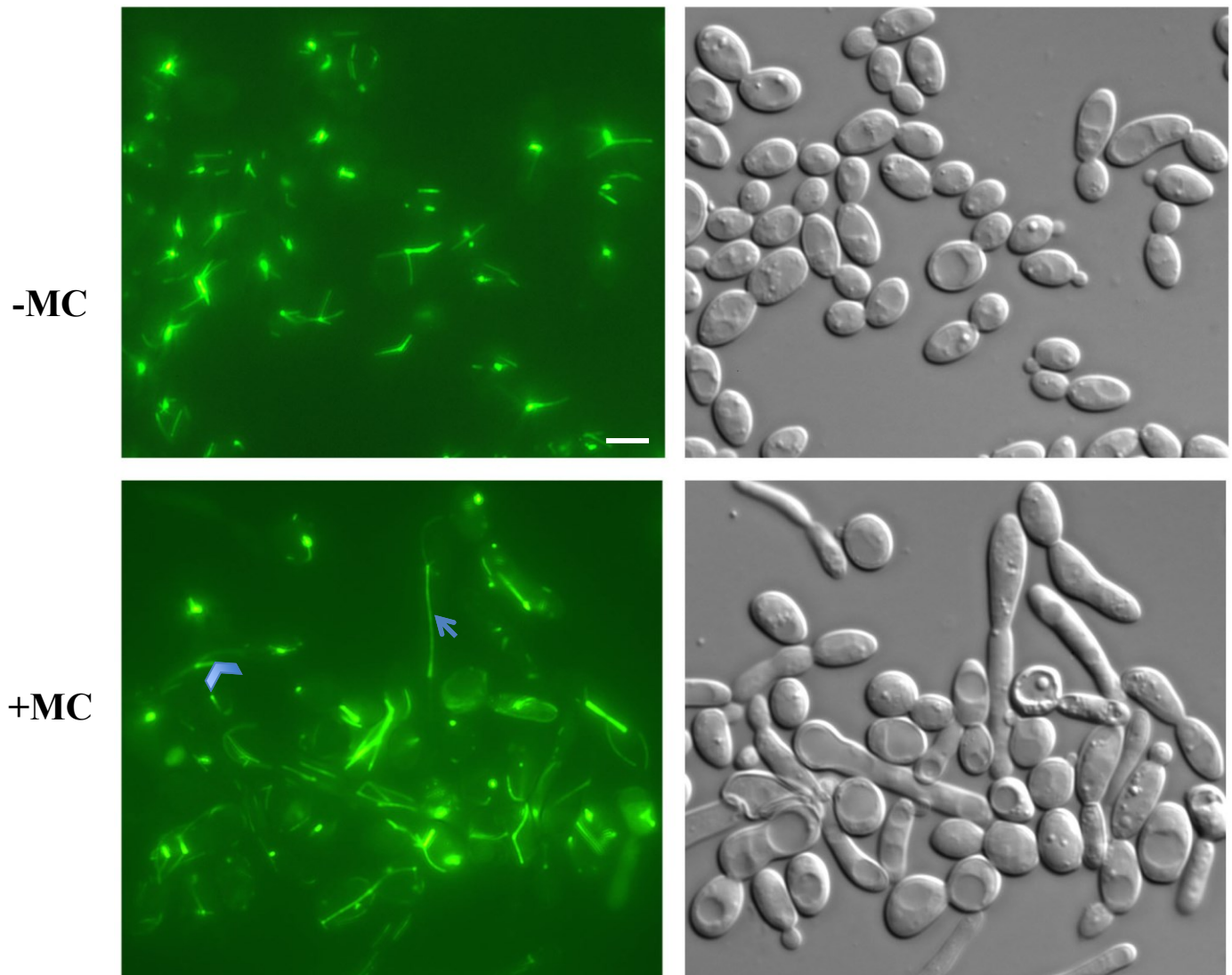


Fig. 24: Cells depleted of Orf19.955p demonstrate abnormalities in spindle and cytoplasmic microtubule organization and position in a proportion of cells.

Strain SS25 (*orf19.955::URA3/MET3::ORF19.955-HIS1*) was incubated in inducing (-MC) or repressing (+MC) medium for 7 h, and imaged live on a LeicaDM6000B microscope. Bar: 10 μm . An arrow denotes a telophase spindle and an arrowhead denotes a metaphase or early anaphase spindle.

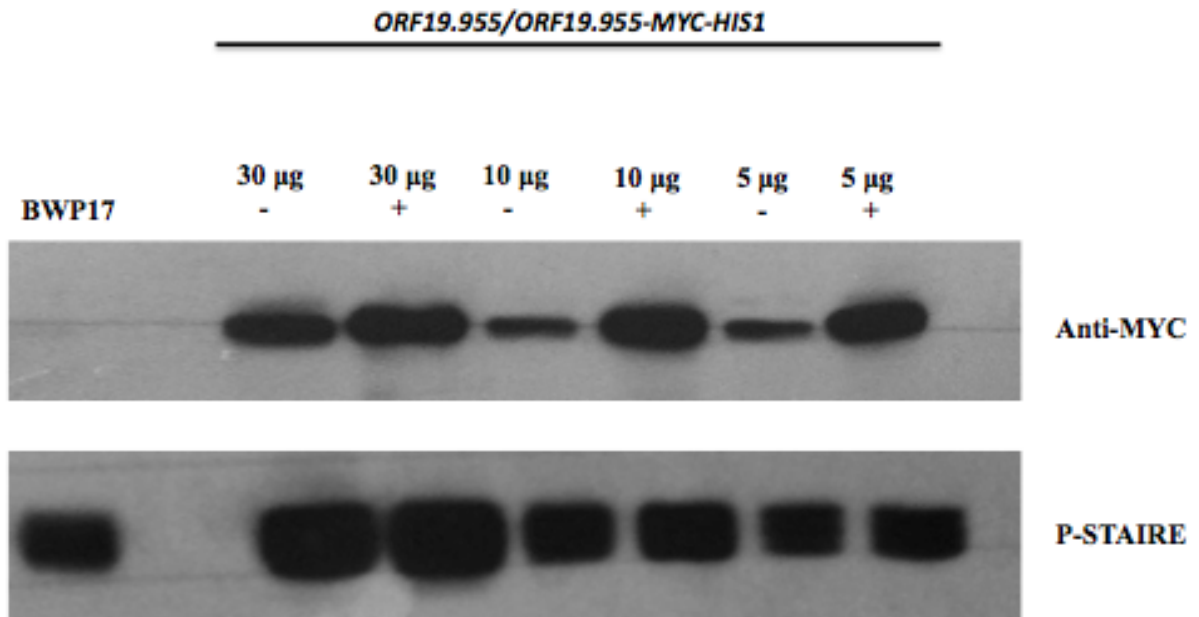


Fig. 25: Orf19.955p levels increase following treatment with methyl methanesulfate (MMS). Strain SS22 was incubated in the presence or absence of 0.02% MMS for 5 h, collected and processed for Western blotting. Treated (+) and untreated (-) samples (30, 10 or 5 μ g) were loaded onto a 10% SDS gel. Blots were incubated with anti-MYC antibody, stripped then incubated in anti-pSTAIRES antibody.

4.0 Discussion

Elucidating the networks that govern mitosis in the fungal pathogen *C. albicans* will further our understanding of the basic biology of this organism, provide insights on the regulation of its cell proliferation, and identify potential new targets for anti-fungal therapies. However, we currently lack a comprehensive understanding of the various mechanisms that control mitosis in *C. albicans*. We previously characterized the APC/C cofactors Cdc20p and Cdh1p in *C. albicans*, and demonstrated that they were conserved in being important for the metaphase-to-anaphase transition and mitotic exit (90). However, the mutant cells showed some unexpected phenotypes, and *C. albicans* lacks a sequence homologue of a securin, a conserved target of Cdc20p that regulates the activity of separase, suggesting that Cdc20p and Cdh1p may also have novel functions and/or mechanism of action in *C. albicans*. This work focusses on the mechanisms of action of Cdc20p and determining how it may regulate the metaphase-to-anaphase transition. In order to address this question, we hypothesized that *C. albicans* contains a divergent securin, which may be revealed through identifying the interacting factors of a conserved securin target, separase. *C. albicans* contains a separase homologue, *ESPI*, but it had not been functionally characterized. Here, we provide the first evidence that Esp1p is required for chromosome segregation in *C. albicans*. We subsequently identified its interacting factors using affinity purification followed by mass spectrometry, and the data revealed strong enrichment of Orf19.955p, a protein of unknown function with close homologues only in *Candida* species. Orf19.955p is not essential, but important for yeast cell growth, phenotype and chromosome organization, and it contains sequences that could potentially mediate Cdc20p-dependent degradation. However, its absence does not phenocopy absence of Esp1p, unlike the situation with cells lacking Pds1p or Esp1p in *S. cerevisiae* (9). If Orf19.955p represents a securin in *C. albicans* that regulates separase, we predict that the manner in which it does this is not identical to that of Pds1p in *S. cerevisiae*. If not a securin, Orf19.955p merits further study as a novel factor having a strong influence on growth and chromosome organization in an important fungal pathogen of humans.

4.1 *C. albicans* Esp1p may be a functional separase

Separases are highly conserved regulators of chromosome segregation at the metaphase-to-anaphase transition (14). They function to liberate cohesin subunit Scc1p from chromatin, allowing sister chromatid separation (14). *C. albicans* contains all the homologues of a conserved cohesion complex, including subunits Smc1p, Smc3p, and Scc1p. However, functional studies on this complex and subunits are lacking. *C. albicans* also contains a sequence homologue of a separase, *ESP1*. A large-scale mutant screen of *C. albicans* strains under control of the *TET* promoter recently demonstrated that *ESP1* was essential and its repression resulted in filamentous growth (63). However, this report did not investigate a putative role in mitosis. Here, we provide the first functional data that supports a role for Esp1p in chromosome segregation at the metaphase-to-anaphase transition. First, cells depleted of the protein were predominantly in a large-budded state, similar to that reported for *esp1* mutants in *S. cerevisiae* (16) and expected if cells were blocked in metaphase. Second, a majority of cells demonstrated unsegregated chromosomes that remained as a single mass in one half of the cell doublet, similar to *esp1* mutants in *S. cerevisiae* (16). Third, localization of tubulin revealed a higher proportion of cells with visible metaphase spindles and a lower proportion with telophase spindles in the absence vs. presence of Esp1p, as expected if cells were blocked in metaphase. However, many cells lacked visible spindles due to weak signal or the presence of extensive cytoplasmic microtubule arrays, and in some cases, bar spindles appeared split. Consistent with this, *esp1* mutants in *S. cerevisiae* show spindle abnormalities, where some cells contained short bar metaphase spindles, and others contained discontinuous, faint or curvilinear microtubule arrays (16). Fourth, affinity purification of Esp1p revealed putative interactions with Cdc14p, a phosphatase involved in regulating mitotic exit in *S. cerevisiae* (25) and *C. albicans* (90). Although Esp1p does not interact with Cdc14p directly in *S. cerevisiae*, it indirectly acts on it through down-regulating the phosphatase PP2A^{cdc55}, which in turn binds and phosphorylates the Cdc14 inhibitor Net1p to allow initial release of Cdc14p from the nucleolus during early anaphase (7). Thus, Esp1p from *C. albicans* functions in a manner consistent with a separase. Future experiments to confirm this role could involve determining whether Scc1p interacts with Esp1p and is released by it from chromatin; investigate the dynamic localization of Esp1p, and image live cells with tagged chromosomes in

order to deduce the timing and patterns of chromosome separation in the presence and absence of Esp1p, for example.

4.2 Putative *C. albicans* Esp1p-interacting proteins include previously unidentified factors, suggesting additional functions

Separases have additional functions in other organisms, including duplication of centrosomes in humans (14) and reorganizing epithelial cells in *D. melanogaster* (26), for example. In *S. cerevisiae*, Esp1p also stabilizes the anaphase spindle through cleaving the kinesin-associated factor Slk19p (8), and regulates mitotic exit and Cdc14p release as part of the FEAR pathway (7). Accordingly, Esp1p in *S. cerevisiae* binds additional factors related to these functions, including the polo kinase Cdc5p, Slk19p and the phosphatase PP2A^{cdc55} (24, 25), for example. However, data obtained from affinity purification of Esp1p followed by mass spectrometry in *C. albicans* did not reveal such interactions, despite the fact that *C. albicans* has close sequence homologues of Slk19p, Cdc5p and PP2A. This could be due to the fact that Esp1p does not interact with these proteins or that there are methodological factors involving the affinity purification such as solutions being too stringent. Some spindles in Esp1p-depleted cells were abnormal, suggesting an additional role in spindle organization, but this requires further quantification and analysis, and Slk19p has not yet been characterized in *C. albicans*. Alternatively, the affinity purification data from exponential-growing cells revealed interactions with histones including H2B, H4 and a homologue of the histone deacetylase complex factor Rco1p, for example, raising the possibility of a novel role in regulating nucleosome organization and gene expression. These factors were not pulled out, however, when Esp1p was purified from cells blocked in mitosis via depletion of Cdc20p. We can also not rule out the possibility that the interaction between Esp1p and Cdc14p in *C. albicans* is unrelated to the functional association observed between these factors in *S. cerevisiae*, and may reflect direct Esp1p regulation of Cdc14p for an unknown function. Thus, Esp1p may have conserved but also novel functions in *C. albicans*, consistent with several other mitotic regulators in *C. albicans*, including Cdc5p (88), Cdc14p (73) Dbf4p (73), and Cdh1p (90). Collectively, the results further underscore differences in the mitotic machinery in *C. albicans* relative to other systems, including mammals.

Another notable and distinct feature of Esp1p includes the fact that yeast lacking the protein initially blocked as large-budded cells that acquired more filamentous growth at much later time points. In contrast, repression of other essential genes required for early stages of mitosis in *C. albicans* results in yeast buds switching into highly elongated filaments at very early stages (73). For example, depletion of the mitotic polo-like kinase Cdc5p results in an initial block in metaphase, but by 4 h, elongated bud growth is evident. The cells continue to grow such that by 8 h, most cells are highly elongated filaments that change fate to the hyphal cell fate, possible due to maintenance of polarized growth and feedback on the hyphal signaling pathways (89). Yeast buds initially grow in a polar manner and switch to isometric growth in early mitosis, although the regulation of this switch in *C. albicans* is not known (69). The block in mitosis is hypothesized to prevent the switch in growth mode, resulting in elongated buds that eventually adapt a hyphal fate, which may provide a growth advantage for the pathogen in the different stressful environments of the host (72, 73, 89). The Esp1p-depleted phenotype does not agree with this model and suggests that other mechanisms are involved, and/or that Esp1p may influence aspects of the polar growth machinery itself. Overall this highlights the multiple strategies that *C. albicans* can employ to alter its phenotype and growth mode.

4.3 Orf19.955p binds Esp1p and influences chromosome organization

Many organisms contain a securin as part of the regulatory network governing the metaphase-to-anaphase transition. These proteins are not well conserved at the sequence level, but in organisms where they have been characterized, there is sufficient homology to be identified with Blast searches. Since *C. albicans* lacked a sequence homologue of any known securin, we reasoned that it may contain a functional securin homologue that is novel in sequence and could be uncovered through purifying conserved securin interacting proteins. Since we could not successfully tag Cdc20p with TAP, we alternatively focused on affinity-purifying the separase Esp1p, and identified Orf19.955p. Orf19.955p is a candidate securin based on many features. First, it was one of the most enriched peptides that co-purified with Esp1p, and was novel in sequence, in agreement with our model. Second, Orf19.955p contains putative destruction and KEN boxes, and contains a weak consensus motif for CDK phosphorylation,

similar to other securins that are targeted for destruction by Cdc20p/APC/C, and regulated in part by CDK phosphorylation (104). Third, Orf19.955p is acidic and charged, similar to other securins (99). Fourth, it influences growth and chromosome organization.

However, Orf19.955p demonstrated some features that were not expected if functioning in a similar manner as Pds1p in *S. cerevisiae* (9), including the null phenotype. In Orf19.955p-depleted cells, chromosomes could clearly segregate, but frequently appeared diffuse, disorganized and at times fragmented, and some cell compartments or cells were missing chromosomes altogether. Thus, Orf19.955p clearly has an influence on chromosome organization and possibly separation, but not in a manner as demonstrated by Pds1p. In contrast, many *pds1* cells phenocopied *esp1* cells in that they contained a single mass of unsegregated chromosomes. One may predict that if a securin is absent, precocious chromosome segregation should result from liberated separase. However, this does not occur in *S. cerevisiae* because Pds1p has both an inhibitory and activating influence on Esp1p (14). Thus, if Orf19.955p is a securin, it is not functioning in an identical manner as Pds1p in *S. cerevisiae*. We also cannot rule out the possibility that *C. albicans* does not have a securin, and uses alternative mechanisms to regulate Esp1p and chromosome separation. In this case, Orf19.955p remains attractive for further study as it represents a novel, fungal-specific factor that strongly affects yeast growth and chromosome organization, yet is not essential.

O'Meara et al. (2015) reported that *ORF19.955* was essential, based on repression from the TET promoter. When we used the same dose of doxycycline for the TET-regulated strain, some residual albeit weak growth was detected on plates, and many cells were capable of chromosome segregation. We obtained similar results when using the *MET3*-regulated strain to repress *ORF19.955*. We suggest that Orf19.955p is important for growth but cells lacking the protein can be viable, depending on the organization of their chromosomes and whether they received the full complement. Successful construction of a deletion strain would clarify this issue, which is underway. It was also previously reported that depletion of Orf19.955p impaired the ability of yeast cells to form hyphae under hyphal-inducing conditions (63). Based on this and our demonstration of the cellular phenotypes of Orf19.955p depletion, we cannot rule out the possibility that Orf19.955p has other or additional functions, including an influence on the polar

growth machinery. Since the cellular phenotype was pleiotropic, it is not clear if the primary defect of Orf19.955p depletion was at the level of chromatin organization, which in turn influenced cell phenotype. Future experiments to further address the function of Orf19.955p and determine whether it is a securin include: 1) investigating whether *ORF19.955* can complement the *S. cerevisiae pds1* mutant; 2) determine whether Orf19.955p is a target of Cdc20p through conducting a Co-IP; 3) mutagenize the KEN and/or Destruction boxes and determine whether a non-degradable form can block cells in metaphase, similar to the situation with Pds1p in *S. cerevisiae*; 4) determine Orf19.955p levels during the course of a cell cycle to see whether it is cyclic and degraded in metaphase, as predicted for a securin; 5) identify interacting proteins of Orf19.955p using affinity purification followed by mass spectrometry; 6) localize the protein and determine any co-localization with Esp1p; 7) image live cells with tagged chromosomes in order to deduce the timing and patterns of chromosome separation in the presence and absence of Orf19.955p; and 8) conduct virulence assays with an *orf9.955/orf19.955* null strain if the gene is not essential.

4.5 Summary

Collectively our results provide new insights on factors that may be involved in regulating a key stage of mitosis, the metaphase-to-anaphase transition, and thus cell proliferation in *C. albicans*. Our work further underscores differences in the mitotic machinery in *C. albicans* relative to other systems, including mammals, which may be exploited for the purposes of new drug target discovery. In this context, Orf19.955p may represent an attractive target, due to the fact that it is fungal-specific, and strongly influences growth and aspects of chromosome organization. That it may not be essential is also an advantage, since drug resistance can develop from targeting genes essential for growth. Targeting two non-essential genes, which may be synthetically lethal, with different drugs can be beneficial in this regard (105).

5.0 References

1. Behl, C. and Ziegler, C. Cell Cycle: The Life Cycle of a Cell. SpringerBriefs in Molecular Medicine. 2007;9-19.
2. De Souza C. P., Osmani S. A. Mitosis, not just open or closed. Eukaryot. Cell. 2007;6:1521–1527.
3. Kitamura E., Tanaka, K., Kitamura, Y., Tanaka, TU. Kinetochore microtubule interaction during S phase in *Saccharomyces cerevisiae*. Genes Dev. 2007;21:3319-30.
4. Dabrieva, Z., Pic-Taylor, A., Boros, J., Spanos, A., Geymonat, M., Reece, R.J., Sedgwick, S.G., Sharrocks, A.D., Morgan, B.A. Cell Cycle-Regulated Transcription through the FHA Domain of Fkh2p and the Coactivator Ndd1p. Curr. Biol. 2003;13:1740-1745.
5. Morgan, D.O. The Cell Cycle Principles of Control. New Science Press Ltd. 2007;96-98.
6. Marston, A.L. Chromosome segregation in budding yeast: Sister chromatid cohesion and related mechanisms. Genetics. 2014;196:31-63.
7. Weiss, E.L. Mitotic exit and separation of mother and daughter cells. Genetics. 2012;192:1165-1202.
8. Peters, J.M., Tedeschi, A., Schmitz, J. The cohesin complex and its roles in chromosome biology. Genes Dev 2008;22:3089-3114
9. Yamamoto, A., Guacci, V., Koshland, D. Pds1p is required for faithful execution of anaphase in the yeast *Saccharomyces cerevisiae*. J. Cell Biol. 1996;133:85-97.
10. Yanagida, M. Cell cycle mechanisms of sister chromatid separation; roles of Cut1/separin and Cut2/securin. Genes to cells. 2000;5:1-8.
11. May, G. S., McGoldrick, C. A., Holt, C. L. and Denison, S. H. The *bimB3* mutation of *Aspergillus nidulans* uncouples DNA replication from the completion of mitosis. J. Biol. Chem. 1992;267:15737-15743.
12. Waizenegger, I.C., Gimenez-Abian, J.F., Wernic, D., Peters, J.M. Regulation of Human Separase by Securin Binding and Autocleavage. Curr. Biol. 2002;12:1368-1378.
13. Siomos MF., Badrinath A., Pasierbek P., Livingstone D., White J., Glotzer M., Nasmyth K. Separase is required for chromosome segregation during meiosis I in *Caenorhabditis elegans*. Curr. Biol. 2001;11:1825-1835.
14. Moschou, P. and Bozhkov, P.V. Separases: biochemistry and function. Physiol. Plant. 2012;145:67-76.
15. Uhlmann F., Lottspeich, F., Nasmyth, K. Sister-chromatid separation at anaphase onset is promoted by cleavage of the cohesin subunit Scc1. Nature. 1999;400:37-42.
16. McGrew, J.T., Goetsch, L., Byers, B., Baum, P. Requirement for ESP1 in the Nuclear Division of *Saccharomyces cerevisiae*. Molecular Biology of the Cell. 1992;3:1443-1445.
17. Baum, P., Yip, C., Goetsch, L., Byers, B. A yeast gene essential for regulation of spindle pole duplication. Mol. Cell. Biol. 1988;8:5386-5397.

18. Ciosk, R., Zachariae, W., Michaelis, C., Shevchenko, A., Mann, M., Nasmyth, K. An ESP1/PDS1 complex regulates loss of sister chromatid cohesion at the metaphase to anaphase transition in yeast. *Cell*. 1998;93:1067-1076.
19. Sumara, I., Vorlaufer, E., Stukenberg, P.T., Kelm, O., Redemann, N., Nigg, E.A., Peters, J.M. The Dissociation of Cohesin from Chromosomes in Prophase Is Regulated by Polo-like Kinase. *Mol Cell*. 2002;9:515-525.
20. Uhlmann F., Wernic, D., Poupart, M.A., Koonin, E.V., Nasmyth, K. Cleavage of Cohesin by the CD Clan Protease Separin Triggers Anaphase in Yeast. *Cell*. 2000;103:375-386.
21. Park, S., Isaacson, R., Kim, H.T., Silver, P.A., Wagner, G. Ufd1 exhibits the AAA-ATPase fold with two distinct ubiquitin interaction sites. *Structure*. 2005;13:995-1005.
22. Alexandru, G., Uhlmann, F., Mechtler, K., Poupart, M.A., Nasmyth, K. Phosphorylation of the cohesin subunit Scc1 by Polo/Cdc5 kinase regulates sister chromatid separation in yeast. *Cell*. 2005;105:459-72.
23. Sullivan, M., Lehane, C., and Uhlmann, F. Orchestrating anaphase and mitotic exit: separase cleavage and localization of Slk19. *Nat. Cell Biol.* 2001;3: 771–777.
24. Sullivan, M. and Uhlmann, F. A non-proteolytic function of separase links the onset of anaphase to mitotic exit. *Nat. Cell Biol.* 2003;5: 249–254.
25. Stegmeier, F., Visintin, R., Amon, A. Separase, polo kinase, the kinetochore protein Slk19, and Spo12 function in a network that controls Cdc14 localization during early anaphase. *Cell*. 2002;108:207-220.
26. Jäger, H., Herzig, A., Lehner, C.F., Heidmann, S. *Drosophila* Separase is required for sister chromatid separation and binds to PIM and THR. *Genes & Dev.* 2001;15:2572-2584.
27. Hornig, N.C.D., Knowles, P.P., McDonald, N.Q., Uhlmann, F. The Dual Mechanism of Separase Regulation by Securin. *Curr. Biol.* 2002;12:973-982.
28. Jensen, S., Segal, M., Clarke, D.J., Reed, S.I. A novel role of the budding yeast separin Esp1 in anaphase spindle elongation: evidence that proper spindle association of Esp1 is regulated by Pds1. *J. Cell. Biol.* 2001;152:27-40.
29. Yaakov, G., K. Thorn, and D. O. Morgan. Separase biosensor reveals that cohesin cleavage timing depends on phosphatase PP2A(Cdc55) regulation. *Dev. Cell*. 2012;23: 124–136.
30. Jallepalli, P.V., Waizenegger, I.C., Bunz, F., Langer, S., Speicher, M.R., Peters, J.M., Kinzler, K.W., Vogelstein, B., Lengauer, C. Securin is required for chromosomal stability in human cells. *Cell*. 2001;105:445-457.
31. Pflieger, K., Heubes, S., Cox, J., Stemmann, O., Speicher, M.R. Securin Is Not Required for Chromosomal Stability in Human Cells. *PLoS Biol.* 2005;3:e416.
32. Gorr, I.H., Boos, D., Stemmann, O. Mutual inhibition of separase and Cdk1 by two-step complex formation. *Mol. Cell*. 2005;19:135-141.
33. Funabiki, H., Yamano, H., Kumada, K., Nagao, K., Hunt, T., and Yanagida, M. Cut2 proteolysis required for sister-chromatid separation in fission yeast. *Nature*. 1996;381:438–441.

34. Agarwal, R. and Cohen-Fix, O. Phosphorylation of the mitotic regulator Pds1/securin by Cdc28 is required for efficient nuclear localization of Esp1/separase. *Genes Dev.* 2002;16:1371-82
35. Cohen-Fix, O., and Koshland D. The anaphase inhibitor of *Saccharomyces cerevisiae* Pds1p is a target of the DNA damage checkpoint pathway. *Proc Natl Acad Sci USA.* 1997;94:14361-14366.
36. Sanchez., Y., Bachant, J., Wang, H., Hu, F., Liu, D., Tetzlaff, M., Elledge, SJ. Control of the DNA damage checkpoint by chk1 and rad53 protein kinases through distinct mechanisms. *Science.* 1999;286:1166-1171.
37. Peters, J.M. The anaphase promoting complex/cyclosome : a machine designed to destroy. *Mol. Cell. Biol.* 2006;7:644-656.
38. Shira, M., Toth, A., Galova, M., and Nasmyth, K. APC(Cdc20) promotes exit from mitosis by destroying the anaphase inhibitor Pds1 and cyclin Clb5. *Nature.* 1999;402:203-207.
39. Baumer, M., Braus, G.H., Irniger, S. Two different modes of cyclin Clb2 proteolysis during mitosis in *Saccharomyces cerevisiae*. *FEBS Lett.* 2000;468:142-148.
40. Irniger, S. Cyclin destruction in mitosis: a crucial task of Cdc20. *FEBS Lett.* 2002;532:7-11.
41. Wasch, R. and Cross, F.R. APC-dependent proteolysis of the mitotic cyclin Clb2 is essential for mitotic exit. *Nature.* 2002;418:556-562.
42. Lim, H.H., Goh, P.Y., Surana, U. Cdc20 is essential for the cyclosome-mediated proteolysis of both Pds1 and Clb2 during M phase in budding yeast. *Curr. Biol.* 1998;8:231-234.
43. Morris, M.C., Kaiser, P., Rudyak, S., Baskerville, C., Watson, M.H., Reed, S.I. Cks1-dependent proteasome recruitment and activation of CDC20 transcription in budding yeast. *Nature.* 2003;423:1009-1013.
44. Visintin, R., Prinz, S., Amon, A. CDC20 and CDH1: a family of substrate-specific activators of APC-dependent proteolysis. *Science.* 1997;278:460– 463.
45. Huang, J. N., Park, I., Ellingson, E., Littlepage, L. E. and Pellman, D. Activity of the APC(Cdh1) form of the anaphase-promoting complex persists until S phase and prevents the premature expression of Cdc20p. *J. Cell Biol.* 2001;154:85-94.
46. Sudakin, V., Chan, G.K., Yen, T.J. Checkpoint inhibition of the APC/C in HeLa cells is mediated by a complex of BUBR1, BUB3, CDC20, and MAD2. *J Cell Biol.* 2001;154:925-936.
47. May, K. M. and K. G. Hardwick. The spindle checkpoint. *J Cell Sci.* 2006;119: 4139-4142.
48. Harper, J.W., Burton, J.L., Solomon, M. The anaphase-promoting complex: it's not just for mitosis any more. *Genes & Dev.* 2002;16:2179-2206.
49. Kramer, E.R, Scheuringer, N., Podtelejniko, A.V., Mann, M., Peters, J.M. Mitotic Regulation of the APC Activator Proteins CDC20 and CDH1. *Mol Cell Bio.* 2000;11:1555-1569.
50. Jorgensen, P., Nishikawa, J.L., Breikreutz, B.J., Tyers, M. Systematic identification of pathways that couple cell growth and division in yeast. *Science.* 2002;297:395-400.
51. Prinz, S., Hwang, E.S., Visintin, R., Amon, A. The regulation of Cdc20 proteolysis

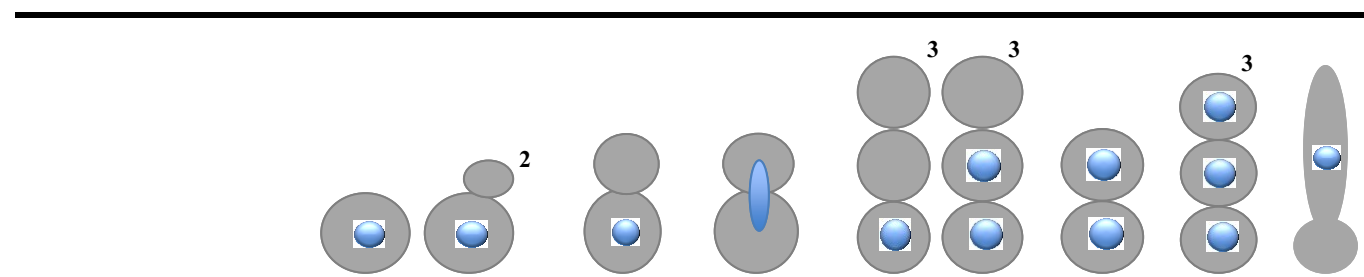
- reveals a role for APC components Cdc23 and Cdc27 during S phase and early mitosis. *Curr Biol.* 1998;8:750-760.
52. Jaspersen, S.L., Charles, J.F., Morgan, D. Inhibitory phosphorylation of the APC regulator Hct1 is controlled by the kinase Cdc28 and the phosphatase Cdc14. *Curr Biol.* 1999;9:227-36.
 53. Yeong, F.M., Lim, H.H., Padmashree, C.G., Surana, U. Exit from mitosis in budding yeast: biphasic inactivation of the Cdc28-Clb2 mitotic kinase and the role of Cdc20. *Mol Cell.* 2000;5:501-11.
 54. Liang, F., Jin, F., Liu, H., Wang, Y. The molecular function of the yeast polo-like kinase Cdc5 in Cdc14 release during early anaphase. *Mol Biol Cell.* 2009;20:3671-3679.
 55. Rahal, R., and Amon, A. The Polo-like kinase Cdc5 interacts with FEAR network components and Cdc14. *Cell Cycle.* 2008;7:3262-3272.
 56. Sanchez-Diaz, A., Nkosi, P.D., Murray, S., Labib, K. The Mitotic Exit Network and Cdc14 phosphatase initiate cytokinesis by counteracting CDK phosphorylations and blocking polarised growth. *EMBO J.* 2012;31:3620-3634.
 57. Queralt, E., and Uhlmann, F. Cdk-counteracting phosphatases unlock mitotic exit. *Curr Opin Cell Biol.* 2008;20:661-668.
 58. Bardin, A.J., Visintin, R., Amon, A. A mechanism for coupling exit from mitosis to partitioning of the nucleus. *Cell.* 2000;102:21-31.
 59. Lim, C.S., Rosli, R., Seow, H.F., Chong, P.P. *Candida* and invasive candidiasis: back to basics. *Eur J Clin Microbiol Infect Dis.* 2012;31:21-31.
 60. Berman, J. *Candida albicans*. *Curr Biol.* 2012;22:R620-622.
 61. Cannon, R.D., Lamping, E., Holmes, A.R., Niimi, K., Tanabe, K., Niimi, M., Monk, B.C. *Candida albicans* drug resistance another way to cope with stress. *Microbiology.* 2007;153:3211-3217.
 62. Xie, J.L., Polvi, E.J., Shekhar-Guturja, T., Cowen, L.E. Elucidating drug resistance in human fungal pathogens. *Future Microbiol.* 2014;9:523-542.
 63. O'Meara, T.R., Veri, A.O., Ketela, T., Jiang, B., Roemer, T., Cowen, L.E. Global analysis of fungal morphology exposes mechanisms of host cell escape. *Nat Commun.* 2015;6:1-10.
 64. Kabir, M.A., Hussain, M.A., Ahmad, Z. *Candida albicans*: A Model Organism for Studying Fungal Pathogens. *ISRN Microbio.* 2012;1-15.
 65. Lim, C.S.Y., Rosli, R., Seow, H.F., Chong, P.P. *Candida* and invasive candidiasis: back to basics. *Eur J Clin Microbiol Infect Dis.* 2012;31:21-31.
 66. Staebell, M., and Soll, D.R. Temporal and spatial differences in cell wall expansion during bud and mycelium formation in *Candida albicans*. *J. Gen Microbiol.* 1985;131:1467-1480.
 67. Hazan, I., Sepulveda-Becerra, M., Liu, H. Hyphal elongation is regulated independently of cell cycle in *Candida albicans*. *Mol Biol Cell.* 2002;13:134-45.
 68. Cramplin, H., Finley, K., Gerami-Nejad, M., Court, H., Gale, C., Berman, J., Sudbery, P. *Candida albicans* hyphae have a Spitzenkorper that is distinct from the polarisome found in yeast and pseudohyphae. *J Cell Sci.* 2005;118:2935-2947.
 69. Sudbery, P. E. The germ tubes of *Candida albicans* hyphae and pseudohyphae show

- different patterns of septin ring localization. *Mol. Microbiol.* 2001;41:19-31.
70. Morschhäuser, J. Regulation of white-opaque switching in *Candida albicans*. *Med. Microbiol. Immunol.* 2010;199:165–172.
 71. Si, R.H., Xu, K., Nicksarlian, M., Calvo, A.M., Harris, S.D. Morphogenetic and developmental functions of the *Aspergillus nidulans* homologues of the yeast bud site selection proteins Bud4 and Axl2. *Mol Microbiol.* 2012;85:252-270.
 72. Sudbery, P. Growth of *Candida albicans* hyphae. *Nat Rev Microbiol.* 2011;16:737-748.
 73. Berman, J. Morphogenesis and cell cycle progression in *Candida albicans*. *Curr Biol.* 2006;9:595-601.
 74. Jones, L., and Sudbery, P. Spitzenkorper, Exocyst, and Polarisome Components in *Candida albicans* Hyphae Show Different Patterns of Localization and Have Distinct Dynamic Properties. *Eukaryotic Cell.* 2010;9:1455-1465.
 75. Carlisle, P.L., and Kadosh, D. A genome-wide transcriptional analysis of morphology determination in *Candida albicans*. *Mol Biol Cell.* 2013;24:246-260.
 76. Gordan, R., Pyne, S., Bulyk, M.L. Identification of cell-cycle regulated, putative hyphal genes in *Candida albicans*. *Pac Symp Biocomput.* 2012;299-310.
 77. Braun, B.R., Head, W.S., Wang, M.X., Johnson, A.D. Identification and characterization of TUP1-regulated genes in *Candida albicans*. *Genetics.* 2000;156:31-44.
 78. Zeidler, U., Lettner, T., Lassnig, C., Müller, M., Lajko, R., Hintner, H., Breitenbach, M., Bito, A. UME6 is a crucial downstream target of other transcriptional regulators of true hyphal development in *Candida albicans*. *FEMS Yeast Res.* 2009;9:126-42
 79. Zhang, X., Wang, Y., Wang, Y. Hgc1, a novel hypha-specific G1 cyclin-related protein regulates *Candida albicans* hyphal morphogenesis. *The EMBO Journal.* 2004;23:1845-1856.
 80. Wang A, Raniga PP, Lane S, Lu Y, Liu H. Hyphal chain formation in *Candida albicans*: Cdc28-Hgc1 phosphorylation of Efg1 represses cell separation genes. *Mol. Cell. Biol.* 2009;29:4406–4416.
 81. Bishop, A., Lane, R., Beniston, R., Chapa-y-Lazo, B., Smythe, C., Sudbery, P. Hyphal growth in *Candida albicans* requires the phosphorylation of Sec2 by the Cdc28-Ccn1/Hgc1 kinase. *EMBO J.* 2010;29:2930-2942.
 82. Cote, P., Hogues, H., Whiteway, M.S. Transcriptional analysis of the *Candida albicans* cell cycle. *Mol. Biol. Cell* 2009;20:3363–3373.
 83. Bensen, E.S., Clemente-Blanco, A., Finley, K.R., Correa-Bordes, J., Berman, J. The mitotic cyclins Clb2p and Clb4p affect morphogenesis in *Candida albicans*. *Mol Biol Cell.* 2005;16:3387-3400.
 84. Umeyama, T., Kaneko, A., Niimi, B., Uehara, Y. Repression of CDC28 reduces the expression of the morphology-related transcription factors, Efg1p, Nrg1p, Rbf1p, Rim101p, Fkh2p and Tec1p and induces cell elongation in *Candida albicans*. *Yeast* 2006;23:537–552.
 85. Clemente-Blanco, A., et al. 2006. The Cdc14p phosphatase affects late cell-cycle events and morphogenesis in *Candida albicans*. *J. Cell Sci.* 2006;119:1130–1143.
 86. Gonzalez-Novo, A., et al. Dbf2 is essential for cytokinesis and correct mitotic spindle

- formation in *Candida albicans*. Mol. Microbiol. 2009;72:1364-1378.
87. Jimenez, J., Castelao, B.A., Gonzalez-Novo, A., Sanchez-Perez, M. The role of MEN (mitosis exit network) proteins in the cytokinesis of *Saccharomyces cerevisiae*. Intern Microbiol. 2005;8:33-42.
 88. Bachewich, C., Thomas, D.Y., Whiteway, M. Depletion of a polo-like kinase in *Candida albicans* activates cyclase-dependent hyphal-like growth. Mol Biol Cell. 2003;14:2163-2180.
 89. Glory, A., Oostende, C., Geitmann, A., Bachewich, C. Depletion of the mitotic kinase Cdc5p in *Candida albicans* results in the formation of elongated buds that switch to the hyphal fate over time in a Ume6p-dependent manner. Submitted to *Eukaryotic Cell* MS# EC00172-14; in revision. 2014.
 90. Chou, H., Glory, A., Bachewich, C. Orthologues of the anaphase-promoting complex/cyclosome coactivators Cdc20p and Cdh1p are important for mitotic progression and morphogenesis in *Candida albicans*. Eukaryot Cell. 2011;10:696-709.
 91. Care, R.S., Trevethick, J., Binley, K.M., Sudbery, P.E. The *MET3* promoter: a new tool for *Candida albicans* molecular genetics. Mol Microbiol. 1999;34:792-798.
 92. Lavoie, H., Sellam, A., Askew, C., Nantel, A., Whiteway, M. A toolbox for epitope-tagging and genome-wide location analysis in *Candida albicans*. BMC Genomics. 2008;9:578.
 93. Chen, D.C., Yang, B.C, Kuo, T.T. One-step transformation of yeast in stationary phase. Curr Genet. 1992;21(1):83-4.
 94. Gietz, R.D., Schiestl, R.H., Willems, A.R., Woods, R.A. Studies on the transformation of intact yeast cells by the LiAc/SS- DNA/PEG procedure. Yeast (Chichester, England). 1995;11:355-60.
 95. Gietz, R.D. and Woods, R.A. Genetic transformation of yeast. BioTechniques. 2001;30: 816-20, 822-6, 828.
 96. Rose, M.D., Winston, F., Hieter, P. Methods in Yeast Genetics: A Laboratory Course Manual. Cold Spring Harbor Laboratory Press. 1990.
 97. Liu, H.L., Osmani, A.H., Ukil, L., Son, S., Markossian, S., Shen, K.F., Govindaraghavan, M., Varadaraj, A., Hashmi, S.B., De Souza, C.P., Osmani, S.A. Single-step affinity purification for fungal proteomics. Eukaryot Cell. 2010;9:831-833.
 98. Rigaut, G., Shevchenko, A., Rutz, B., Wilm, M., Mann, M., Séraphin B. A generic protein purification method for protein complex characterization and proteome exploration. Nat Biotechnol. 1999;17:1030-1032.
 99. Han, X., and Poon, R.Y.C. Critical Differences between Isoforms of Securin Reveal Mechanisms of Separase Regulation. Mol Cell Biol. 2013;33:3400-3415.
 100. Gola, S., Martin, R., Walther, A., Dunkler, A., Wendland, J. New modules for PCR-based gene targeting in *Candida albicans*: rapid and efficient gene targeting using 100 bp of flanking homology region. Yeast. 2003;20:1339-1347.
 101. Guacci, V., and Koshland, D. Cohesin-independent segregation of sister chromatids in budding yeast. Mol Cell Biol. 2011;23:729-739.
 102. Suzuki, K., Sako, K., Akiyama, K., Isoda, M., Senoo, C., Nakajo, N., Sagata, N. Identification of non-Ser/Thr-Pro consensus motifs for Cdk1 and their roles in mitotic

- regulation of C2H2 zinc finger proteins and Ect2. *Scientific Reports*. 2015; 5:1-9.
103. Wang, H., Gao, J., Li, W., Wong, A.H.H., Hu, K., Chen, K., Wang, Y., Sang, J. Pph3 Dephosphorylation of Rad53 Is Required for Cell Recovery from MMS-Induced DNA Damage in *Candida albicans*. *Plos One*. 2012;7:1-13.
 104. Rahal, R., and Amon, A. Mitotic CDKs control the metaphase-anaphase transition and trigger spindle elongation. *Genes & Dev*. 2008;22:1534-1548.
 105. Roemer, T., and Boone, C. Systems-level antimicrobial drug and drug synergy discovery. *Nature*. 2013;9:222-231.

Table S2: Cell phenotype and position of nuclei in cells depleted of Esp1p or Orf19.955p for 8 h¹



+DOX

<i>ESP1::URA3/ TET::ESP1-HIS1</i> (n=129)	16.3	26.4	10.9	16.3	7.8	5.4	1.6	15.5
<i>ORF19.955::URA3/ TET::ORF19.955- HIS1</i> (n=123)	28.5	13.0	4.1	2.4	9.8	17.1	17.1	8.1

-DOX

<i>ESP1::URA3/ TET::ESP1-HIS1</i> (n=133)	70.0	9.8	6.0	-	-	10.5	3.0	-
<i>ORF19.955::URA3/ TET::ORF19.955- HIS1</i> (n=126)	57.1	18.3	3.2	-	-	15.1	7.0	-

¹Percentage of cells showing the indicated patterns. GRACE strain (*esp1::URA3/TET::ESP1-HIS1*) and GRACE strain (*orf19.955::URA3/TET::ORF19.955-HIS1*) were incubated in YPD medium with doxycycline (+DOX) or YPD medium without doxycycline (-DOX) for 8 h, fixed, and stained with DAPI.

²Includes unbudded and small-budded cells.

³Pattern includes multibudded and pseudohyphal cells.

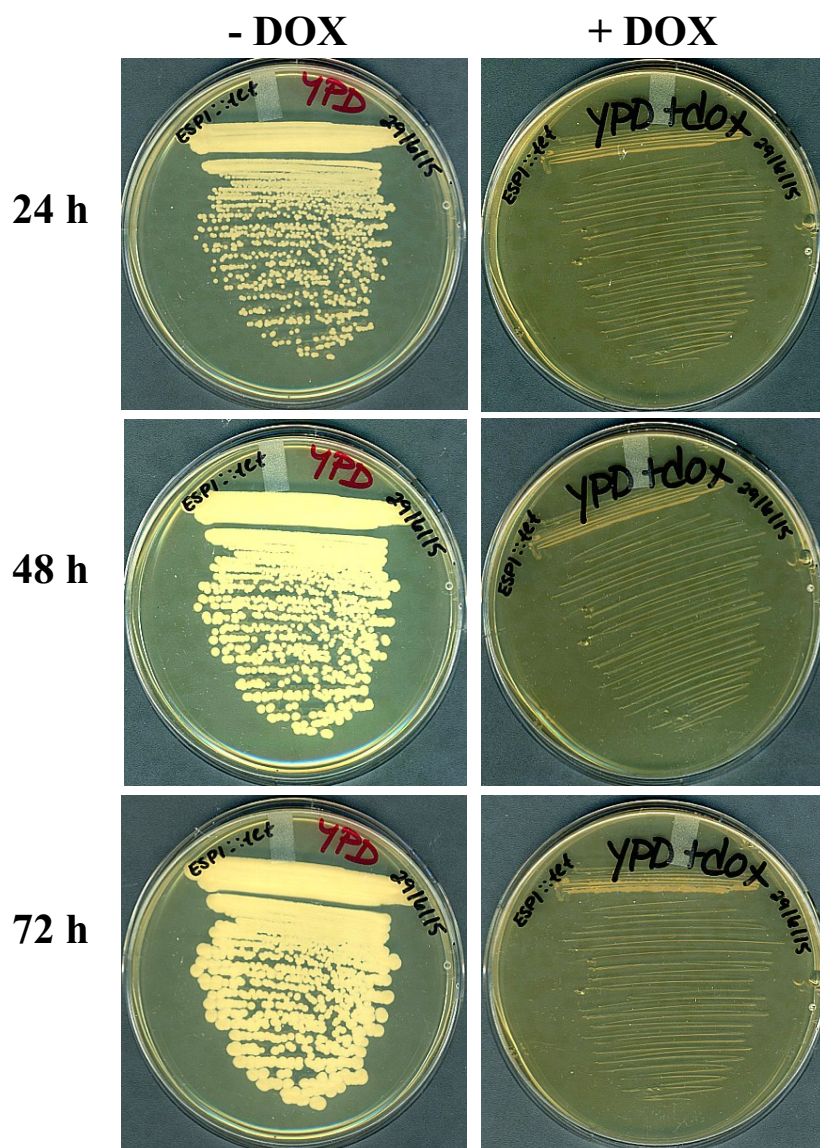


Fig S1: Esp1p depletion shows inviability.

GRACE strain *esp1::URA3/TET::ESP1-HIS1* was plated on YPD medium with 10 $\mu\text{g/ml}$ doxycycline (+DOX) or YPD medium without doxycycline (-DOX) and incubated at 30°C for select times.

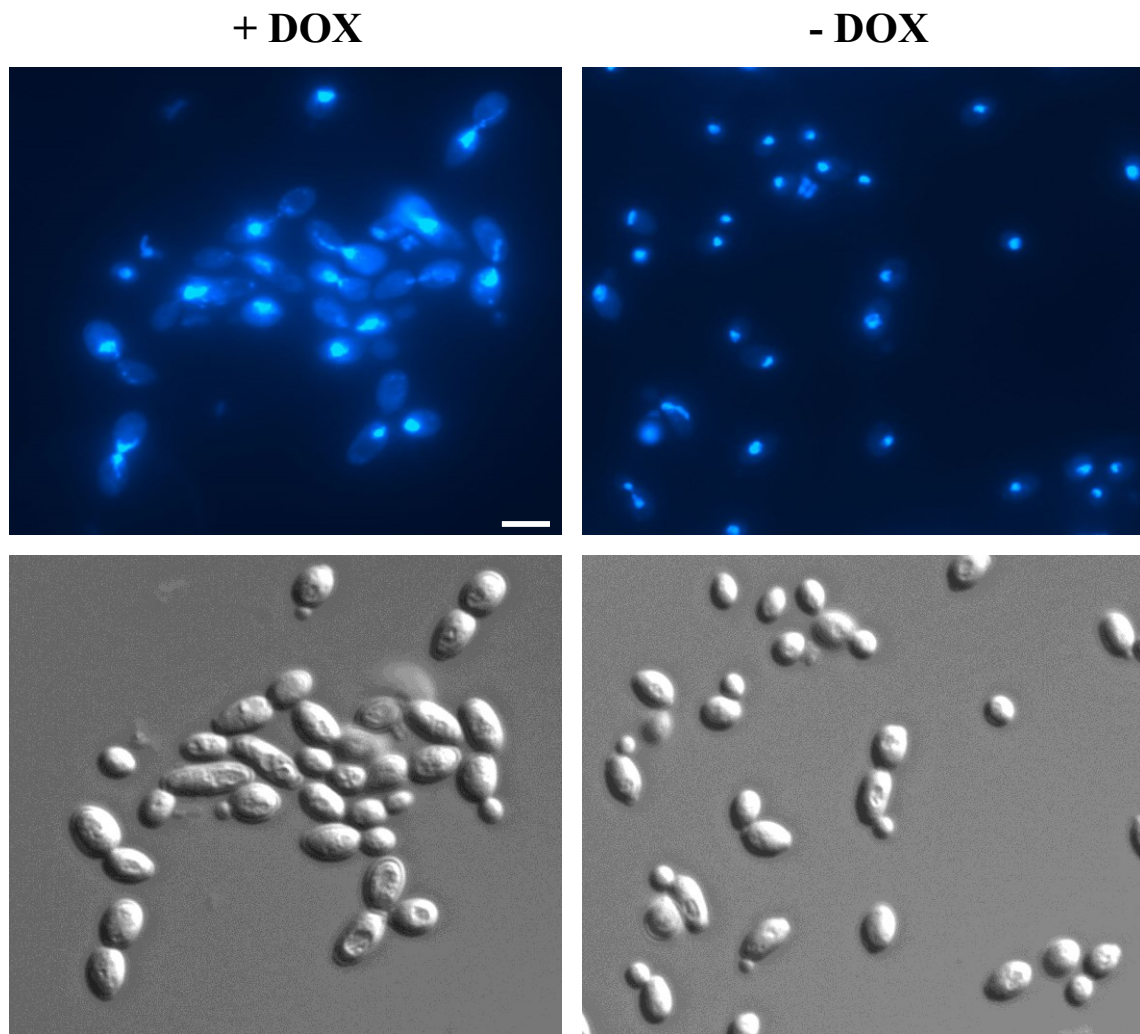


Fig S2: Absence of Esp1p impairs chromatin separation.

GRACE strain *esp1::URA3/TET::ESP1-HIS1* was incubated in YPD medium with 10 $\mu\text{g/ml}$ doxycycline (+DOX) or YPD medium without doxycycline (-DOX) at 30 degrees C for 5 h, fixed and stained with DAPI. Bar: 10 μm .

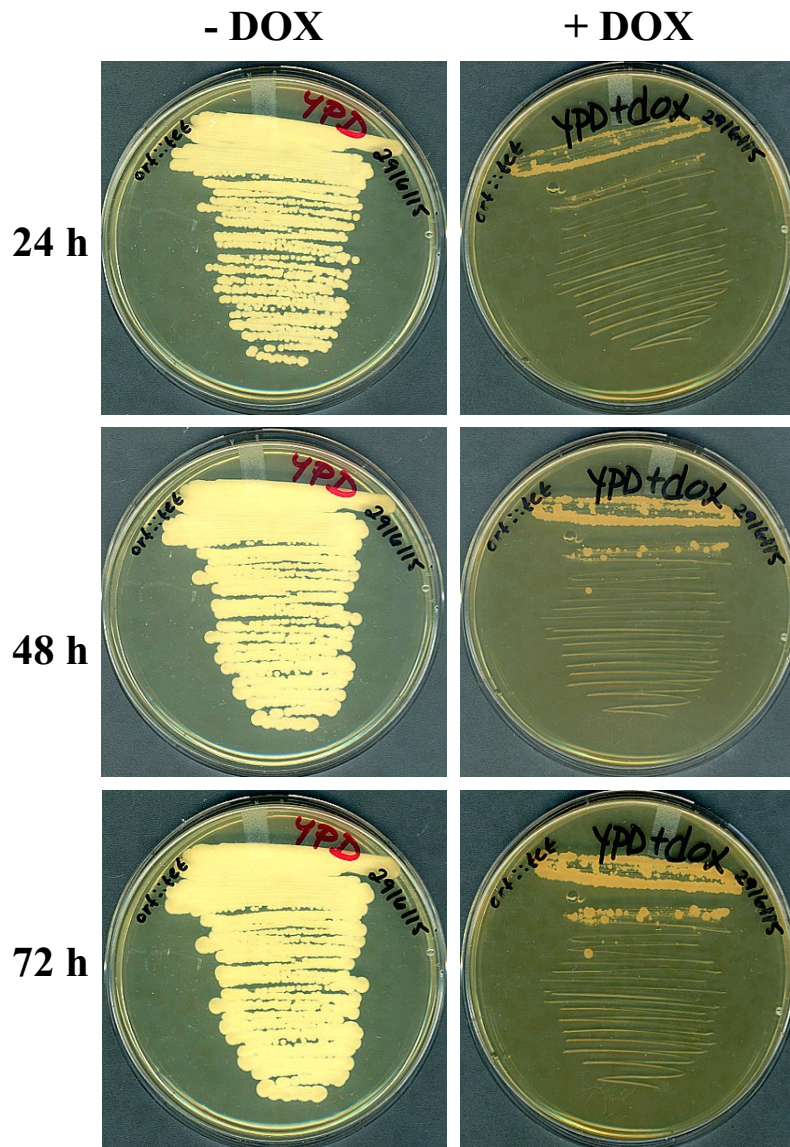


Fig S3: Depletion of Orf19.955p results in slow growing small colonies.

GRACE strain *orf19.955::URA3/TET::ORF19.955-HIS1* was plated on YPD medium with 10 $\mu\text{g/ml}$ doxycycline (+DOX) or YPD medium without doxycycline (-DOX) and incubated at 30°C for select times.

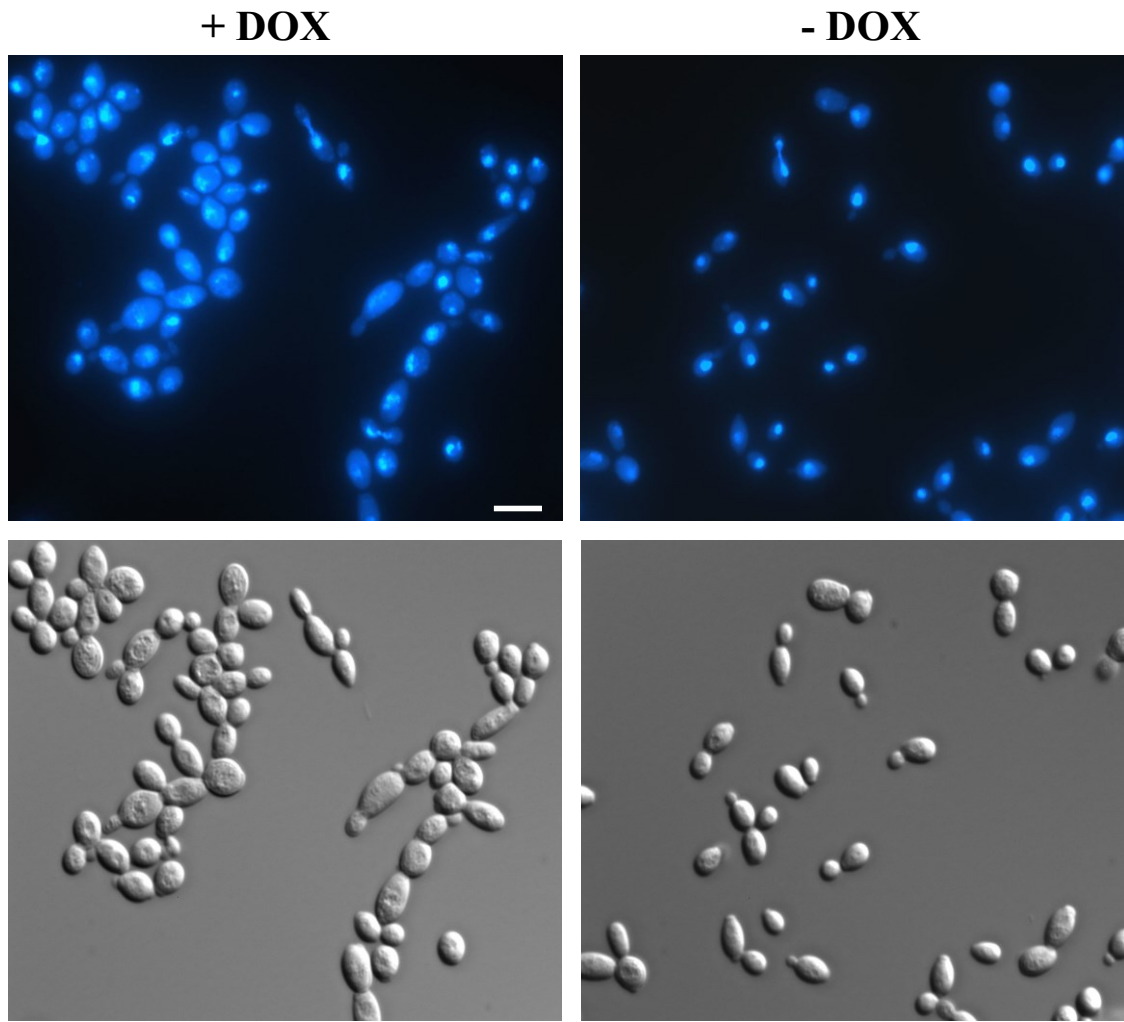


Fig S4: Cells depleted of Orf19.955p show abnormalities in chromosome organization. GRACE strain *orf19.955::URA3/TET::ORF19.955* was incubated in YPD medium with 10 $\mu\text{g/ml}$ doxycycline (+DOX) or YPD medium without doxycycline (-DOX) at 30 degrees C for 5 h, fixed and stained with DAPI. Bar: 10 μm .

MWM ***ESP1/ESP1*** ***esp1/ESP1-TAP***



Fig S5: Tandem affinity purification of Esp1p.

Protein extracted from 2 L cultures of strains BH440 (*ESP1/ESP1, URA3+HIS1+*) or SS1 (*esp1::HIS1/ESP1-TAP-URA3*) were subjected to tandem affinity purification. Elutions were TCA precipitated and run on an SDS-PAGE gel for silver staining.